Universität Rostock Traditio et Innovatio

Untersuchungen zum Reaktionsverhalten niedrigkoordinierter Phosphor-Stickstoffkationen gegenüber perfluorierten Anionen

Diplomarbeit

zum

Diplomverfahren

am Institut für Chemie

der Mathematisch-Naturwissenschaftlichen Fakultät

der Universität Rostock

Marcus Kuprat

Untersuchungen zum Reaktionsverhalten niedrigkoordinierter Phosphor-Stickstoffkationen gegenüber perfluorierten Anionen

Diplomarbeit

zum

Diplomverfahren

am Institut für Chemie

der Mathematisch-Naturwissenschaftlichen Fakultät

der Universität Rostock

vorgelegt von Marcus Kuprat,

geb. am 19.11.1984 in Ludwigslust

Rostock, August 2010

Gutachter: Prof. Dr. Axel Schulz

Dr. Alexander Villinger

Datum der Verteidigung: 09. September 2010

Die vorliegende Arbeit wurde von April bis September 2010 am Lehrstuhl für Anorganische und Elementorganische Chemie der Universität Rostock unter Betreuung von Prof. Dr. Axel Schulz angefertigt.

Erklärung

Ich versichere hiermit an Eides statt, dass ich die vorliegende Arbeit selbstständig angefertigt und ohne fremde Hilfe verfasst habe, keine außer den von mir angegebenen Hilfsmitteln und Quellen dazu verwendet habe und die den benutzten Werken inhaltlich und wörtlich entnommenen Stellen als solche kenntlich gemacht habe.

Marcus Kuprat

Rostock, den 07.09.2010

Mein ganz besonderer Dank gilt Herrn **Prof. Dr. Axel Schulz** für die Bereitstellung des interessanten Themas, das in mich gesetzte Vertrauen, für die mir eingeräumte wissenschaftliche Freiheit und das große Interesse an meiner Arbeit.

Des Weiteren gilt mein großer Dank Herrn **Dr. Alexander Villinger** für die intensive, wertvolle Betreuung im Labor, die anregenden wissenschaftlichen Diskussionen sowie für die Übernahme der Zweitgutachtertätigkeit.

Überdies bedanke ich mich bei Herrn **Dr. Ronald Wustrack** sowie Frau **Dipl.-Chem. Andrea Westenkirchner**, Herrn **Dipl.-Chem. Mathias Lehmann** und Herrn **Dipl.-Chem. René Kuzora** für die außerordentlich freundliche und produktive Arbeitsatmosphäre.

Ferner danke ich sowohl allen weiteren Mitarbeitern des Arbeitskreises, als auch den analytischen Abteilungen der Instituts für Chemie der Universität Rostock und des Leibniz Instituts für Katalyse an der Universität Rostock e.V., die ebenfalls zum Gelingen dieser Arbeit beigetragen haben.

Mein weiterer besonderer Dank gilt meinem familiären Umfeld für Unterstützung, Verständnis und Ermöglichung des Studiums.

Für Jenny

Inhaltsverzeichnis

1. Zielstellung 1

2. Allgemeiner Teil 2

2.1 Abkürzungen 2

2.2 Maßeinheiten 2

3. Bisheriger Kenntnisstand 3

3.1 PN-Monomer-Dimer-Gleichgewichte und PN-Kationen 3

3.2 Schwachkoordinierende Anionen 5

4. Ergebnisse und Diskussion 7

4.1 Silbertetrakis(hexafluorisopropoxy)aluminat als Hexafluorisopropyl-Transfer-Reagenz für den Chlor/Hexafluorisopropylaustausch in Iminophosphanen 7

4.2 Lewis-Säure katalysierte Synthese von Pentafluorphenylsilber : Struktur von Silber-Lösemittel-Komplexen 11

4.3 Blaues Imino(pentafluorphenyl)phosphan und seine Eisencarbonyl-Adduktkomplexe 15

5. Originalpublikationen 18

5.1 Silver tetrakis(hexafluoroisopropoxy)aluminate as hexafluoroisopropyl transfer reagent for the chlorine/hexafluoroisopropyl exchange in imino phosphanes 19

5.2 Synthesis of Pentafluorophenyl Silver by Means of Lewis Acid Catalysis: Structure of Silver Solvent Complexes 26

5.3 Blue Imino(pentafluorophenyl)phosphane and Its Iron Carbonyl Complexes 34

6. Zusammenfassung 43

7. Literatur 44

1. Zielstellung

Ziel der vorliegenden Diplomarbeit war es zum einen, reaktive PN-Kationen wie $[Mes^*NP]^+$ (Mes* = 2,4,6-tri-*tert*-butylphenyl) oder $[Hyp_2N_2P_2Cl]^+$ (Hyp = $(Me_3Si)_3Si$) durch chemisch inerte, schwachkoordinierende Anionen (WCAs) zu stabilisieren. Daran anschließend sollte die Stabilität von Silbersalzen des WCAs Tetrakis(pentafluorphenyl)borat, $[B(C_6F_5)_3]^-$, in verschiedenen Lösemitteln untersucht und in diesem Zusammenhang entsprechende Silber- und Lithium-Lösemittelkomplexe des Pentafluorphenylborats strukturell charakterisiert werden. Das dritte Ziel dieser Arbeit war, pentafluorphenyl-substituierte Iminophosphane und *cyclo*-Diphosphadiazane über einen Chlor-/Pentafluorphenylaustausch durch Reaktion von AgC_6F_5 mit Mes*NPCl oder $[DippNPCl]_2$ (Dipp = 2,6-Di*iso*propylphenyl) darzustellen.
Die Untersuchung der Struktur sowie des chemischen Verhaltens der Verbindungen sollte durch schwingungsspektroskopische Methoden (IR,Raman-Spektroskopie) und multinukleare Kernresonanzspektroskopie (^{31}P-, ^{29}Si-, ^{13}C- und ^{1}H-NMR) in Lösung zum einen, zum anderen mit Hilfe der Röntgendiffraktometrie an geeigneten Einkristallen erfolgen. Diese Daten sollten zudem mit den Ergebnissen von *ab-initio*- und DFT-Rechnungen verglichen werden, und die Bindungsverhältnisse innerhalb der synthetisierten Moleküle aufgeklärt und charakterisiert werden. Dadurch sollte sowohl der Zusammenhang zwischen Struktur und chemischer Bindung als auch die Ladungsverteilung und Reaktivität erklärt werden.

2. Allgemeiner Teil

Die in der vorliegenden Arbeit verwendeten Abkürzungen sind in Tabelle 1 aufgeführt.

2.1 Abkürzungen

Ar^F	fluorierter Arylligand	MS	Massenspektrometrie
CB	Carborat	NMR	*nuclear magnetic resonance*
CI	Chemische Ionisation	Ph	Phenyl-
Dipp	Di*iso*propylphenyl-	R^F	fluorierter Alkylligand
FT	Fourier-Transformation	RAMAN	RAMAN-Spektroskopie
EI	Elektronenstoß-Ionisation	RT	Raumtemperatur
Et	Ethyl-	s	stark
Hyp	Hypersilyl-	T	Temperatur
i-Pr	*iso*-Propyl-	*t*-Bu	*tert*-Butyl-
IR	Infrarot-Spektroskopie	Ter	Terphenyl-
m	mittel	w	schwach (engl. weak)
Me	Methyl-	WCA	schwachkoordinierendes Anion
Mes*	Supermesityl-	X-ray	Röntgendiffraktometrie

Tabelle 1. Verwendete Abkürzungen.

2.2 Maßeinheiten

Es wurden die im internationalen Einheitensystem (SI) geltenden Maßeinheiten verwendet, alle davon abweichenden, in der Arbeit verwendeten Einheiten und deren Umrechnungen in SI-Einheiten sind in Tabelle 2 aufgeführt.

Größe	**Symbol**	**Bezeichnung**	**Umrechnung in SI-Einheit**
Länge	Å	Ångström	1 Å = 100 pm
Temperatur	℃	Grad Celsius	x ℃ = (x + 273.15) K
Zeit	d	Tag	1 d = 86400 s
	h	Stunde	1 h = 3600 s
Energie	kcal	Kilokalorie	1 kcal = 4.2 kJ

Tabelle 2. Vom SI-System abweichende Einheiten.

3. Bisheriger Kenntnisstand

3.1 PN-Monomer-Dimer-Gleichgewichte und PN-Kationen

Verbindungen der Zusammensetzung $[RNPX]_n$ (R = sterisch anspruchsvoller Rest, z.B. Alkyl, Aryl; X = Halogen, Alkyl, Aryl; n = 1,2) stellen eine gut untersuchte Stoffklasse dar. Bereits im Jahre 1894 wurde von Michaelis und Schroeter am chemischen Institut der Universität Rostock der erste viergliedrige Phosphor(III)-Stickstoff-Ring entdeckt, indem sie Anilinhydrochlorid mit einem Überschuss an PCl_3 unter Rückfluss zur Reaktion brachten.

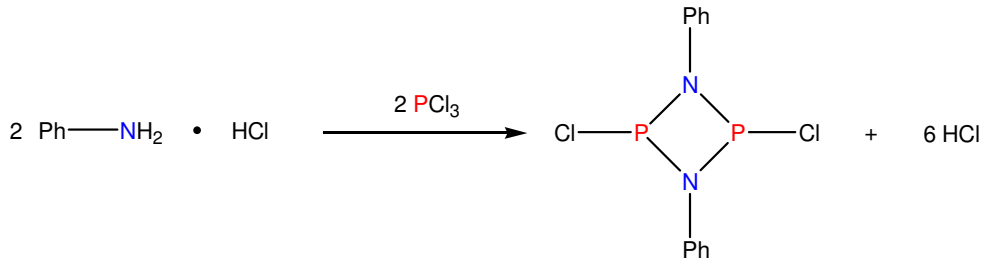

Schema 1. Darstellung des ersten viergliedrigen Phosphor(III)-Stickstoff-Ringes.

Allerdings gingen sie fälschlicherweise von der Annahme aus, die monomere Spezies PhNPCl gefunden zu haben.[1] Heute ist jedoch bekannt, dass in diesem Falle das Dimer die stabile Form repräsentiert; Burford *et al.* nehmen hierzu an, dass mit abnehmendem sterischen Anspruch der Reste R das Dimer begünstigt ist.[2,3] Hierbei ist das Supermesityl-substituierte Iminochlorphosphan Mes*NPCl (Mes* = 2,4,6-Tri-*tert.*-butylphenyl) bislang die einzige Verbindung, die intensiv rot gefärbt ist, und bei der das formale Monomer-Dimer-Gleichgewicht sowohl in Lösung als auch im Festkörper vollständig auf der Seite des Monomers liegt,[4] während in Systemen mit weniger voluminösen 2,6-Di*iso*propyphenyl- oder Hypersilyl-Resten praktisch nur das cyclische, farblose Dimer existiert.

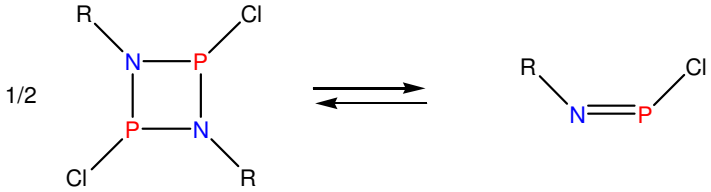

Schema 2. Formales Monomer-Dimer Gleichgewicht.

Deutlich weniger bekannt sind allerdings die entsprechenden kationischen Verbindungen. Das erste 1-Halogeno-*cyclo*-diphosphazeniumkation $[R_2N_2P_2X]^+$ (R = ^{t}Bu, X = Cl) wurde von Cowley *et al*. in einer ^{31}P-NMR-Studie beobachtet, in der ein Chlorid-Ion durch Zugabe von $AlCl_3$ aus der entsprechenden Neutralverbindung $[RNPCl]_2$ abstrahiert wurde[5]. Burford *et al.* berichteten später über die intermediäre Bildung von 1-Halogen-2,4-di(aryl)-*cyclo*-1,3-dipnicta-2,4-diazeniumkationen bei der Umsetzung von $[RNPX]_2$ (R = 2,6-Dimethylphenyl, 2,6-Di*iso*propylphenyl; X = Cl, Br) mit GaX_3, wobei sich über eine GaX_3 - induzierte Ringerweiterung Trimere $[RNPX]_3$ bildeten[3]. Jüngst konnten sogar ausgehend von $[TerNECl]_2$ (Ter = 2,6-Bis(2,4,6-trimethylphenyl)phenyl, E = P, As) *cyclo*-1,3-dipnicta-2,4-diazeniumkationen dargestellt werden.[6]

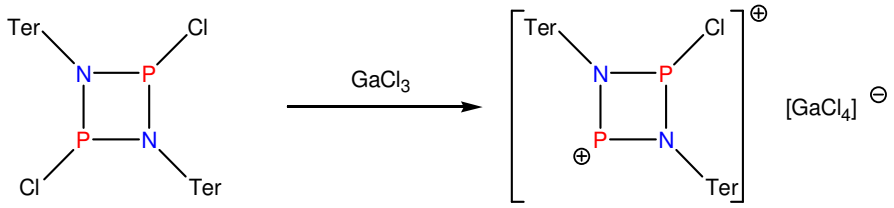

Schema 3. Synthese des *cyclo*-1,3-diphospha-2,4-diazenium Salzes.

Monomere PN-Kationen wie das Supermesityl-substituierte Iminophospheniumkation wurde erstmals von Niecke *et al*. als Tetrachloroaluminat [Mes*NP][$AlCl_4$] dargestellt; auch hier wurde $AlCl_3$ als Lewis-Säure eingesetzt, um Chlorid vom Mes*NPCl zu abstrahieren.[4] Ein derartiges Kation konnte beispielsweise von Niecke *et al*. erfolgreich in einer [2+3] - Cyclo-Addition durch Umsetzung mit *tert.*-Butylazid zur Darstellung des Tetrazaphospholium-tetrachloroaluminates eingesetzt werden.[7] Überdies konnte durch Umsetzung von Mes*NPCl mit Me_3SiN_3 durch $GaCl_3$-assistierte [2+3] - Cyclo-Addition ein Weg zu Tetrazaphospholen eröffnet werden.[8]

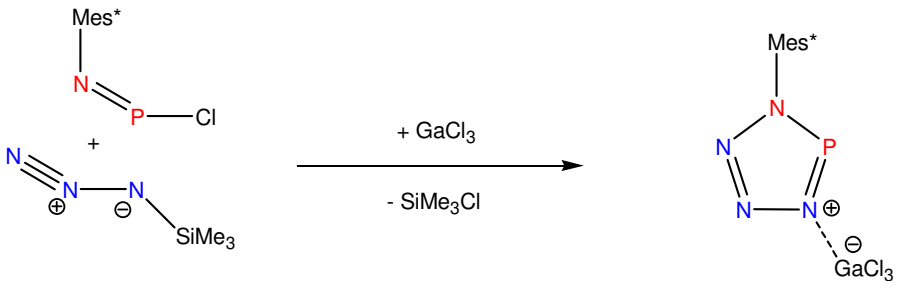

Schema 4. Synthese von Tetrazaphosphol stabilisiert als $GaCl_3$-Addukt.

3.2 Schwachkoordinierende Anionen

Für die Isolierung und kinetische Stabilisierung reaktiver PN-Kationen ist, neben dem Einfluss der Größe eines sterisch anspruchsvollen Restes, auch die Anwesenheit eines chemisch möglichst robusten und gleichzeitig schwach koordinierenden Anions von entscheidender Bedeutung. Diese sogenannten *Weakly Coordinating Anions*, kurz WCAs, waren in der Vergangenheit bereits Gegenstand zahlreicher Forschungsbeiträge.

Allgemeiner Anspruch an WCAs ist unter anderem ein möglichst geringfügig koordinierender Effekt. Dies erreicht man durch Delokalisierung der negativen Ladung über ein großes Volumen von möglichst nicht-nucleophilen und chemisch robusten, funktionellen Gruppen. Da stets die basischste Gruppierung die Koordinationskraft eines Anions bestimmt, koordiniert das WCA immer mit der sterisch zugänglichsten, nucleophilen Gruppe an das Kation. Der Idealfall wäre somit ein „nicht-koordinierendes" Anion.[9]

Als bekannte Vertreter der WCAs sind als erstes die fluorierten Tetraarylborate zu nennen, dessen einfachstes Derivat das $[B(C_6F_5)_4]^-$ darstellt. Ebenso sind verbrückte Borate wie z.B. $[(C_6F_5)_3B(\mu\text{-}CN)B(C_6F_5)_3]^-$ bekannt.

Eine Stoffklasse von WCAs die extrem schwachkoordinierend und zugleich chemisch sehr inert ist, stellt die Gruppe der *closo*-Carborat-Anionen, wie das ikosaedrische $[CB_{11}H_{12}]^-$ oder das $[CB_9H_{10}]^-$ dar. Sehr viel schwächer koordinierend und zugleich stabiler gegen Oxidation werden die Carborate durch partiellen oder vollständigen Austausch von H gegen Halogene oder auch kurze Alkylreste. So haben Reed *et al.* verschiedene halogenierte Derivate wie z. B. $[CB_{11}H_6X_6]^-$, oder $[CHB_{11}Me_5Cl_6]^-$ synthetisiert, wobei die korrespondierenden Brönsted-Säuren dieser Anionen zu den stärksten bekannten Supersäuren zählen.[10]

Weitere wichtige Vertreter der WCAs sind poly- oder perfluorierte Alkoxy- und Arylalkoxymetallate, wie z.B. $[Nb(OC_6F_5)_6]^-$ oder auch $[Al\{OC(CF_3)_3\}_4]^{-}$, da diese Anionen ähnlich schwach koordinierende Eigenschaften aufweisen wie $[CB_{11}H_6Cl_6]^-$.[11,1213] Neben den sogenannten Teflaten, wie $[B(OTeF_5)_4]^-$ und $[M(OTeF_5)_6]^-$ (M = z.B. As, Sb, Bi), gibt es auch mehrkernige Fluorometallat-WCAs; hierbei handelt es sich um Anionen aus Lewis-Säuren wie SbF_5, also in diesem Falle z.B. $[Sb_2F_{11}]^-$ oder $[Sb_4F_{21}]^-$.

WCAs finden in der präparativen Chemie eine breite Anwendung, da es nur durch die besonderen Eigenschaften der WCAs möglich wird, beispielsweise hochreaktive Kationen wie R_3Si^+, R_2Al^+ oder auch R_2F^+ zu stabilisieren.[14,15,16,17]

Die Darstellung von Siliceniumionen R_3Si^+ gelingt durch Hydridabstraktion in Silanen, wofür sich besonders $[Ph_3C][B(C_6F_5)_4]$ eignet. Darauf aufbauend lassen sich bissilylierte Halonium-

Ionen $[Me_3Si\text{-}X\text{-}SiMe_3][B(C_6F_5)_4]$ (X = F, Cl, Br, I) darstellen, indem $[Me_3Si]^+$-Salze, welche nur mit Carboraten oder dem Tetrakis(pentafluorphenyl)borat als Gegenion stabil sind, mit Trimethylhalogensilanen $Me_3Si\text{-}X$ (X = F, Cl, Br, I) zur Reaktion gebracht werden, wobei $Me_3Si\text{-}X$ sowohl Ausgangsverbindung als auch Lösemittel in einem ist.

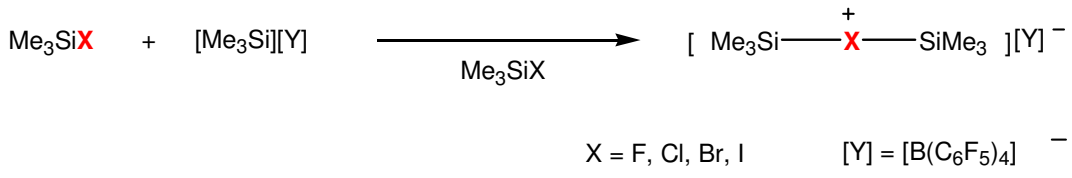

Schema 5. Darstellung bissilylierter Haloniumionen.

Ein weiteres Anwendungsgebiet erschließt sich durch die protonierte Form der Carborane, die sogenannten Supersäuren. Diese sind Brönsted-Säuren, die die Acidität reiner H_2SO_4 übertreffen, deren Superacidität idealerweise aber nicht mit der Lewis-Acidität einher geht. Dadurch werden außergewöhnliche Protonierungsreaktionen möglich, z.B. die Protonierung von C_{60}, Benzol oder Toluol.[8] Möglich sind auch nucleophile Substitutionen am Kation des WCA-Salzes; hier sei beispielhaft die Substitution eines Fluoratoms in $[N_2F]^+[X]^-$ durch eine Azideinheit unter Bildung des Pentastickstoffkations N_5^+ sowie HF genannt.[18]

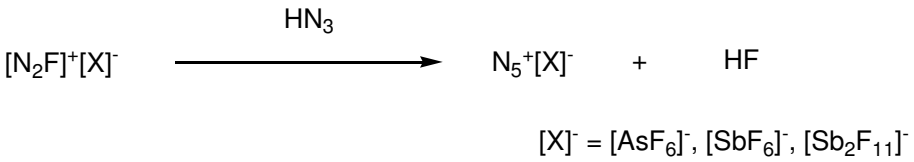

Schema 6. Darstellung von N_5^+-Salzen.

4. Ergebnisse und Diskussion

4.1 Silbertetrakis(hexafluorisopropoxy)aluminat als Hexafluorisopropyl-Transfer-Reagenz für den Chlor/Hexafluorisopropylaustausch in Iminophosphanen

Marcus Kuprat, René Kuzora, Mathias Lehmann, Axel Schulz, Alexander Villinger, Ronald Wustrack.

J. Organomet. Chem. **2010**, *695*, 1006-1011.

Wie bereits in der Einleitung erwähnt, sollte versucht werden, ein stabiles $[Mes^*NP]^+$-Kation durch das schwachkoordinierende Anion Tetrakis(hexafluorisopropoxy)aluminat darzustellen. Hierzu wurde Silbertetrakis(1,1,1,3,3,3-hexafluor-2-propoxy)-aluminat, $Ag[Al(OCH(CF_3)_2)_4]$, zu einer Lösung von Mes*NPCl in CH_2Cl_2 gegeben. Doch statt der erwarteten Bildung des $[Mes^*NP]^+$-Ions mit dem Aluminatanion $[Al(OCH(CF_3)_2)_4]^-$ als schwachkoordinierendem Gegenion, wurde die Bildung vom *N*-(2,4,6-tri-*tert*-butylphenyl)imino-(1,1,1,3,3,3-hexafluor-2-propoxy)phosphan, $Mes^*NPOCH(CF_3)_2$ und Bis[tris(1,1,1,3,3,3-hexafluor-2-propoxy)aluminium], $[Al(OCH(CF_3)_2)_3]_2$ beobachtet.

Hierbei wird das schwachkoordinierende Anion $[Al(OCH(CF_3)_2)_4]^-$ unter Ausbildung der freien Lewis-Säure $[Al(OCH(CF_3)_2)_3]_2$ zersetzt. Offensichtlich unterliegt die Bildung der freien Lewis-Säure der Instabilität des Anions $[Al(OCH(CF_3)_2)_4]^-$ gegenüber dem stark elektrophilen Kation $[Mes^*NP]^+$.

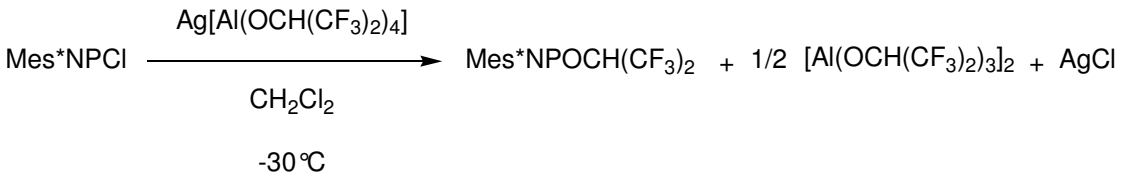

Schema 7. Synthese von *N*-(2,4,6-Tri-*tert*-butylphenyl)imino-(1,1,1,3,3,3-hexafluor-2-propoxy)-phosphan.

Dies bedeutet, dass das $[Mes^*NP]^+$-Kation im Vergleich zu $[Al(OCH(CF_3)_2)_3]_2$ die stärkere Lewis-Säure darstellt.

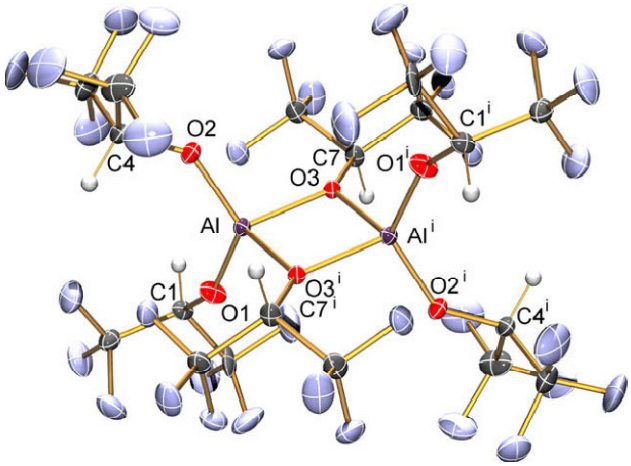

Abbildung 1. Molekülstruktur von Bis[tris(1,1,1,3,3,3-hexafluor-2-propoxy)aluminium].

In einer weiteren Untersuchung wurde das dimere $[HypNPCl]_2$ ebenfalls mit $Ag[Al(OCH(CF_3)_2)_4]$ in CH_2Cl_2 umgesetzt. Die anfangs farblose Lösung begann sich schnell kräftig rot zu färben, was einen ersten Anhaltspunkt für die mögliche Existenz des Vorliegens eines Kations ergab. In einer ^{31}P-NMR-Untersuchung konnte nachgewiesen werden, dass sich das 1-Chlor-2,4-bis[tris(trimethysilyl)silyl]-*cyclo*-diphosphazeniumion $[Hyp_2N_2P_2Cl]^+$ tatsächlich gebildet hatte. Weiterhin ergaben Messungen, dass das Kation in Lösung mehr als 12 h stabil ist. Durch anschließendes Entfernen des Lösungsmittels im Hochvakuum resultierte ein rotes Öl, aus dem sich langsam farblose Kristalle bildeten, welche durch Einkristallstrukturanalyse als 1-Chlor-3-(1,1,1,3,3,3-hexafluor-2-propoxy)-2,4-bis[tris(trimethyl-silyl)silyl]-*cyclo*-diphosphadiazan identifiziert werden konnten. Analog zur vorangegangenen Umsetzung mit dem Monomer entsteht auch hier das Dimer der freien Lewis-Säure.

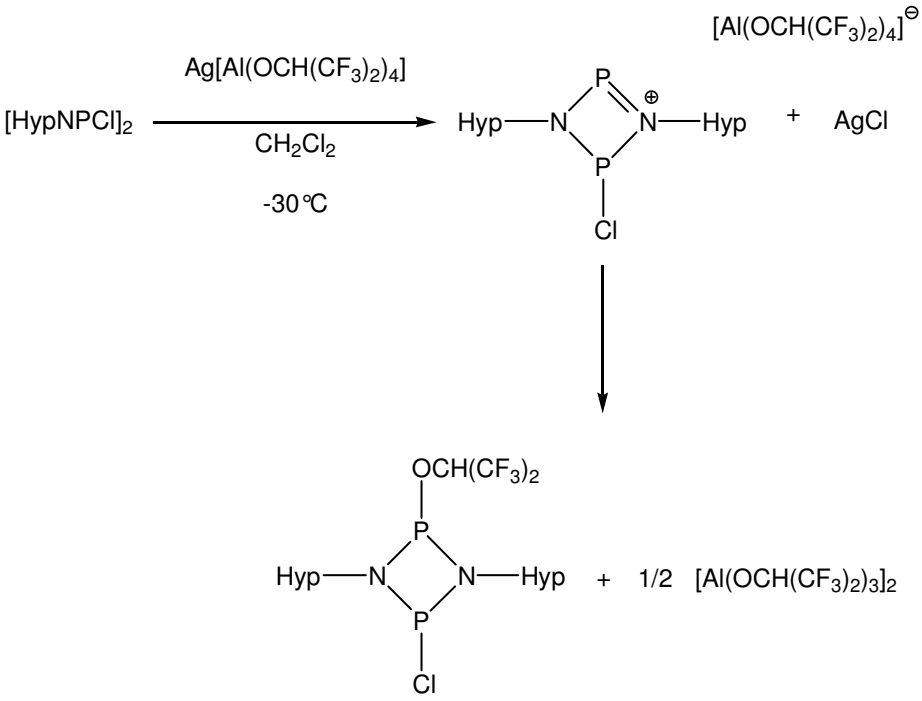

Schema 8. Synthese von 1-Chlor-3-(1,1,1,3,3,3-hexafluor-2-propoxy)-2,4-bis[tris(trimethylsilyl)silyl]-*cyclo*-diphosphadiazan.

Die Abrennung des *cyclo*-Diphosphadiazans vom Bis[tris(1,1,1,3,3,3-hexafluor-2-propoxy)aluminium] konnte erreicht werden, indem eine Lösung von $Li[OCH(CF_3)_2]$ zugegeben wurde, wobei ein Niederschlag von $Li[Al(OCH(CF_3)_2)_4]$ ausfiel, während das *cyclo*-Diphosphadiazan in Lösung blieb.

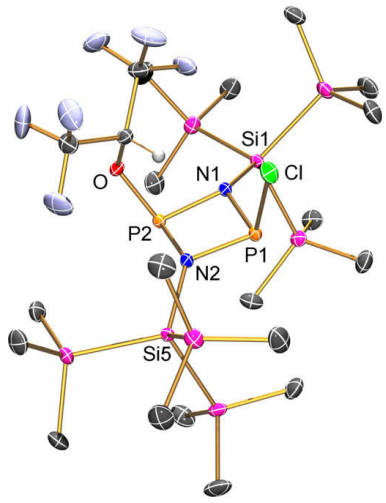

Abbildung 2. Molekülstruktur von 1-Chlor-3-(1,1,1,3,3,3-hexafluor-2-propoxy)-2,4-bis[tris(trimethylsilyl)silyl]-*cyclo*-diphosphadiazan.

Anschließend wurde versucht, dieses *cyclo*-Diphosphadiazan auf direktem Wege durch Umsetzung des *cyclo*-Dichlordiphosphadiazans mit Lithiumhexafluorisopropanolat zu synthetisieren.

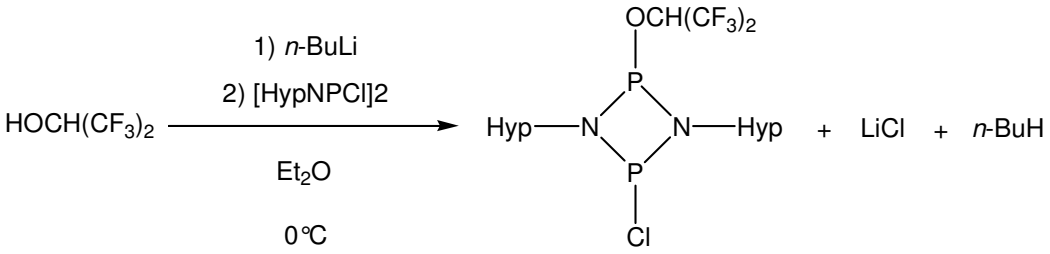

Schema 9. Versuchte direkte Synthese von 1-Chloro-3-(1,1,1,3,3,3-hexafluoro-2-propoxy)-2,4-bis[tris(trimethylsilyl)silyl]-*cyclo*-diphosphadiazan.

Die Zugabe von $Li[OCH(CF_3)_2]$ zu $[HypNPCl]_2$ in Diethylether ergab zunächst jedoch keine Reaktion. Erst nach Zugabe von Ethylendiamin zu Steigerung der Reaktivität von $Li[OCH(CF_3)_2]$ bildete sich ein weißer kristalliner Niederschlag.

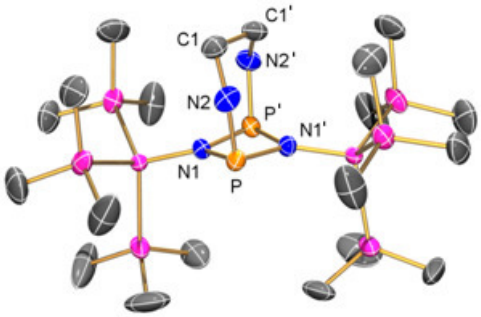

Abbildung 3. Ethylendiamin-überbrücktes *cyclo*-Diphosphadiazan.

Die Analytik der erhaltenen Kristalle mit Hilfe von Röntgenbeugungsmethoden ergab, dass es sich hierbei überraschenderweise um ein Ethylendiamin-überbrücktes *cyclo*-Diphosphadiazan handelte. Die direkte Synthese des gemischt-substituierten *cyclo*-Diphosphadiazan war somit zwar nicht erfolgreich, zeigt aber auf der anderen Seite, dass die gefundene Hexafluoro*iso*propyl-Transfer-Reaktion mit Silbertetrakis(hexafluoro*iso*propoxy)aluminat ein großes synthetisches Potential besitzt.

4.2 Lewis-Säure katalysierte Synthese von Pentafluorphenylsilber : Struktur von Silber-Lösemittel-Komplexen

Marcus Kuprat, Mathias Lehmann, Axel Schulz, Alexander Villinger
Organometallics **2010**, *29*, 1421-1427.

Die Silbersalze schwachkoordinierender Anionen stellen wertvolle Synthesebausteine dar. Tetrakis(pentafluorophenyl)borat Salze sind präparativ gut zugänglich, und aufgrund der enormen Stabilität von großem Interesse. Das entsprechende Silbersalz war bisher nur in Form eines Ether-Solvates bekannt, was jedoch den Einsatzbereich erheblich einschränkt, da das Ethermolekül leicht an starke, elektrophile Kationen koordinieren kann.
Aus diesem Grund wurde die Stabilität verschiedener Silber- und Lithium-Boratsalze in unterschiedlichen Lösemitteln untersucht. Zunächst wurde der Silbersalz-Lösemittelkomplex $[Ag(Et_2O)_3][B(C_6F_5)_4]$ ausgehend vom Lösemittelkomplex $[Li(Et_2O)][B(C_6F_5)_4]$ durch Reaktion mit $AgNO_3$ über einen Silber-/Lithium-Austausch dargestellt. Durch angemessene Druckreduzierung und thermische Behandlung war es möglich, den Lösemittelgehalt der Substanz bis auf nur ein Diethylethermolekül zu reduzieren, welches sich allerdings nicht weiter entfernen ließ.
Durch anschließende Umkristallisation konnte $[Ag(Toluol)_3][B(C_6F_5)_4]$ erhalten werden. In diesem Falle gelang es somit, ein etherfreies Salz, welches für Metathesereaktionen in schwach nucleophilen Lösemitteln von hoher Bedeutung sein kann, darzustellen.

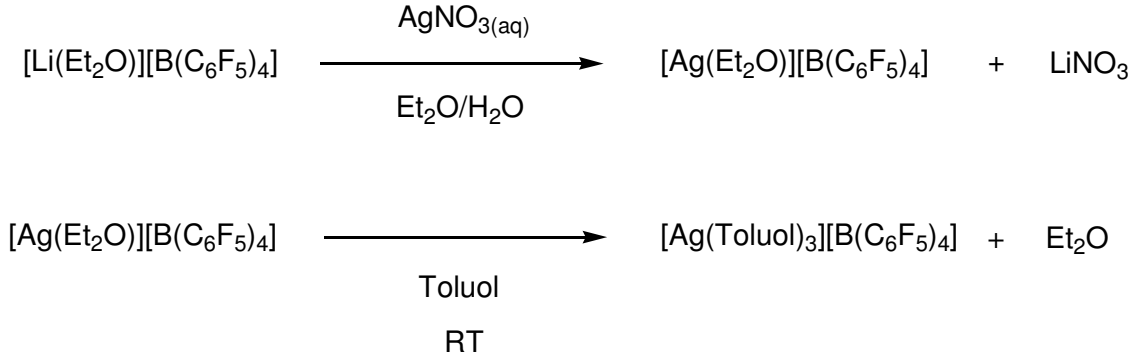

Schema 10. Syntheseroute zum Pentafluorphenylsilber-Toluolkomplex.

Um dennoch ein entsprechendes lösemittelfreies Silbersalz zu erhalten, wurde alternativ dazu nun vom lösemittelfreien Lithium-Salz $Li[B(C_6F_5)_4]$ ausgegangen, welches in CH_2Cl_2 mit

AgF unter mehrstündigem Einwirken von Ultraschall zu lösemittelfreiem AgC_6F_5 und $B(C_6F_5)_3$ neben LiF reagierte. Mit *n*-Hexan konnte das $B(C_6F_5)_3$ von AgC_6F_5 abgetrennt und durch Sublimation zu einem hohen Anteil zurückgewonnen werden, wodurch es wieder für erneute AgC_6F_5-Synthese einsetzbar war. Es ist also möglich, hier von einem formalen Katalysezyklus in Bezug auf das $B(C_6F_5)_3$ zu sprechen.

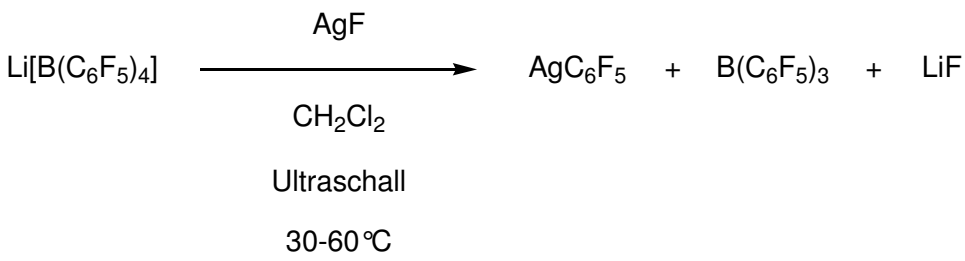

Schema 11. Synthese von AgC_6F_5.

Da in CH_2Cl_2 unsolvatisiertes $Ag[B(C_6F_5)_4]$ als Intermediat entsteht, dieses aber aufgrund fehlender Donor-Akzeptor-Wechselwirkungen durch Lösemittelmoleküle wie Toluol oder Et_2O instabil ist, zersetzt sich das Borat-Anion. Hierbei bildet sich AgC_6F_5 durch Abstraktion von $C_6F_5^-$ durch das Ag^+ als Lewis-Säure. Dies zeigt, dass es nicht möglich ist, $Ag[B(C_6F_5)_4]$ ohne zusätzliche stabilisierende Lösemittelmoleküle darzustellen.

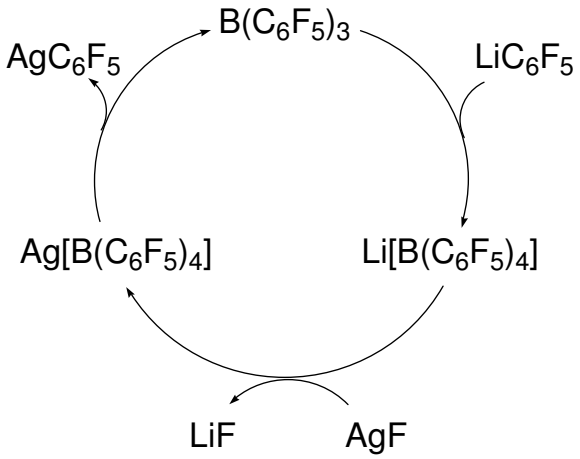

Schema 12. Formaler Katalysezyklus für die Darstellung von Pentafluorphenylsilber.

Ergänzend dazu wurden die Strukturen von $[Li(Et_2O)_4][B(C_6F_5)_4]$, $[Li(Toluol)][B(C_6F_5)_4] \cdot Toluol$, $[Li(Et_2O)_2][B(C_6F_5)_4] \cdot CH_2Cl_2$, $[Ag(Et_2O)_3][B(C_6F_5)_4]$, $[Ag(Toluol)_3][B(C_6F_5)_4]$ sowie $AgC_6F_5 \cdot CH_3CN$ kristallografisch untersucht.

Folgende Beispiele seien dazu näher erläutert:

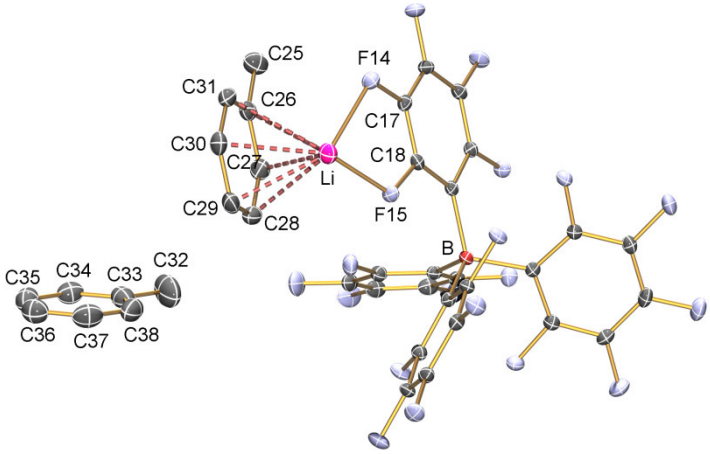

Abbildung 4. Molekülstruktur von $[Li(Toluol)][B(C_6F_5)_4] \cdot Toluol$.

Im $[Li(Toluol)][B(C_6F_5)_4] \cdot Toluol$ besteht die asymmetrische Einheit aus einer $[Li(Toluol)]^+$-Einheit und dem $[B(C_6F_5)_4]^-$-Anion, sowie aus einem nichtkoordinierenden Toluolmolekül. Interessanterweise bindet das Li^+-Ion hierbei an neun Atome, und zwar in η^6-Koordination an alle sechs Ring-Kohlenstoff-Atome, wobei man zusätzlich vier Li···F Kontakte mit drei verschiedenen $B(C_6F_5)_4]^-$Ionen findet, was vergleichbar mit dem bekannten $[Li(Benzol)][B(C_6F_5)_4] \cdot Benzol$ ist.

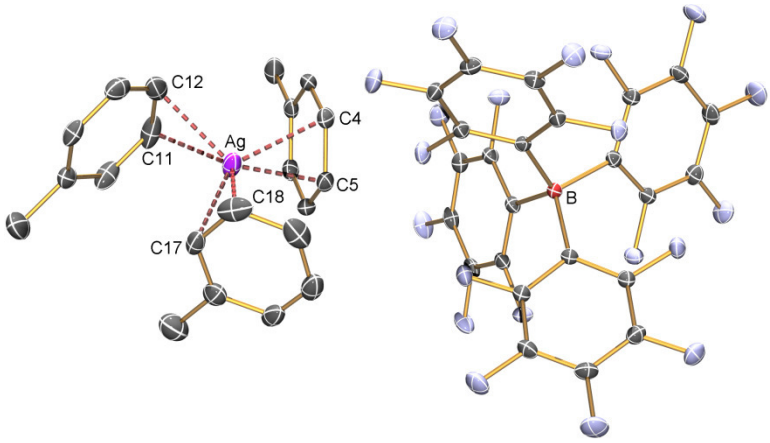

Abbildung 5. Asymmetrische Einheit der Molekülstruktur von $[Ag(Toluol)_3][B(C_6F_5)_4]$.

Im Falle des $[Ag(Toluol)_3][B(C_6F_5)_4]$ ist das Silberkation durch jeweils zwei Kohlenstoffatome der drei Toluolmoleküle in einer η^2-Koordination komplexiert, was zur

Koordinationszahl sechs führt. Im Gegensatz zu Komplexen wie z.B. $[Ag(Toluol)_2\{Al(OR^F)_4\}]$ (R^F = $CH_3(CF_3)_2$) konnten hierbei jedoch keine kurzen, stabilisierenden Silber···Anion-Wechselwirkungen gefunden werden. Die Koordinationsumgebung des Silbers ist nicht exakt trigonal planar, sondern leicht verzerrt. Diese ungewöhnliche Dreifachkoordination des Silbers wurde erst kürzlich in der Literatur beschrieben. So konnten Krossing *et al.* ein $[Ag(\eta^2\text{-}C_2H_4)_3]^+$-Ion isolieren, während Kitagawa, Komatsu *et al.* die Darstellung von $[Ag(Benzol)_3][B(C_6F_5)_4]$ berichteten.[19,20]

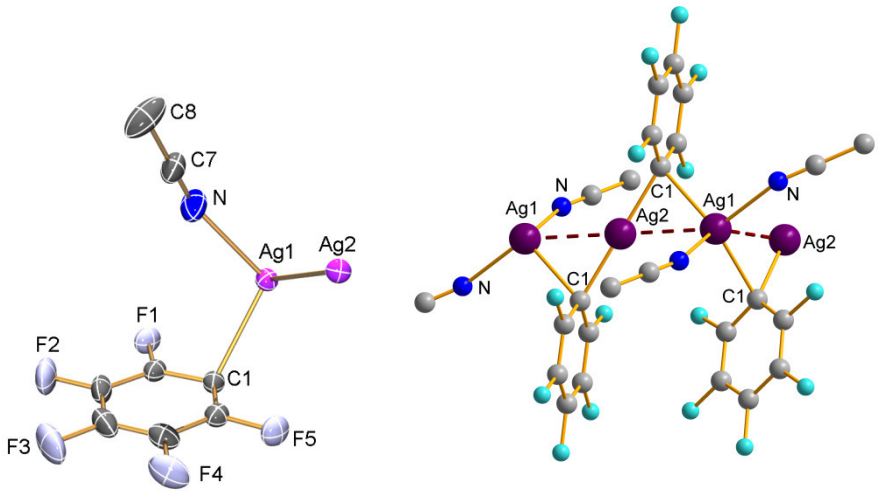

Abbildung 6. Molekülstruktur von $Ag(C_6F_5)(CH_3CN)$, asymmetrische Einheit (links), Ausschnitt aus Packungsdiagramm (rechts).

In $Ag(C_6F_5)(CH_3CN)$ besteht die asymmetrische Einheit aus zwei kristallografisch verschiedenen Silberionen, Ag1 und Ag2, mit Ag2 in einer linearen Koordination durch zwei Kohlenstoffatome zweier verbrückender Phenylgruppen, während durch koordinierendes CH_3CN an Ag1 für dieses eine verzerrt tetraedrische Koordination resultiert. Durch die C_6F_5-Brücken kommt es zur Ausbildung unendlicher Ketten in der Einheitszelle.

4.3 Blaues Imino(pentafluorphenyl)phosphan und seine Eisencarbonyl-Adduktkomplexe

Marcus Kuprat, Mathias Lehmann, Axel Schulz, Alexander Villinger

Die direkte Umsetzung von *N*-(2,4,6-Tri-*tert*-butylphenyl)imino(chloro)phosphan, Mes*NPCl mit AgC_6F_5 in CH_2Cl_2 führte zur Bildung von AgCl und einer in Lösung vorliegenden tiefblauen Komponente, welche sich äußerst instabil gegenüber Luft, Feuchtigkeit und Vakuum verhält und sich aufgrund der großen Löslichkeit weder aus polaren, noch aus unpolaren Lösemitteln kristallisieren ließ. Das vermutete Vorliegen von Mes*NPC_6F_5 lässt sich so mit Hilfe analytischen Methoden nicht zweifelsfrei klären, allerdings weist die Verbindung einen charakteristischen n→π* Elektronenübergang bei 592 nm auf, der auf der Basis von TD-B3LYP-Rechnungen dem *trans*-Monomer zugeordnet werden konnte. Rechnungen auf dem B3LYP/6-31G(d,p)-Level ergaben, dass nur eine äußerst geringe Energiedifferenz von ΔG^{298} = 0.8 kcal/mol zwischen dem *cis*- und *trans*-Isomer vorliegt.

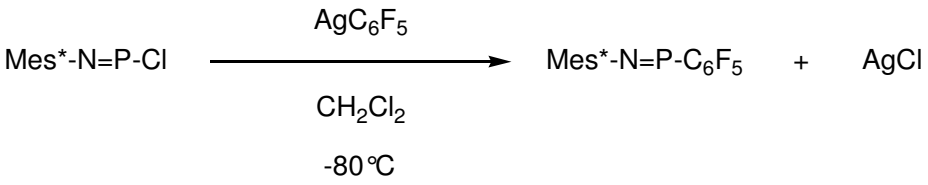

Schema 13. Umsetzung von Mes*NPCl mit AgC_6F_5.

Um einen tieferen Einblick in den Cl/C_6F_5-Austausch zu bekommen, wurde LiC_6F_5 in Ether als $C_6F_5^-$-Quelle herangezogen, und mit Mes*NPCl umgesetzt. Überraschenderweise entstand hierbei neben LiCl allerdings keine blaue, sondern eine kräftig orange Komponente in Lösung, welche sich aus *n*-Hexan sehr gut kristallisieren ließ. Die Einkristallstrukturanalyse ergab, dass es sich hierbei um ein Dimer von Mes*NPC_6F_5 handelte, allerdings nicht in Form einer viergliedrigen PN-*cyclo*-Verbindung, sondern in Gestalt einer PNPN-Kette.

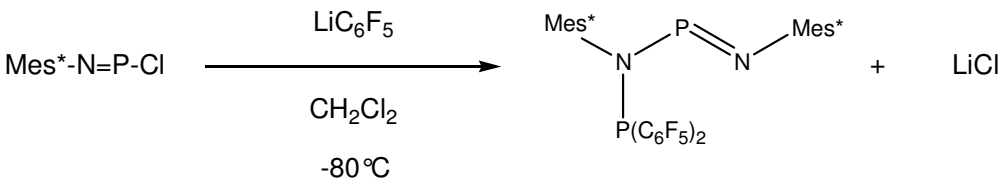

Schema 14. Umsetzung von Mes*NPCl mit LiC_6F_5.

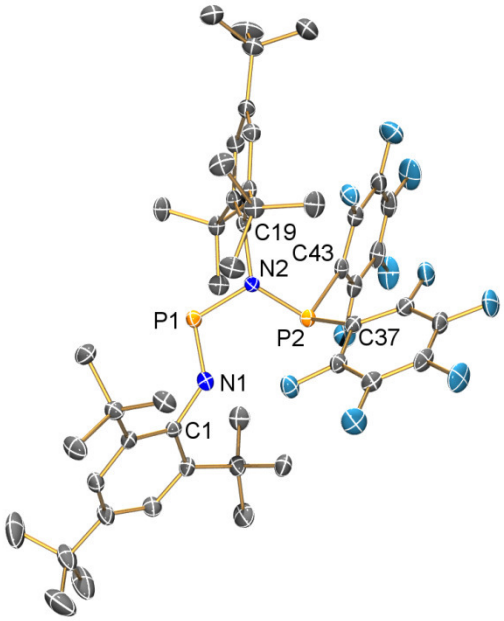

Abbildung 7. Molekülstruktur von $P(C_6F_5)_2N(Mes^*)PN(Mes^*)$.

Die orange kristalline Verbindung erweist sich bei Raumtemperatur für einige Minuten als luftstabil. Die N-P-N-P-Einheit weist eine *trans*-Konformation an der PN-Doppelbindung, sowie eine annähernd planare Anordnung aller vier Atome auf.

Im Weiteren wurde $[DippNPCl]_2$ (Dipp = 2,5-Diisopropylphenyl) mit AgC_6F_5 umgesetzt, das anders als Mes*NPCl als Dimer vorliegt. Neben AgCl entstand hierbei das zu erwartende dimere $[DippNPC_6F_5]_2$, dessen Kristalle allerdings von hellgelber Farbe sind. Die Umsetzung mit LiC_6F_5 führte unselektiv zu einem Reaktionsgemisch, in welchem unter anderem $P(C_6F_5)_3$ enthalten war.

Um die zuvor erhaltene blaue Verbindung zweifelsfrei zu identifizieren und Kristalle zu erhalten, wurde die Komplexierung mit Hilfe von $Fe_2(CO)_9$ untersucht. Die Einkristallstrukturanalyse der resultierenden roten Kristalle ergab eine Struktur, in welcher das Fe-Ion an vier Carbonyl-Liganden sowie an das Phosphor-Atom einer $Mes^*NPC_6F_5$-Einheit gebunden ist.

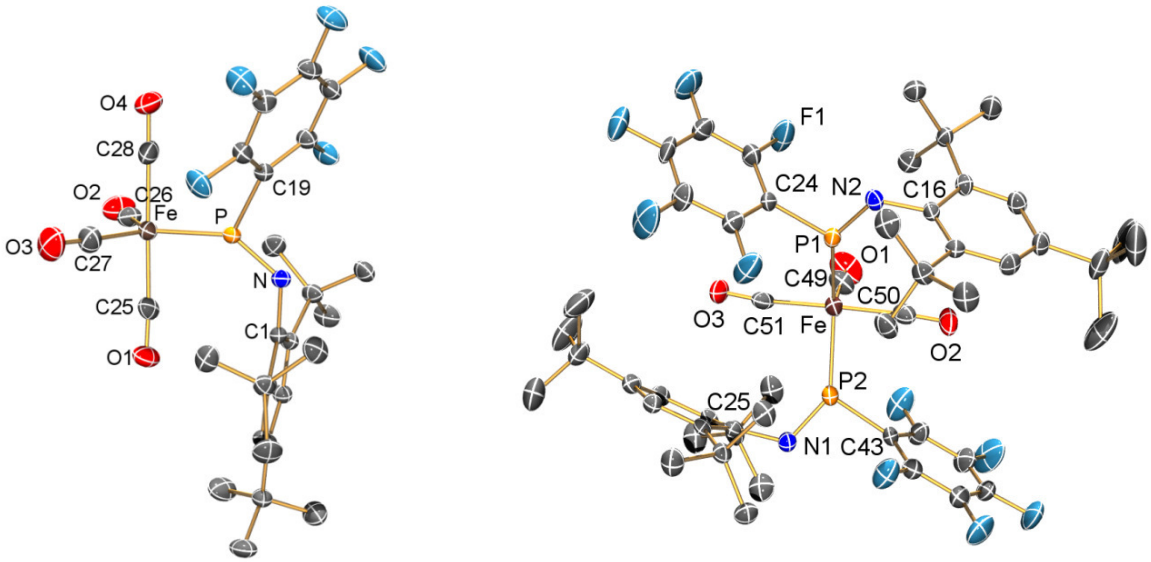

Abbildung 8. Molekülstrukturen von $(Mes^*NPC_6F_5)Fe(CO)_4$ und $(Mes^*NPC_6F_5)_2Fe(CO)_3$.

In dem Tetracarbonyleisenkomplex ist das Fe-Atom in einer trigonal bipyramidalen Anordnung von den CO-Liganden und dem *trans*-$Mes^*NPC_6F_5$ Liganden umgeben. Aufgrund von Van-der-Waals-Wechselwirkungen sind im Kristall die Eisenkomplexe in einer Art gezackter Ketten angeordnet, die durch alternierende polare $Fe(CO)_4$-Einheiten und nicht-polare Mes*-Einheiten geformt werden.

Es konnte gezeigt werden, dass sich je nach Reaktionsführung und Lösemittel eine Mischung von Trieisendodekacarbonyl $Fe_3(CO)_{12}$ und $[Mes^*NPC_6F_5]_2 \cdot Fe(CO)_3$ bildete, wenn $Fe_2(CO)_9$ nicht im Überschuss zugegeben wurde. Der Tricarbonyleisenkomplex weist hierbei ähnliche strukturelle Eigenschaften auf. Das Fe liegt ebenfalls zentriert in einer trigonal bipyramidalen Koordinationsumgebung, wobei die beiden $Mes^*NPC_6F_5$-Liganden jeweils eine Position in der trigonalen Ebene einnehmen und gegeneinander versetzt ausgerichtet sind. Auch hier nehmen die $Mes^*NPC_6F_5$-Liganden eine *trans*-Konfiguration ein.

5. Originalpublikationen

Dieses Kapitel beinhaltet die Originalpublikationen bzw. Manuskripte zu den in Kapitel 4 vorgestellten Arbeiten.

5.1 Silver tetrakis(hexafluoroisopropoxy)aluminate as hexafluoroisopropyl transfer reagent for the chlorine/hexafluoroisopropyl exchange in imino phosphanes

Marcus Kuprat, René Kuzora, Mathias Lehmann, Axel Schulz, Alexander Villinger, Ronald Wustrack.

Journal of Organometallic Chemistry **2010**, *695*, 1006-1011.

Journal of Organometallic Chemistry 695 (2010) 1006–1011

Contents lists available at ScienceDirect

Journal of Organometallic Chemistry

journal homepage: www.elsevier.com/locate/jorganchem

Silver tetrakis(hexafluoroisopropoxy)aluminate as hexafluoroisopropyl transfer reagent for the chlorine/hexafluoroisopropyl exchange in imino phosphanes

Marcus Kuprat [a], René Kuzora [a], Mathias Lehmann [a], Axel Schulz [a,b,*], Alexander Villinger [a], Ronald Wustrack [a]

[a] Institut für Chemie Abt. Anorganische Chemie, Albert-Einstein-Straße 3a, 18059 Rostock, Germany
[b] Leibniz-Institut für Katalyse e.V. an der Universität Rostock, Albert-Einstein-Str. 29a, 18059 Rostock, Germany

ARTICLE INFO

Article history:
Received 30 September 2009
Received in revised form 12 November 2009
Accepted 13 November 2009
Available online 18 November 2009

On the occasion of the 75th birthday of Dr. C.N.R. Rao.

Keywords:
Hypersilyl
Lewis acid
PN chemistry
Structure
Weakly coordinating anions

ABSTRACT

Treating 1,3-dichloro-2,4-bis[tris(trimethylsilyl)silyl]-*cyclo*-diphosphadiazane, $[HypNPCl]_2$ ($(Me_3Si)_3Si$ = Hyp), or *N*-(2,4,6-tri-*tert*-butylphenyl)imino(chloro)phosphane, Mes*–N=P–Cl (Mes* = 2,4,6-tri-*tert*-butylphenyl), with $Ag[Al(OCH(CF_3)_2)_4]$ leads to the abstraction of $[OCH(CF_3)_2]^-$ from the counter ion $[Al(OCH(CF_3)_2)_4]^-$ in a formal Lewis acid/Lewis base reaction. The final products $Hyp_2N_2P_2(Cl)(OCH(CF_3)_2)$, Mes*–N=P–$OCH(CF_3)_2$ and the dimeric Lewis acid $[Al(OCH(CF_3)_2)_3]_2$ have been characterized by means of X-ray analysis.

© 2009 Elsevier B.V. All rights reserved.

1. Introduction

In the last two decades 1,3-dichloro-*cyclo*-diphosphadiazanes $[RNPCl]_2$ with several groups R have been intensively studied, as they are used as potential starting materials for e.g., ring-opening and transformation reactions, oligomerization and polymerization [1–4] or the preparation of macrocycles, polymers, main-group complexes and the generation of cyclic binary PN cations [5,6]. Only little is known of 1-chloro-*cyclo*-diphosphadiazenium salts of the type $[R_2N_2P_2Cl]^+$ [6a]. These cyclic phosphorus–nitrogen cations have been synthesized by chloride abstraction from kinetically stabilized 1,3-dichloro-*cyclo*-diphosphadiazanes. The monochlorodiphosphadiazenium cation ($[R_2N_2P_2Cl]^+$, R = ^{t}Bu) was first observed by Cowley et al. [7] in the reaction of the corresponding *cyclo*-diphosphadiazane with $AlCl_3$. Burford et al. [8] assumed 1-halo-2,4-di(aryl)-*cyclo*-1,3-dipnicta-2,4-diazenium cations as reactive intermediate species in the reaction of $[RNPX]_2$ (R = 2,6-dimethylphenyl, 2,6-diisopropylphenyl; X = Cl, Br) with GaX_3, which led to trimeric species $[RNPX]_3$ via GaX_3 induced heterocycle expansion [9]. The supermesityl substituted iminophosphenium cation as tetrachloridoaluminate salt [Mes*–N≡P][$AlCl_4$] was first prepared by Niecke et al. by means of chloride abstraction from Mes*–N=P–Cl with $AlCl_3$ as Lewis acid [15].

Recent work in our group [10] has focused on a new strategy for the generation and stabilization of cyclic and acyclic P(III)–N cations utilizing bulky groups such as the hypersilyl ($(Me_3Si)_3Si$ = hyp) [11,12] and the supermesityl group (Mes* = 2,4,6-tri-*tert*-butylphenyl). For this reason we have studied a number of differently substituted 1,3-dichloro-*cyclo*-diphosphadiazanes $[RNPCl]_2$. Moreover, since Michaelis and Schroeter [13] discovered the first example of a *cyclo*-diphosphadiazane, it is known, that there is a formal monomer–dimer equilibrium depending on the organic group R: 2 RNPCl ⇆ $[RNPCl]_2$. Burford et al. assumed that dependent upon steric strain in derivatives of $[RPNR]_2$ the dimer can be destabilized with respect to the monomer [8,9,14]. The intriguing equilibrium is best illustrated by the fact, that Mes*–N=P–Cl is observed as an iminophosphane monomer in the solid state [15], while slightly smaller substituents such as 2,6-diisopropylphenyl or the *m*-terphenyl allow dimerization [6,14].

To be able to isolate reactive PN^+ ions two things need to be considered: (i) A bulky group should be used to kinetically protect the cation as well as (ii) a weakly coordinating anion, which should be chemically robust [16]. Here we report on attempts to isolate [Mes*–N≡P]$^+$ and $[Hyp_2N_2P_2Cl]^+$ ions as tetrakis(hexafluoroisopropoxy)aluminate salts, which led unintentionally to the

* Corresponding author. Address: Institut für Chemie Abt. Anorganische Chemie, Albert-Einstein-Straße 3a, 18059 Rostock, Germany. Fax: +49 381 4986382.
E-mail address: axel.schulz@uni-rostock.de (A. Schulz).
URL: http://www.chemie.uni-rostock.de/ac/schulz (A. Schulz).

0022-328X/$ - see front matter © 2009 Elsevier B.V. All rights reserved.
doi:10.1016/j.jorganchem.2009.11.014

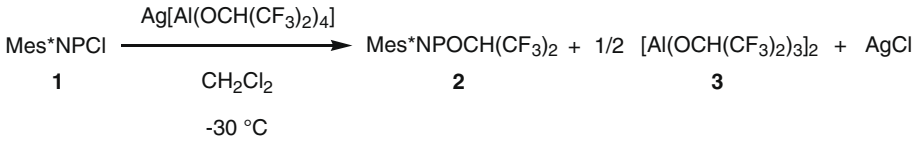

Scheme 1. Synthesis of *N*-(2,4,6-tri-*tert*-butylphenyl)imino-(1,1,1,3,3,3-hexafluoro-2-propoxy)phosphane (**2**).

discovery of a new hexafluoroisopropyl transfer reaction. The decomposition of the aluminate anion $[Al(OCH(CF_3)_2)_4]^-$ which is accompanied by the formation of the free acid $[Al(OCH(CF_3)_2)_3]_2$ clearly demonstrates the reactivity of weakly coordinating anions and illustrates the limitations of the use of such weakly coordinating anions in the presence of highly electrophilic cations.

2. Results and discussion

2.1. Reaction of Mes*–N=P–Cl with Ag[Al(OCH(CF3)2)4]

The stabilization of highly electrophilic cations such as $[R–NP]^+$ is commonly achieved by replacing the small and strongly coordinating counter ion by a large and weakly coordinating anion (wca) such as tetrakis(hexafluoroisopropoxy)aluminate [16]. The easiest way to introduce wca's is to treat R–N=P–Cl with a wca containing silver salt (see Scheme 1).

Supermesityl iminochlorophosphane, Mes*–N=P–Cl (**1**), which does not dimerize to give a 1,3-dichloro-*cyclo*-diphosphadiazane, is easily prepared in the reaction of supermesityl amine Mes*–NH_2 with PCl_3 followed by a basic work-up [15,17]. Addition of silver tetrakis(1,1,1,3,3,3-hexafluoro-2-propoxy)aluminate, Ag[Al(OCH(CF3)2)4], to a solution of Mes*–N=P–Cl in CH_2Cl_2 should result in the formation of a solvated $[Mes^*–N{\equiv}P]^+$ ion with $[Al(OCH(CF_3)_2)_4]^-$ as counter ion as well as in the precipitation of AgCl. However, instead we observed the formation of *N*-(2,4,6-tri-*tert*-butylphenyl)imino-(1,1,1,3,3,3-hexafluoro-2-propoxy)phosphane, Mes*–N=P–$OCH(CF_3)_2$ (**2**) and bis[tris(1,1,1,3,3,3-hexafluoro-2-propoxy)aluminium], $[Al(OCH(CF_3)_2)_3]_2$ (**3**), respectively. Obviously, the driving force of the formation of **2** is the instability of the anion $[Al(OCH(CF_3)_2)_4]^-$ towards strong electrophilic ions such as $[Mes^*–N{\equiv}P]^+$. Thus $[Mes^*–N{\equiv}P]^+$ seems to be the stronger Lewis acid compared to $[Al(OCH(CF_3)_2)_3]_2$ resulting in the abstraction of $[OCH(CF_3)_2]^-$ from the $[Al(OCH(CF_3)_2)_4]^-$ ion finally yielding **2** and **3**. The whole process can formally be regarded as a Lewis acid/Lewis base reaction, which is triggered by the precipitation of AgCl and the formation of the free electronically unstabilized $[Mes^*–N{\equiv}P]^+$ ion representing the stronger Lewis acid. Krossing et al. have already shown in a series of papers [18] that wca's such as $[Al(OR^F)_4]^-$ decompose in the presence of very electrophile cations such as $P_2X_5^+$ (X = Br, I) or Ag^+/PCl_3 or $SiCl_4$ mixtures leading to fluoride bridged $[(R^FO)_3Al–F–Al(OR^F)_3]^-$ anions [18b,c]. They already mentioned the $[OR^F]^-$ abstraction, triggered by the action of oxophilic cations such as $P_2Cl_5^+$, results in the intermediate formation of $R^FO–PCl_2$ [18d], while the generated free Lewis acid $Al(OR^F)_3$ then abstracts a F^- ion from $R^FO–PCl_2$ finally forming the bridged anion $[(R^FO)_3Al–F–Al(OR^F)_3]^-$. In case of the reaction of Mes*–N=P–Cl with Ag[Al(OCH(CF3)2)4], it was possible to isolate the free acid and to stop the whole decomposition process prior to F^- abstraction and formation of the bridged ion.

In a next series of experiments it was interesting to see if **2** can be generated in a direct synthesis. The attempted synthesis of acid **3** from $AlMe_3$ and $HOCH(CF_3)_2$ has already been reported by Krossing et al. but was not successful [19]. Mes*–N=P–$OCH(CF_3)_2$ (**2**) is readily generated in good yields (95%) upon treatment of $HOCH(CF_3)_2$ with *n*-BuLi (intermediate formation of $Li[OCH(CF_3)_2]$) and addition of Mes*–N=P–Cl in diethyl ether at 0 °C as illustrated in Scheme 2.

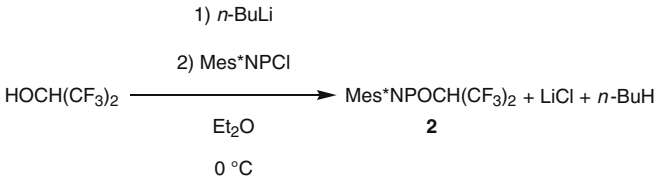

Scheme 2. Direct synthesis of *N*-(2,4,6-tri-*tert*-butylphenyl)imino-(1,1,1,3,3,3-hexafluoro-2-propoxy)-phosphane (**2**).

2.2. Reaction of [HypNPCl]2 with Ag[Al(OCH(CF3)2)4]

The dimer $[HypNPCl]_2$ is stable in CH_2Cl_2 at ambient temperature for several days as shown by ^{31}P NMR studies [$\delta(^{31}P)$ = 257.0 ppm] and does not dissociate into monomeric Hyp–N=P–Cl [6b]. However, after adding $Ag[Al(OCH(CF_3)_2)_4]$ the NMR spectra showed rapid, quantitative formation of a new phosphorus species within 10 min at ambient temperatures. Furthermore, the colourless solution of the beginning turned dark red. NMR spectroscopic investigations revealed the formation of the 1-chloro-2,4-bis[tris(trimethylsilyl)silyl]-*cyclo*-diphosphadiazenium ion $[Hyp_2N_2P_2Cl]^+$, which is stable in solution for more than 12 h as shown by NMR spectroscopy. Removal of solvent *in vacuo* yields a red oil, in which the slow formation of white crystals was observed. X-ray studies revealed the formation of 1-chloro-3-(1,1,1,3,3,3-hexafluoro-2-propoxy)-2,4-bis[tris(trimethylsilyl)silyl]-*cyclo*-diphosphadiazane, $[HypNPX]_2$ (X = Cl and $OCH(CF_3)_2$) (**4**), and again the dimer of the free Lewis acid **3** (Scheme 3). It can be assumed, that upon removal of CH_2Cl_2, the reactive PN^+ cation approaches

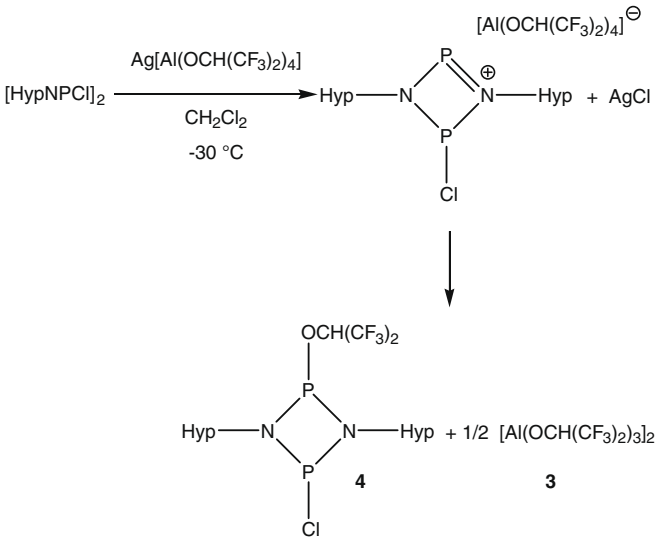

Scheme 3. Synthesis of 1-chloro-3-(1,1,1,3,3,3-hexafluoro-2-propoxy)phosphane-2,4-bis[tris(trimethylsilyl)silyl]-*cyclo*-diphosphadiazane (**4**).

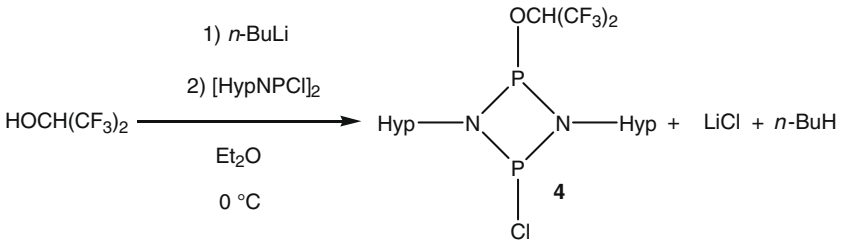

Scheme 4. Attempted direct synthesis of 1-chloro-3-(1,1,1,3,3,3-hexafluoro-2-propoxy)phosphane-2,4-bis[tris(trimethylsilyl)silyl]-*cyclo*-diphosphadiazane (**4**).

the $[Al(OCH(CF_3)_2)_4]^-$ ion finally undergoing a similar Lewis acid/Lewis base reaction as discussed before.

Again, several attempts were made to generate **4** in a direct synthetic route. Firstly, a solution of $Li[OCH(CF_3)_2]$ was treated with a solution of $[HypNPCl]_2$ in diethyl ether (Scheme 4). No reaction occurred, which nicely demonstrates the kinetic protection of the two hypersilyl groups in the dimer in contrast to the insufficient protection of the Mes* group in monomeric Mes*–N=P–Cl. Secondly, the reactivity of $Li[OCH(CF_3)_2]$ was increased by addition of ethylenediamine, which however resulted in an ethylenediamine bridged *cyclo*-diphosphadiazane (see supporting information).

Separation of **3** and **4** obtained from the decomposition of the red oil (see above) is possible when $Li[OCH(CF_3)_2]$ was directly added to a mixture of **3** and **4** in *n*-hexane. A rapid reaction was observed leading to the precipitation of $Li[Al(OCH(CF_3)_2)_4]$ and unreacted **3** which remains dissolved in *n*-hexane.

Compounds **2, 3** and **4** are thermally stable, moisture sensitive but stable under argon atmosphere over a long period as solid and in polar solvents at ambient temperature. Compound **2** is easily prepared in bulk and stable for a long time when stored in a sealed tube.

2.3. X-ray crystallography

The solid-state structures of compounds **1**, **2**, **3** and **4** are shown in Figs. 1–4. Crystallographic details are given in Table 1. More details are found in the supporting information file. X-ray quality crystals of Mes*–N=P–Cl (**1**), Mes*–N=P–$OCH(CF_3)_2$ (**2**), $[Al(OCH(CF_3)_2)_3]_2$ (**3**), and $Hyp_2N_2P_2(Cl)OCH(CF_3)_2$ (**4**) were selected in Fomblin YR-1800 perfluoroether (Alfa Aesar) at ambient temperatures. All samples were cooled to 173(2) K during measurement. It should be mentioned, that a solid-state structure of compound **1** has been reported [15], but in the present structure redetermination, a different modification was found with significantly different structural data (see below).

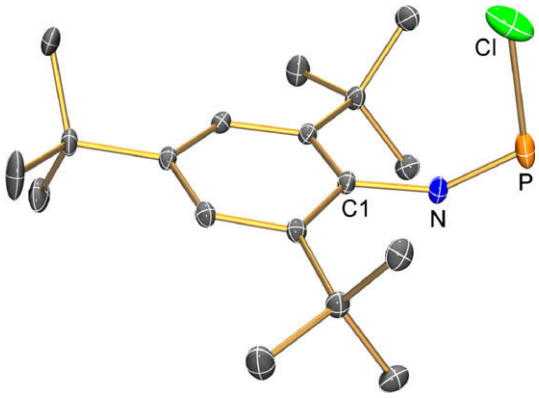

Fig. 1. ORTEP drawing of the molecular structure of **1** in the crystal. Thermal ellipsoids with 50% probability at 173 K. Hydrogen atoms are omitted for clarity. Selected bond lengths in Å, angles in °: N–C1 1.413(3), N–P 1.506(2), P–Cl 2.118(1); C1–N–P 146.7(2), N–P–Cl 111.30(9), C1–N–P–Cl 0.3(3).

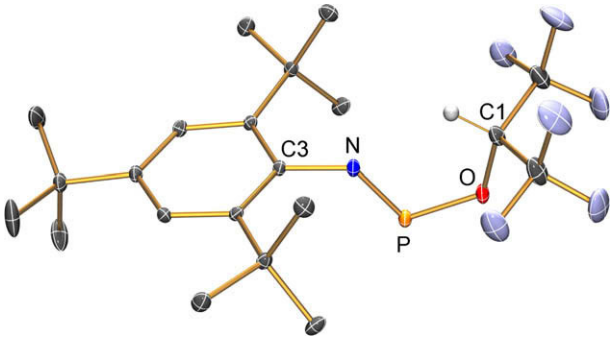

Fig. 2. ORTEP drawing of the molecular structure of **2** in the crystal. Thermal ellipsoids with 50% probability at 173 K. Hydrogen atoms of the *tert*-Bu groups are omitted for clarity. Selected bond lengths in Å, angles in °: P–N 1.540(2), P–O 1.642(2), N–C3 1.429(2), O–C1 1.405(3); N–P–O 105.17(9), C3–N–P 127.0(1), C1–O–P 125.1(1).

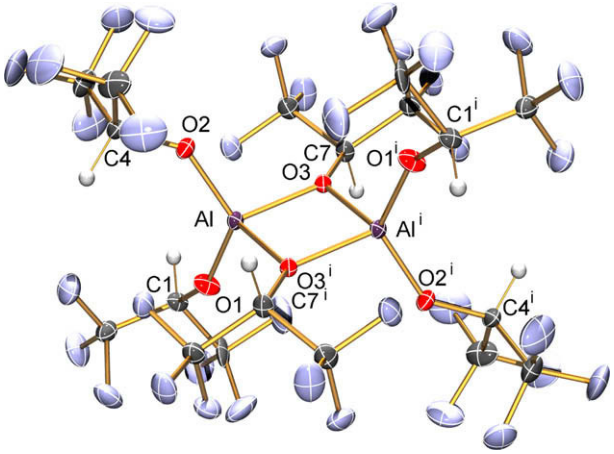

Fig. 3. ORTEP drawing of the molecular structure of **3** in the crystal. Thermal ellipsoids with 50% probability at 173 K. Selected bond lengths in Å, angles in °: Al–O2 1.666(2), Al–O1 1.685(2), Al–$O3^i$ 1.843(2), Al–O3 1.854(2), Al–Al^i 2.818(2), O1–C1 1.371(3); O2–Al–O1 124.9(1), O2–Al–$O3^i$ 114.5(1), O1–Al–$O3^i$ 108.11(9), O2–Al–O3 109.14(9), O1–Al–O3 110.77(8), $O3^i$–Al–O3 80.68(8), O2–Al–Al^i 119.12(9), O1–Al–Al^i 115.89(7), C1–O1–Al 142.1(2).

Mes–N=P–Cl* (**1**) crystallizes in the monoclinic space group $P2_1/n$ with four formula units per cell. One of the *t*-Bu groups is found to be disordered and was split in two parts. The structure consists of Mes*–N=P–Cl (Fig. 1) molecules arranged in parallel layers allowing π stacking. Mes*–N=P–Cl adopts a *cis* configuration with respect to the position of the C1-atom and chlorine (<(C1–N–P–Cl) = 0.3(3)°). A fairly short P–N bond lengths of N–P 1.506(2) Å is

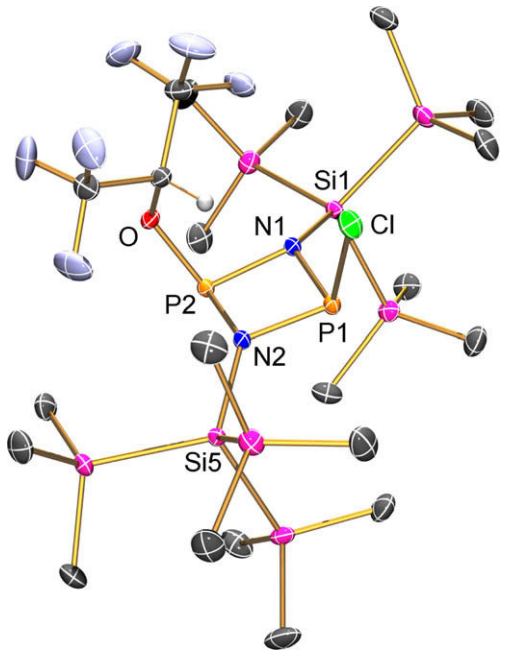

Fig. 4. ORTEP drawing of the molecular structure of **4** in the crystal. Thermal ellipsoids with 50% probability at 173 K. Hydrogen atoms of the Me_3Si groups are omitted for clarity. Selected bond lengths in Å, angles in °: P1–N1 1.697(2), P1–N2 1.711(1), P1–Cl1 2.139(1), P1–P2 2.521(1), P2–O1 1.658(1), P2–N1 1.721(1), P2–N2 1.725(2), N1–Si1 1.801(2), N2–Si5 1.806(1); O1–C1 1.409(2), N1–P1–N2 85.50(7), N1–P1–Cl1 104.58(5), N2–P1–Cl1 102.46(5), N1–P1–P2 42.83(4), N2–P1–P2 43.01(5), Cl1–P1–P2 112.80(4), O1–P2–N1 106.05(7), O1–P2–N2 104.91(6), N1–P2–N2 84.36(6), O1–P2–P1 115.26(5), N1–P2–P1 42.11(5), N2–P2–P1 42.58(4), P1–N1–P2 95.07(7), P1–N1–Si1 127.88(8), P2–N1–Si1 127.14(7), P1–N2–P2 94.41(7), P1–N2–Si5 125.44(7), P2–N2–Si5 132.49(7), C1–O1–P2 125.82(9).

observed, which indicates a bond order larger than two due to hyperconjugation [20] (cf. $\sum r_{cov}$(N–P) = 1.8, $\sum r_{cov}$(N=P) = 1.6 Å) [21]. As expected, a large C1–N–P angle of 146.7(2)° is found for the imino nitrogen atom, while the N–P–Cl angle amounts to 111.30(9)°. Interestingly, Niecke et al. published a modification of **1** which crystallized in the space group *Pnma* and shows significantly different structural data (cf. *d*(P–N) 1.495(4) Å, <(P–N–C1) 154.8(4)°, and N–P–Cl 112.4(2)°, nicely displaying the influence and magnitude of lattice effects in the solid state [15].

*Mes**–N=P–$OCH(CF_3)_2$ (***2***) crystallizes in the monoclinic space group $P2_1/m$ with two formula units per cell. One of the *t*-Bu groups is found to be disordered and was split in two parts. As depicted in Fig. 2, the structure consists of Mes*–N=P–$OCH(CF_3)_2$ molecules also arranged in parallel layers in the unit cell. Mes*–N=P–$OCH(CF_3)_2$ adopts a *cis* configuration with respect to the position of the C3-atom and the oxygen atom (<(O–P–N–C3) = 180.0°), while a *trans* arrangement is found along the C1–O–P–N moiety (0.0 °C). Compared to **1** the P–N distance is slightly increased with 1.540(2) Å (cf. **1**: 1.506(2) Å) and the P–O bond length of 1.642(2) Å is slightly shorter than a typical P–O single bond ($\sum r_{cov}$(O–P) = 1.76 Å) [21]. A short non-classical intramolecular C–H···N hydrogen bond is found with a donor–acceptor distance of 2.872(3) Å.

[Al(OCH($CF_3)_2)_3]_2$ (***3***) crystallizes in the monoclinic space group $P2_1/n$ with two formula units per cell. One of the $OCH(CF_3)_2$ groups in **3** is found to be disordered and was split in two parts. The occupancy of each part was refined freely (0.672(3)/0.328(3)) and the group with larger occupancy is displayed in Fig. 3. As depicted in Fig. 3, the Al_2O_2 ring is planar, but slightly distorted with two longer Al–O bond lengths (*d*(Al–O3) = 1.854(2) Å) and two slightly shorter Al–O bond lengths (*d*(Al–$O3^i$) = 1.843(2) Å; cf. $\sum r_{cov}$(O–Al) = 1.81 Å, Fig. 3). These Al–O bond lengths are again substantially longer than those of the exocyclic Al–O bonds (*d*(Al–O2) = 1.666(2), *d*(Al–O1) = 1.685(2) Å). The Al···Al distance is rather short with 2.818(2) Å and compares to the Al···Al distance in aluminium metal (d_{metal}(Al–Al) = 2.864 Å) [21].

$Hyp_2N_2P_2$(Cl)OCH($CF_3)_2$ (***4***) crystallizes in the triclinic space group $P\bar{1}$ with four formula units per cell. The crystallographic asymmetric unit contains two crystallographically independent molecules, which are arranged in the unit cell in such a manner that stacked chains of alternating polar "NPCl-units" and non-polar "hyp-units" are formed as already observed for Hyp–N(H)–PCl_2

Table 1
Crystallographic details of **1**–**4**.

	1	**2**	**3**	**4**
Chemcal formula	$C_{18}H_{29}ClNP$	$C_{21}H_{30}F_6NOP$	$C_{18}H_6Al_2F_{36}O_6$	$C_{21}H_{55}ClF_6N_2OP_2Si_8$
Formula weight (g mol^{-1})	325.84	457.43	1056.19	787.78
Colour	Red	Orange	Colourless	Colourless
Crystal system	Monoclinic	Monoclinic	Monoclinic	Triclinic
Space group	$P2_1/n$	$P2_1/m$	$P2_1/n$	$P\bar{1}$
a (Å)	5.8515(12)	5.930(2)	10.394(8)	14.748(7)
b (Å)	33.661(7)	14.828(6)	10.206(9)	16.885(9)
c (Å)	9.6883(19)	13.051(5)	16.211(15)	18.920(9)
α (°)	90.00	90.00	90.00	86.82(2)
β (°)	98.72(3)	91.064(11)	91.439(18)	69.247(16)
γ (°)	90.00	90.00	90.00	71.949(10)
V (Å^3)	1886.2(7)	1147.4(7)	1719(3)	4181(4)
Z	4	2	2	4
$\rho_{calc.}$ (g cm^{-3})	1.147	1.324	2.040	1.251
μ (mm^{-1})	0.283	0.180	0.316	0.443
$\lambda_{MoK\alpha}$ (Å)	0.71073	0.71073	0.71073	0.71073
T (K)	173(2)	173(2)	173(2)	173(2)
Measured reflections	16 368	11 716	14 477	98 586
Independent reflections	4322	3128	3922	24 279
Reflections with $I > 2\sigma(I)$	3157	2329	2490	18 042
$R_{int.}$	0.0412	0.0355	0.0353	0.0411
F(0 0 0)	704	480	1024	1664
R_1 ($R[F^2 > 2\sigma(F^2)]$)	0.0590	0.0470	0.0504	0.0397
wR_2 (F^2)	0.1346	0.1310	0.1406	0.1033
Goodness-of-fit (GOF)	1.071	1.045	1.020	1.047
Parameters	212	160	344	775
CCDC #	753943	753944	753946	753945

[6b]. Only very weak intermolecular contacts are observed. As depicted in Fig. 4, the P_2N_2 ring is almost planar (deviation from planarity: <(N–P1–N–P2) = 7.7°), but slightly distorted with two longer P–N bond lengths (*d*(P2–N1) = 1.721(1), *d*(P2–N2) 1.725(2) Å) and two slightly shorter P–N bond lengths (*d*(P1–N1) = 1.697(2), *d*(P1–N2) = 1.711(1). These P–N bond lengths are again substantially shorter than the sum of the covalent radii (see above). The P–O bond length is rather short with 1.658(1) Å, and the P–Cl bond length amounts to 2.139(1) Å. A difference of *ca.* 10° is found between the N–P–N and P–N–P angles (85.5/84.4° vs. 95.1/94.4°), in accord with that found e.g. in $[(C_6H_5)NPCl]_2$ (80.1° vs. 99.7°) [3]. A short non-classical intramolecular C–H···Cl hydrogen bond is found for both molecules in the asymmetric unit with donor–acceptor distances of 3.482(2) and 3.555(3) Å.

3. Conclusion

In conclusion, we present here highly reactive hypersilylated *cyclo*-diphosphadiazenium $[Hyp_2N_2P_2Cl]^+$ and supermesityl substituted iminophosphenium $[Mes^*–N{\equiv}P]^+$ cations, which are capable of abstracting $[OCH(CF_3)_2]^-$ from the $[Al(OCH(CF_3)_2)_4]^-$ counter ion in formal Lewis acid/Lewis base reactions. By this approach the hitherto unknown $Mes^*–N{=}P–OCH(CF_3)_2$ and $Hyp_2N_2P_2(Cl)OCH(CF_3)_2$ as well as the dimer of the free Lewis acid $[Al(OCH(CF_3)_2)_3]_2$ have been obtained and fully characterized.

4. Experimental details

4.1. General Information

All manipulations were carried out under oxygen- and moisture-free conditions in an argon atmosphere using standard Schlenk or dry box techniques.

Dichloromethane was dried over P_4O_{10} and freshly distilled prior to use. Diethyl ether was dried over Na/benzophenone, *n*-hexane was dried over Na/benzophenone/tetraglyme and freshly distilled prior to use. 1,1,1,3,3,3-hexafluoro-2-propanole (99%, DuPont) was distilled prior to use. *N*-BuLi (2.5 M, Acros) was used as received. Silver tetrakis(1,1,1,3,3,3-hexafluoro-2-propoxy)aluminate $Ag[Al(OCH(CF_3)_2)_4]$, *N*-(2,4,6-tri-*tert*-butylphenyl)imino-(chloro)phosphane Mes^*NPCl (**1**), and 1,2-dichloro-2,4-bis [tris(trimethylsilyl)silyl]-*cyclo*-diphosphadiazane $[HypNPCl]_2$, were prepared as previously reported [6b,15,17,19].

NMR: ^{29}Si INEPT, $^{19}F\{^1H\}$, $^{13}C\{^1H\}$, ^{13}C DEPT, and ^1H NMR spectra were obtained on a Bruker AVANCE 250, or 300 spectrometer and were referenced internally to the deuterated solvent (^{13}C, CD_2Cl_2: $\delta_{reference}$ = 54 ppm) or to protic impurities in the deuterated solvent (^1H, $CDHCl_2$: $\delta_{reference}$ = 5.31 ppm). CD_2Cl_2 was dried over P_4O_{10} and freshly distilled prior to use.

IR: Nicolet 6700 FT-IR spectrometer with a Smart Endurance ATR device was used. *Raman:* Bruker VERTEX 70 FT-IR with RAM II FT-Raman module, equipped with a Nd:YAG laser (1064 nm) was used. *CHN analyses:* C/H/N/S-Mikronalysator TruSpec-932 from Leco was used. Melting points are uncorrected (EZ-Melt, Stanford Research Systems). Heating-rate 20 °C/min (clearing-points are reported).

4.2. Reaction of N-(2,4,6-tri-tert-butylphenyl)imino(chloro)phosphane (1) with silver tetrakis(1,1,1,3,3,3-hexafluoro-2-propoxy)aluminate

To a stirred solution of *N*-(2,4,6-tri-*tert*-butylphenyl)imino-(chloro)phosphane Mes^*NPCl (**1**) (0.326 g, 1.0 mmol) in dichloromethane (10 mL), silver tetrakis(1,1,1,3,3,3-hexafluoro-2-propoxy)aluminate $Ag[Al(OCH(CF_3)_2)_4]$ (0.883 g, 1.1 mmol) in dichloromethane (5 mL) is added dropwise at −30 °C over a period of 10 min. The resulting orange suspension is warmed to ambient temperatures over a period of 30 min, and filtered (F4). The resulting clear orange solution is concentrated to an approximate volume of 3 mL *in vacuo* and is stored at −25 °C for 10 h, which results in the deposition of colourless crystals. The crystals were identified as bis[tris(1,1,1,3,3,3-hexafluoro-2-propoxy)aluminium] (**3**), the only phosphorous containing product was identified as *N*-2,4,6-tri-*tert*-butylphenyl)imino-(1,1,1,3,3,3-hexafluoro-2-propoxy)phosphane (**2**) by ^{31}P NMR.

4.3. Reaction of 1,3-dichloro-2,4-bis[tris(trimethylsilyl)silyl]-cyclo-diphosphadiazane with silver tetrakis(1,1,1,3,3,3-hexafluoro-2-propoxy)aluminate

To a stirred solution of 1,3-dichloro-2,4-bis-[tris(trimethylsilyl)silyl]-*cyclo*-diphosphadiazane $[HypNPCl]_2$ (0.656 g, 1.0 mmol) in dichloromethane (10 mL), silver tetrakis(1,1,1,3,3,3-hexafluoro-2-propoxy)aluminate $Ag[Al(OCH(CF_3)_2)_4]$ (0.883 g, 1.1 mmol) in dichloromethane (5 mL) is added dropwise at −30 °C over a period of 10 min. The resulting dark red suspension is warmed to ambient temperatures over a period of 30 min, and filtered (F4). Removal of solvent *in vacuo* at ambient temperature yields a red oil, which is characterized as 2-chloro-3,4-bis[tris(trimethylsilyl)silyl]-*cyclo*-diphosphadiazenium tetrakis(1,1,1,3,3,3-hexafluoro-2-propoxy)-aluminate $[Hyp_2N_2P_2Cl][Al(OCH(CF_3)_2)_4]$ by NMR. Storage at ambient temperatures for 10 h, results in the deposition of colourless crystals. The crystals were identified as 1-chloro-3-(1,1,1,3,3,3-hexafluoro-2-propoxy)-2,4-bis-[tris(trimethylsilyl)silyl]-*cyclo*-diphosphadiazane $Hyp_2N_2P_2(Cl)OCH(CF_3)_2$ (**4**).

$[Hyp_2N_2P_2Cl][Al(OCH(CF_3)_2)_4]$: ^1H NMR (25 °C, CD_2Cl_2, 300.13 MHz): δ = 0.36 (s, 54 H, $Si(Si(CH_3)_3)_3$), 4.50 (sept, 4H, $CH(CF_3)_2$, $^3J(^{19}F–^1H)$ = 6.0 Hz). $^{13}C\{^1H\}$ NMR (25 °C, CD_2Cl_2, 75.5 MHz): δ = 0.95 (s, $Si(Si(CH_3)_3)_3$). 71.5 (sept, $CH(CF_3)_2$, $^2J(^{19}F–^{13}C)$ = 32.9 Hz), 123.7 (q, CF_3, $^1J(^{19}F–^{13}C)$ = 283.3 Hz). ^{29}Si NMR (25 °C, CD_2Cl_2, 59.6 MHz): δ = −26.0 (m, $Si(Si(CH_3)_3)_3$), −12.8 (m, $Si(Si(CH_3)_3)_3$).$^{19}F\{^1H\}$ NMR (25 °C, CD_2Cl_2, 282.4 MHz): δ = −77.3 (s, CF_3).

4.4. Synthesis of N-(2,4,6-tri-tert-butylphenyl)imino-(1,1,1,3,3,3-hexafluoro-2-propoxy)phosphane (2)

To a stirred solution of 1,1,1,3,3,3-hexafluoro-2-propanole $HOCH(CF_3)_2$ (0.252 g, 1.5 mmol) in diethyl ether (10 mL), *n*-BuLi (2.5 M, 0.6 mL, 1.5 mmol) is added dropwise at 0 °C over a period of 5 min. The resulting colourless, clear solution is stirred for 10 min at this temperature, and is then added dropwise to a stirred solution of *N*-(2,4,6-tri-*tert*-butylphenyl)imino(chloro)phosphane Mes^*NPCl (**1**) (0.489 g, 1.5 mmol) in diethyl ether (8 mL) over a period of 5 min at 0 °C. The resulting orange suspension is stirred at this temperature for 30 min and is then slowly warmed to ambient temperatures. The solvent is removed *in vacuo,* resulting in an orange residue which is extracted with *n*-hexane (15 mL), and filtered (F4). The resulting clear orange solution is concentrated to an approximate volume of 3 mL *in vacuo* and is stored at −25 °C for 10 h, which results in the deposition of orange needlelike crystals. The supernatant is removed by syringe and the crystalline residue is dried *in vacuo*, which yields 0.652 g (1.43 mmol, 95%) of **2** as an orange crystalline solid. M.p. 102 °C (dec.). Anal. Calc.: C, 55.14; H, 6.61; N, 3.06. Found: C, 54.91; H, 6.59; N, 3.30%. ^1H NMR (25 °C, CD_2Cl_2, 300.13 MHz): δ = 1.33 (s, 9H, *p*-$C(CH_3)_3$), 1.47 (s, 18H, *o*-$C(CH_3)_3$), 5.18 (m, 1H, $CH(CF_3)_2$, $^4J(^{31}P–^{19}F)$ = 5.9 Hz), 7.35 (d, 2H, *m*-CH, $^5J(^{31}P–^1H)$ = 1.4 Hz). $^{13}C\{^1H\}$ NMR (25 °C, CD_2Cl_2, 75.5 MHz): δ = 30.8 (d, *o*-$C(CH_3)_3$, $^5J(^{13}C–^{31}P)$ = 2.4 Hz), 31.8 (s, *p*-$C(CH_3)_3$), 35.4 (s, *p*-$C(CH_3)_3$), 36.2 (d, *o*-$C(CH_3)_3$, $^4J(^{13}C–^{31}P)$ = 0.9 Hz), 68.4 (m, $CH(CF_3)_2$, $^2J(^{19}F–^{13}C)$ = 34.7 Hz, $^2J(^{31}P–^{13}C)$ = 10.4 Hz), 121.5 (m, CF_3, $^1J(^{19}F–^{13}C)$ = 283.2 Hz, $^3J(^{31}P–^{13}C)$ = 3 Hz),

122.5 (d, *m*-*C*H, $^4J(^{31}P-^{13}C)$ = 2.3 Hz), 137.7 (d, *p*-*C*, $^5J(^{31}P-^{13}C)$ = 31.4 Hz), 140.9 (d, *o*-*C*, $^3J(^{31}P-^{13}C)$ = 9.1 Hz), 146.6 (d, *ipso*-*C*, $^2J(^{31}P-^{13}C)$ = 4.2 Hz). $^{19}F\{^1H\}$ NMR (25 °C, CD_2Cl_2, 282.4 MHz): δ = −74.4 (m, *C*F_3, $^3J(^{19}F-^1H)$ = 5.9 Hz). $^{31}P\{^1H\}$ NMR (25 °C, CD_2Cl_2, 121.5 MHz): δ = 138.4. IR (ATR, 16 scans): 3100 (w), 2962 (m), 2935 (m), 2911 (m), 2872 (m), 2744 (w), 1506 (w), 1477 (w), 1471 (w), 1464 (w), 1456 (w), 1451 (w), 1421 (m), 1390 (w), 1382 (m), 1362 (m), 1337 (m), 1310 (w), 1278 (m), 1260 (m), 1229 (s), 1219 (s), 1188 (s), 1145 (w), 1134 (w), 1106 (s), 1083 (s), 1020 (w), 979 (w), 925 (w), 901 (m), 878 (m), 868 (s), 811 (s), 786 (m), 764 (m), 730 (w), 710 (w), 686 (s), 669 (w), 644 (m), 567 (m), 552 (w), 535(m). Raman (200 mW, 25 °C, 219 scans, cm^{-1}): = 3101 (1), 2965 (10), 2933 (9), 2910 (9), 2880 (5), 2776 (1), 2710 (2), 1598 (4), 1470 (2), 1449 (3), 1423 (4), 1390 (2), 1364 (2), 1336 (3), 1310 (8), 1199 (3), 1153 (1), 1081 (1), 1055 (1), 1026 (1), 927 (2), 868 (1), 823 (3), 784 (1), 731 (2), 687 (1), 568 (2), 537 (1), 509 (1), 475 (1),,421 (1), 389 (1), 338 (1), 299 (1), 256 (1), 126 (5). MS (Cl^+, isobutane): 458 $[M+H]^+$, 402 $[M-t\text{Bu}+2H]^+$.

Crystals suitable for X-ray crystallographic analysis were obtained directly from the above reaction solution.

4.5. Attempted synthesis of 1-chloro-3-(1,1,1,3,3,3-hexafluoro-2-propoxy)-2,4-bis-[tris(tri-methylsilyl)silyl]-cyclo-diphosphadiazane (**4**)

To a stirred solution of 1,1,1,3,3,3-hexafluoro-2-propanole $HOCH(CF_3)_2$ (0.168 g, 1.0 mmol) in diethylether (10 mL), *n*-BuLi (2.5 M, 0.4 mL, 1.0 mmol) is added dropwise at 0 °C over a period of 5 min. The resulting colourless, clear solution is stirred for 10 min at this temperature, and is then added dropwise to a stirred solution of 1,3-dichloro-2,4-bis-[tris(trimethylsilyl)silyl]-*cyclo*-diphosphadiazane $[HypNPCl]_2$ (0.656 g, 1.0 mmol) in diethyl ether (8 mL) over a period of 5 min at 0 °C. The resulting colourless solution is then slowly warmed to ambient temperatures. Even after several hours at ambient temperatures, no reaction is observed as shown by ^{31}P NMR. The solvent is removed *in vacuo,* resulting in a colourless residue which is extracted with *n*-hexane (15 mL), and filtered (F4). The resulting clear colourless solution is concentrated to an approximate volume of 3 mL *in vacuo* and is stored at −25 °C for 10 h, which results in the deposition of colourless crystals of the starting material 1,3-dichloro-2,4-bis[tris(trimethylsilyl)silyl]-*cyclo*-diphosphadiazane $[HypNPCl]_2$ almost quantitatively.

4.6. Synthesis of 1-chloro-3-(1,1,1,3,3,3-hexafluoro-2-propoxy)-2,4-[tris(tri-methylsilyl)silyl]-cyclo-diphosphadiazane (**4**)

The mixture of **3** and **4** (from the decomposition reaction of 2-chloro-3,4-bis[tris(trimethylsilyl)silyl]-*cyclo*-diphosphadiazenium tetrakis(1,1,1,3,3,3-hexafluoro-2-propoxy)aluminate $[Hyp_2N_2P_2Cl]^+[Al(OCH(CF_3)_2)_4]^-$) is dissolved in *n*-hexane (10 mL) resulting in a yellowish suspension, which is added dropwise to a colourless suspension of $Li[OCH(CF_3)_2]$ (prepared from 1,1,1,3,3,3-hexafluoro-2-propanole $HOCH(CF_3)_2$ (0.168 g, 1.0 mmol) and *n*-BuLi (2.5 M, 0.4 mL, 1.0 mmol) in *n*-hexane (5 mL) at ambient temperatures over a period of 10 min. The resulting colourless suspension is stirred for 1 h at ambient temperatures and filtered (F4). The resulting colourless solution is concentrated to an approximate volume of 5 mL *in vacuo* and is stored at –25 °C for 10 h which leads to the deposition of colourless crystals. Removal of supernatant by syringe and drying *in vacuo* yields 0.190 g (0.24 mmol, 24%) of **4** as colourless crystalline solid. Mp 127 °C; T_{dec} 186 °C. Anal. Calc.: C, 32.02; H, 7.04; N, 3.56. Found: C, 31.72; H, 7.03; N, 3.46%. ^1H NMR (25 °C, CD_2Cl_2, 300.13 MHz): δ = 0.27 (s, 54 H, $Si(Si(CH_3)_3)_3$), 5.38 (m, 1H, *C*$H(CF_3)_2$, $^3J(^{19}F-^1H)$ = 3.9 Hz). $^{13}C\{^1H\}$ NMR (25 °C, CD_2Cl_2, 75.5 MHz): δ = 1.6 (s, $Si(Si(CH_3)_3)_3$). 71.4 (sept, *C*$H(CF_3)_2$, $^2J(^{19}F-^{13}C)$ = 33.4 Hz). ^{29}Si NMR (25 °C, CD_2Cl_2, 59.6 MHz): δ = −33.3 (m, *Si*$(Si(CH_3)_3)_3$), −13.5 (m, $Si(Si(CH_3)_3)_3$). $^{19}F\{^1H\}$ NMR (25 °C, CD_2Cl_2, 282.4 MHz): δ = −72.0 (d, *C*F_3, $^4J(^{19}F-^{31}P)$ = 4.3 Hz). $^{31}P\{^1H\}$ NMR (25 °C, CD_2Cl_2, 121.5 MHz): δ = 199.8 (d, $^2J(^{31}P-^{31}P)$ = 100 Hz), 233.1 (d, $^2J(^{31}P-^{31}P)$ = 100 Hz). IR (ATR, 16 scans): 2949 (w), 2894 (w), 1371 (w), 1290 (m), 1258 (m), 1244 (m), 1220 (m), 1192 (s), 1162 (m), 1105 (m), 1075 (m), 1012 (w), 1000 (w), 953 (w), 898 (w), 890 (m), 875 (m), 820 (vs), 787 (s), 748 (m), 740 (m), 685 (s), 623 (s), 561 (m). MS (Cl^+, isobutane): 787 $[M+H]^+$, 771 $[M-Me]^+$, 751 $[M-Cl]^+$, 713 $[M-SiMe_3]^+$, 678 $[M-SiMe_3-Cl]^+$, 619 $[M-OCH(CF_3)_2]^+$.

Acknowledgements

We thank Dr. Dirk Michalik (Universität Rostock) for helpful advice.

Appendix A. Supplementary material

CCDC 753943, 753944, 753946 and 753945 contains the supplementary crystallographic data for this paper. These data can be obtained free of charge from The Cambridge Crystallographic Data Centre via www.ccdc.cam.ac.uk/data_request/cif. Supplementary data associated with this article can be found, in the online version, at doi:10.1016/j.jorganchem.2009.11.014.

References

[1] R. Keat, Top. Curr. Chem. 102 (1982) 89–116. and references therein.
[2] L. Stahl, Coord. Chem. Rev. 210 (2000) 203–250. and references therein.
[3] H.-J. Chen, R.C. Haltiwanger, T.G. Hill, M.L. Thompson, D.E. Coons, A.D. Norman, Inorg. Chem. 24 (1985) 4725–4730.
[4] N. Burford, T.S. Cameron, K.-C. Lam, D.J. LeBlanc, C.L.B. Macdonald, A.D. Phillips, A.L. Rheingold, L. Stark, D. Walsh, Can. J. Chem. 79 (2001) 342–348.
[5] (a) R. Keat, Top. Curr. Chem. 102 (1982) 89–116;
(b) M.S. Balakrishna, V.S. Reddy, S.S. Krishnamurthy, J.F. Nixon, J.C. Laurent, Coord. Chem. Rev. 129 (1994) 1–90.
[6] (a) D. Michalik, A. Schulz, A. Villinger, N. Weding, Angew. Chem. 120 (2008) 6565–6568. Angew. Chem., Int. Ed. 47 (2008) 6465–6468;
(b) R. Kuzora, A. Schulz, A. Villinger, R. Wustrack, Dalton Trans. (2009) 9304–9311.
[7] A.H. Cowley, M. Lattman, J.C. Wilburn, Inorg. Chem. 20 (1981) 2916–2919.
[8] N. Burford, J.C. Landry, M.J. Ferguson, R. McDonald, Inorg. Chem. 44 (2005) 5897–5902.
[9] N. Burford, K.D. Conroy, J.C. Landry, P.J. Ragogna, M.J. Ferguson, R. McDonald, Inorg. Chem. 43 (2004) 8245–8251.
[10] A. Villinger, A. Westenkirchner, R. Wustrack, A. Schulz, Inorg. Chem. 47 (2008) 9140–9142.
[11] H. Gilman, R.L. Harrell, J. Organomet. Chem. 5 (1966) 199–200.
[12] M. Westerhausen, W. Schwarz, Z. Anorg. Allg. Chem. 619 (1993) 1053–1063.
[13] A. Michaelis, G. Schroeter, Ber. Dtsch. Chem. Ges. 27 (1894) 490–497.
[14] (a) N. Burford, T.S. Cameron, K.D. Conroy, B. Ellis, M.D. Lumsden, C.L.B. McDonald, R. McDonald, A.D. Phillips, P.J. Ragogna, R.W. Schurko, D. Walsh, R.E. Wasylishen, J. Am. Chem. Soc. 124 (2002) 14012–14013;
(b) N. Burford, J.A.C. Clyburne, M.S.W. Chan, Inorg. Chem. 36 (1997) 3204–3206.
[15] E. Niecke, M. Nieger, F. Reichert, Angew. Chem. 12 (1988) 1781–1782; Angew. Chem., Int. Ed. 27 (1988) 1715–1716.
[16] (a) Reviews: I. Krossing, I. Raabe, Angew. Chem. 116 (2004) 2016–2142. Angew. Chem. Int. Ed. 43 (2004) 2066–2090;
(b) C. Reed, Acc. Chem. Res. 31 (1998) 133–139;
(c) S.H. Strauss, Chem. Rev. 93 (1993) 927–942. and references therein.
[17] N. Burford, J.A.C. Clyburne, P. Losier, T.M. Parks, in: H.H. Karsch (Ed.), Handbuch der Präparativen Anorganischen Chemie (Engl.), fourth ed., Thieme-Verlag, Stuttgart, 1996.
[18] (a) I. Krossing, A. Reisinger, Coord. Chem. Rev. 250 (2006) 2721–2744;
(b) M. Gonsior, I. Krossing, L. Müller, I. Raabe, M. Jansen, L. Van Wullen, Chem. Eur. J. 8 (2002) 4475–4492;
(c) I. Krossing, Dalton Trans. 4 (2002) 500–512;
(d) I. Krossing, I. Raabe, Chem. Eur. J. 10 (2004) 5017–5030.
[19] I. Krossing, Chem. Eur. J. 7 (2001) 490–502.
[20] F. Weinhold, C. Landis, Valency and Bonding. A Natural Bond Orbital Donor–Acceptor Perspective, Cambridge University Press, 2005.
[21] Holleman Wiberg, Lehrbuch der Anorganischen Chemie, Aufl., Walter de Gruyter, Berlin, 2007, p. 102 (Anhang IV).

5.2 Synthesis of Pentafluorophenyl Silver by Means of Lewis Acid Catalysis: Structure of Silver Solvent Complexes

Marcus Kuprat, Mathias Lehmann, Axel Schulz, Alexander Villinger

Organometallics **2010**, *29*, 1421-1427.

ORGANOMETALLICS
Article

Organometallics **2010,** *29,* 1421–1427 1421
DOI: 10.1021/om901063a

Synthesis of Pentafluorophenyl Silver by Means of Lewis Acid Catalysis: Structure of Silver Solvent Complexes§

Marcus Kuprat,† Mathias Lehmann,† Axel Schulz,*,†,‡ and Alexander Villinger*,†

†*Institut für Chemie, Abteilung Anorganische Chemie, Universität Rostock, Albert-Einstein-Strasse 3a, 18059 Rostock, Germany, and* ‡*Leibniz-Institut für Katalyse e.V. an der Universität Rostock, Albert-Einstein-Strasse 29a, 18059 Rostock, Germany*

Received December 11, 2009

The synthesis and structure of lithium and silver tetrakis(pentafluorophenyl)borate salts have been studied in different solvents ranging from polar (CH_2Cl_2, diethyl ether) to nonpolar (toluene, pentane). While $Li[B(C_6F_5)_4]$ is stable in all studied solvents and crystallizes with four ether molecules from ether and with two toluene molecules from toluene, the silver salt is only stable when the Ag^+ ion is strongly coordinated such as in $[Ag(toluene)_3][B(C_6F_5)_4]$ or $[Ag(Et_2O)_3][B(C_6F_5)_4]$. In weakly coordinating solvents such as CH_2Cl_2 $Ag[B(C_6F_5)_4]$ decomposes, yielding AgC_6F_5 and $B(C_6F_5)_3$. The overall process of the AgC_6F_5 synthesis starting from $B(C_6F_5)_3$ and LiC_6F_5 can formally be regarded as a $B(C_6F_5)_3$-catalyzed reaction. The salt $[Ag(toluene)_3][B(C_6F_5)_4]$ presents an easily accessible, ether-free, stable silver salt of the $[B(C_6F_5)_4]^-$ anion. All compounds have been fully characterized.

1. Introduction

As early as 1970,[1] pentafluorophenylsilver, AgC_6F_5, was synthesized in the reaction of $Ag[CF_3COO]$ and LiC_6F_5 or $Ag((CF_3)_2CF)$ and C_6F_5Br (Chart 1).[2−4] Ever since several synthetic routes to pentafluorophenylsilver have been published as summarized in Chart 1.[5] While most reactions gave AgC_6F_5 in good yields, they have in common that either they are rather inconvenient to handle or toxic compounds are involved. The best synthetic route to AgC_6F_5 so far seems to be the reaction of AgF with $Me_3Si(C_6F_5)$ in propionitrile, EtCN. The major drawback of this reaction is the necessary preparation of $Me_3Si(C_6F_5)$ from Me_3SiCl and C_6F_5MgBr.[5,6]

AgC_6F_5 was shown to be an excellent transfer reagent for pentafluorophenyl groups in synthetic metal- and nonmetal organic chemistry, although moisture and oxygen sensitive.[5,7−14] By heating (> 276 °C) and exposure to light, AgC_6F_5 is easily converted into perfluorobiphenyl and silver metal.[1,5]

A few mono- and polynuclear arylsilver(I) complexes of the type AgR (e.g., R = C_6H_5, C_6F_5, C_6Cl_5, MeC_6H_4, $Me_2C_6H_3$, $(MeO)_2C_6H_3$), $AgC_6F_5 \cdot L$ (L = EtCN), and $Ag_2R_2 \cdot L$ have been reported.[15−19] However, examples of structurally characterized organosilver(I) complexes are still rare, appearing mostly as monomeric or tetrameric species in the solid state.[2,20−23] Diarylargentate complexes are composed of separated ion pairs.[24]

Recently, we studied the generation and stability of silver and lithium salts containing new weakly coordinating anions,[25]

§ Dedicated to Prof. Dr. Uwe Rosenthal on the occasion of his 60th birthday.

*Corresponding authors. E-mail: axel.schulz@uni-rostock.de; alexander.villinger@uni-rostock.de.

(1) Miller, W. T.; Sun, K. K. *J. Am. Chem. Soc.* **1970**, *92*, 6985.
(2) Smith, V. B.; Massey, A. G. *J. Organomet. Chem.* **1970**, *23*, C9.
(3) Uson, R.; Laguna, A.; Abad, J. A. *J. Organomet. Chem.* **1983**, *246*, 341.
(4) Fernandez, E. J.; Laguna, A.; Mendigrave, A. *Inorg. Chim. Acta* **1994**, *223*, 161.
(5) Tyrra, W.; Wickleder, M. S. *Z. Anorg. Allg. Chem.* **2002**, *628*, 1841.
(6) Respess, W. L.; Tamborski, C. *J. Organomet. Chem.* **1969**, *18*, 263.
(7) Naumann, D.; Tyrra, W.; Herrmann, R.; Pantenburg, I.; Wickleder, M. S. *Z. Anorg. Allg. Chem.* **2002**, *628*, 833.
(8) Doucette, W. J.; Kim, J.; Kautz, J. A.; Gipson, S. L. *Inorg. Chim. Acta* **2000**, *304*, 237.
(9) Garcia, M. P.; Jimenez, M. V.; Lahoz, F. J.; Oro, L. A. *Inorg. Chem.* **1995**, *34*, 2153.
(10) Danopoulos, A. A.; Wilkinson, G.; Sweet, T. K. N.; Hursthouse, M. B. *J. Chem. Soc., Dalton Trans.* **1994**, 1037.
(11) Laguna, A.; Fernandez, E. J.; Mendia, A.; Ruiz-Romero, M. E.; Jones, P. G. *J. Organomet. Chem.* **1989**, *365*, 201.
(12) Yagupolskii, Yu. L.; Gerus, I. I.; Yagupolskii, L. M. *Zh. Org. Khim.* **1981**, *17*, 2512.
(13) Bennett, R. L.; Bruce, M. I.; Gardner, R. C. F. *J. Chem. Soc., Dalton Trans.* **1973**, 2653.
(14) Bennett, R. L.; Bruce, M. I.; Goodfellow, R. J. *J. Fluorine Chem.* **1973**, *2*, 447.
(15) van Koten, G.; Noltes, G. *Comprehensive Organometallic Chemistry*, Vol. *2*; Pergamon: Oxford, 1982; p 709.
(16) Uson, R.; Laguna, A.; Abad, J. A. *J. Organomet. Chem.* **1983**, *246*, 341.
(17) Lingnau, R.; Strähle, J. *Angew. Chem., Int. Ed. Engl.* **1988**, *27*, 436.
(18) Uson, R.; Luguna, A.; Uson, A.; Jones, P. G.; Meyer-Bäse, K. *J. Chem. Soc., Dalton Trans.* **1988**, 341.
(19) Fernandez, E. J.; Laguna, A.; Mendia, A. *Inorg. Chim. Acta* **1994**, *223*, 161.
(20) Gambarotta, S.; Floriani, C.; Chiesa-Villa, A.; Guastini, C. *J. Chem. Soc., Chem. Commun.* **1983**, 1087.
(21) Meyer, E. M.; Gambarotta, S.; Floriani, C.; Chiesa-Villa, A.; Guastini, C. *Organometallics* **1989**, *8*, 1067.
(22) Edwards, D. A.; Harker, R. M.; Mahon, M. F.; Molloy, K. C. *J. Chem. Soc., Dalton Trans.* **1997**, 3509.
(23) Voelker, H.; Labahn, D.; Bohnen, F. M.; Herbst-Irmer, R.; Roesky, H. W.; Stalke, D.; Edelmann, F. T. *New J. Chem.* **1999**, *23*, 905.
(24) Hwang, C.-S.; Power, P. P. *J. Organomet. Chem.* **1999**, *589*, 234.
(25) Bernsdorf, A.; Brand, H.; Hellmann, R.; Köckerling, M.; Schulz, A.; Villinger, A.; Voss, K. *J. Am. Chem. Soc.* **2009**, *131*, 8958.

© 2010 American Chemical Society
Published on Web 02/19/2010

Chart 1. Synthetic Routes to AgC_6F_5[a]

(1) $Li(C_6F_5) + Ag(CF_3COO) \longrightarrow Ag(C_6F_5) + Li(CF_3COO)$

(2) $C_6F_5Br + Ag(CF(CF_3)_2) \longrightarrow Ag(C_6F_5) + (CF_3)_2CFBr$

(3) $NBu_4Ag(C_6F_5)_2 + AgClO_4 \longrightarrow 2\,Ag(C_6F_5) + NBu_4ClO_4$

(4) $M(C_6F_5)_2 + 2\,AgNO_3 \longrightarrow 2\,Ag(C_6F_5) + M(NO_3)_2$

(5) $AgF + Me_3Si(C_6F_5) \longrightarrow Ag(C_6F_5) + Me_3SiF$

[a] M = e.g., Cd, Zn.

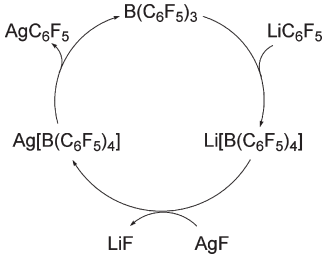

Figure 1. Formal catalytic cycle with $B(C_6F_5)_3$ as catalyst in the generation of AgC_6F_5.

in comparison with the known chemically robust tetrakis(pentafluorophenyl)borate, $[B(C_6F_5)_4]^-$. During this study, we realized that pure solvent-free $Ag[B(C_6F_5)_4]$ is labile with respect to decomposition into AgC_6F_5 and $B(C_6F_5)_3$, which finally led to a new synthetic approach to AgC_6F_5. Here we report on a new synthetic route to AgC_6F_5 in a facile two-step reaction (Figure 1), which formally uses tris(pentafluorophenyl)borane, $B(C_6F_5)_3$, as catalytic reagent. Moreover, the structures of several lithium and silver tetrakis(pentafluorophenyl)borate solvent complexes are discussed.

2. Results and Discussion

Synthesis of Lithium and Silver Tetrakis(pentafluorophenyl)-borate Solvent Complexes. The stabilization of highly electrophilic metal cations such as Li^+ or Ag^+ or as solvent (Lewis acid base) complexes is commonly achieved by replacing the small and strongly coordinating counterion by a large and weakly coordinating anion (wca) such as tetrakis(pentafluorophenyl)borate, $[B(C_6F_5)_4]^-$.[26]

Solvent-free lithium tetrakis(pentafluorophenyl)borate is easily prepared in the reaction of *n*-BuLi with tris(pentafluorophenyl)borane in pentane,[27] while the reaction in donor solvents such as diethyl ether (σ donor) and toluene (π donor) yields the corresponding solvent complex salts $Li[B(C_6F_5)_4]\cdot Et_2O$ and $Li[B(C_6F_5)_4]\cdot 2$ toluene, respectively, as shown in Chart 2. A closer look at the reaction in diethyl ether revealed that at first $Li[B(C_6F_5)_4]\cdot 4Et_2O$ (crystallizes at −80 °C) was formed, which releases readily 1.5 Et_2O at ambient temperatures and 10^{-3} Torr to give $Li[B(C_6F_5)_4]\cdot 2.5Et_2O$ with a melting point of 120 °C (cf. $Li[B(C_6F_5)_4]$: mp 253 °C). Constant heating at this temperature *in vacuo* finally affords $Li[B(C_6F_5)_4]\cdot Et_2O$ with a melting point of 184 °C. The last diethyl ether molecule cannot be removed thermally, which is a major drawback, when for example diethyl ether free salts are needed.

Chart 2. Synthesis of $Li[B(C_6F_5)_4]$ and Its Solvent Complexes

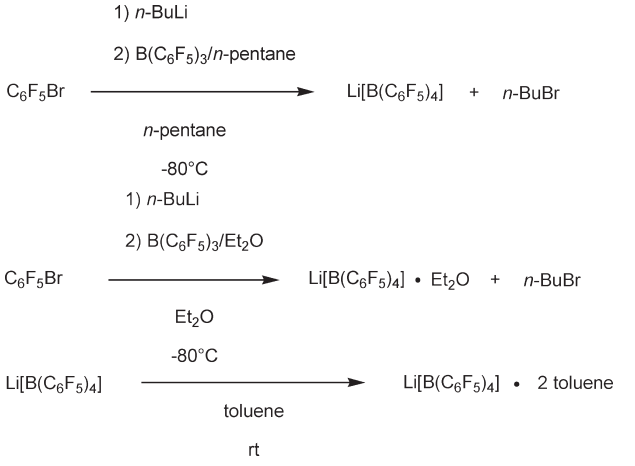

We studied two synthetic routes to silver tetrakis(pentafluorophenyl)borate (Chart 3): (i) $Li[B(C_6F_5)_4]\cdot Et_2O$ was treated with $AgNO_3$,[27] which gave after separation from $LiNO_3$ and recrystallization from dichloromethane crystalline $Ag[B(C_6F_5)_4]\cdot Et_2O$, while (ii) recrystallization of $Ag[B(C_6F_5)_4]\cdot Et_2O$ from toluene over three hours at 50 °C resulted in the formation of $Ag[B(C_6F_5)_4]\cdot 2$ toluene (decomposition above 94 °C). Starting from $Li[B(C_6F_5)_4]\cdot Et_2O$, we did not succeed in preparing solvent-free $Ag[B(C_6F_5)_4]$ by means of recrystallization. A closer look at the reaction in diethyl ether and toluene revealed, depending on the reaction condition, that in diethyl ether first $Ag[B(C_6F_5)_4]\cdot 3Et_2O$ crystallizes at ambient temperatures, while in toluene $Ag[B(C_6F_5)_4]\cdot 3$ toluene (= $[Ag(toluene)_3][B(C_6F_5)_4]$, see section X-ray Crystallography) is formed. Stepwise release of up to two Et_2O molecules or one toluene molecule, respectively, readily occurs at slightly elevated temperatures (50−60 °C) and reduced pressure (10^{-3} Torr) to give $Ag[B(C_6F_5)_4]\cdot Et_2O$ with a melting point of 117 °C (decomposition) and $Ag[B(C_6F_5)_4]\cdot 2$ toluene with a melting point of 94 °C (decomposition). The last diethyl ether/toluene molecules cannot be removed thermally. The $Ag[B(C_6F_5)_4]\cdot 2$ toluene complex is thermally stable at ambient temperatures, can be prepared in high yields, and displays an ether-free species, which makes this silver toluene complex interesting for salt metathesis reaction in low nucleophilicity solvents, where diethyl ether molecules remain attached to the cations.

Synthesis of Pentafluorophenylsilver by Means of Formal $B(C_6F_5)_3$ Catalysis. Since Li^+/Ag^+ cation exchange reactions starting from $Li[B(C_6F_5)_4]\cdot Et_2O$ to obtain ether-free Ag^+ salts were not successful, solvent-free $Li[B(C_6F_5)_4]$ was reacted with AgF in CH_2Cl_2 at 30−60 °C under ultrasonic irradiation for eight hours, a methods that has been introduced by Krossing et al. and successfully been applied in the synthesis of $AgAl(OR^F)_4$ (e.g., $R^F = -CH(CF_3)_2$, $-C(CH_3)(CF_3)_2$, $-C(CF_3)_3$).[28] Surprisingly, in the analogous reaction (with AgF and $Li[B(C_6F_5)_4]$) solvent-free pentafluorophenylsilver, AgC_6F_5, was obtained in high yields (90%) besides free $B(C_6F_5)_3$ and LiF (Chart 4). Separation of LiF was achieved by filtration, while $B(C_6F_5)_3$ was removed by repeatedly washing with *n*-hexane. Almost three-fourths of the utilized Lewis acid $B(C_6F_5)_3$ can be

(26) Reviews: (a) Krossing, I.; Raabe, I. *Angew. Chem., Int. Ed.* **2004**, *43*, 2066. (b) Reed, C. *Acc. Chem. Res.* **1998**, *31*, 133. (c) Strauss, S. H. *Chem. Rev.* **1993**, *93*, 927, and references therein.

(27) Massey, A. G.; Park, A. J. *J. Organomet. Chem.* **1964**, *2*, 245.

(28) Krossing, I. *Chem.—Eur. J.* **2001**, *7*, 490.

Chart 3. Synthesis of $Ag[B(C_6F_5)_4]$ and Its Solvent Complexes

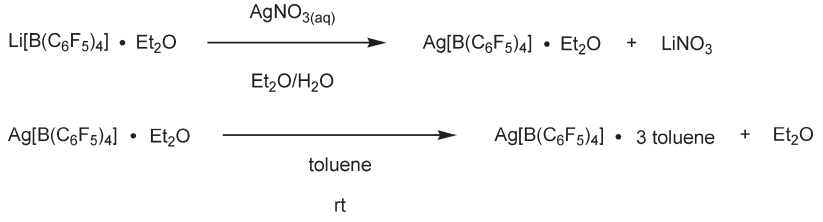

Chart 4. Synthesis of AgC_6F_5

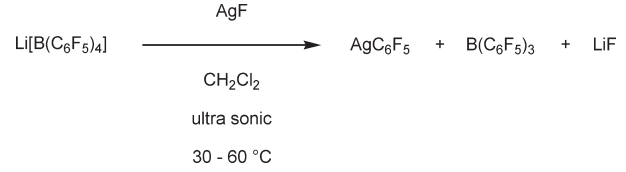

Table 1. Crystallographic Details of $[Li(Et_2O)_4][B(C_6F_5)_4]$, $[Li(Et_2O)][B(C_6F_5)_4]\cdot CH_2Cl_2$, and $[Li(toluene)][B(C_6F_5)_4]\cdot$toluene

	$[Li(Et_2O)_4][B(C_6F_5)_4]$	$[Li(Et_2O)][B(C_6F_5)_4]\cdot CH_2Cl_2$	$[Li(toluene)][B(C_6F_5)_4]\cdot$toluene
chem formula	$C_{40}H_{40}BF_{20}LiO_4$	$C_{28.50}H_{11}BClF_{20}LiO$	$C_{38}H_{16}BF_{20}Li$
fw [g mol^{-1}]	982.47	802.57	870.26
color	colorless	colorless	colorless
cryst syst	triclinic	monoclinic	triclinic
space group	$P\bar{1}$	$P2_1/n$	$P\bar{1}$
a [Å]	11.15(1)	10.909(7)	9.981(5)
b [Å]	11.18(1)	13.662(9)	13.158(7)
c [Å]	17.84(2)	19.69(1)	14.992(8)
α [deg]	78.19(2)	90.00	107.899(8)
β [deg]	85.85(2)	95.36(2)	96.979(9)
γ [deg]	89.76(2)	90.00	108.65(1)
V [Å^3]	2170(3)	2921(3)	1722(2)
Z	2	4	2
$\rho_{calc.}$ [g cm^{-3}]	1.503	1.825	1.679
μ [mm^{-1}]	0.152	0.285	0.173
$\lambda_{Mo K\alpha}$ [Å]	0.71073	0.71073	0.71073
T [K]	173(2)	173(2)	173(2)
measd reflns	18 964	26 944	32 497
indep reflns	5548	6643	8256
reflns with $I > 2\sigma(I)$	4127	5006	6010
$R_{int.}$	0.0332	0.0284	0.0303
$F(000)$	1000	1580	864
R_1 ($R[F^2 > 2\sigma(F^2)]$)	0.0406	0.0351	0.0387
wR_2 (F^2)	0.1105	0.0909	0.1061
GooF	1.097	1.064	1.068
parameters	659	565	543
CCDC #	757606	757607	757608

recovered in high purity by subsequent sublimation at 110 °C for six hours. The driving force of the AgC_6F_5 formation is the instability of the solvent-free $Ag[B(C_6F_5)_4]$ intermediate. If the Ag^+ ion is not stabilized by significant donor−acceptor interactions as in $Ag[B(C_6F_5)_4]\cdot n$ toluene (n = 2, 3) or $Ag[B(C_6F_5)_4]\cdot nEt_2O$ (n = 1−3), Ag^+ seems to be the stronger Lewis acid, resulting in the abstraction of $C_6F_5^-$ from the $[B(C_6F_5)_4]^-$ ion, yielding AgC_6F_5 and $B(C_6F_5)_3$. Since $B(C_6F_5)_3$ can be recovered, the overall process, as shown in Figure 1, can formally be regarded as a Lewis acid-catalyzed synthesis of AgC_6F_5. Bochmann et al. demonstrated the degradation of the $[B(C_6F_5)_4]^-$ ion in the reaction of $[Ph_3C]^+[B(C_6F_5)_4]^-$ with $AlMe_3$ in which the *in situ*-generated $[AlMe_2]^+[B(C_6F_5)_4]^-$ immediately decomposes to $B(C_6F_5)_3$ and $AlMe_2(C_6F_5)$. The authors assumed cations such as $[AlMe_2]^+$ are too electrophilic to be stabilized even by $[B(C_6F_5)_4]^-$ and immediately react with abstraction of $[C_6F_5]^-$.[29,30]

Table 2. Crystallographic Details of $[Ag(toluene)_3][B(C_6F_5)_4]$ and $Ag(C_6F_5)(CH_3CN)$

	$[Ag(toluene)_3][B(C_6F_5)_4]$	$AgC_6F_5\cdot CH_3CN$
chem formula	$C_{45}H_{24}AgBF_{20}$	$C_8H_3AgF_5N$
fw [g mol^{-1}]	1063.32	315.98
color	colorless	colorless
cryst syst	triclinic	monoclinic
space group	$P\bar{1}$	$C2/c$
a [Å]	10.898(5)	22.159(9)
b [Å]	13.413(7)	10.009(4)
c [Å]	14.514(8)	9.140(5)
α [deg]	77.47(2)	90.00
β [deg]	87.50(2)	113.57(1)
γ [deg]	76.42(1)	90.00
V [Å^3]	2013(2)	1858(1)
Z	2	8
ρ_{calcd} [g cm^{-3}]	1.754	2.259
μ [mm^{-1}]	0.629	2.209
$\lambda_{Mo K\alpha}$ [Å]	0.71073	0.71073
T [K]	173(2)	173(2)
measd reflns	40 833	12 262
indep reflns	10 612	3354
reflections with $I > 2\sigma(I)$	8101	3028
$R_{int.}$	0.0393	0.0339
$F(000)$	1052	1200
R_1 ($R[F^2 > 2\sigma(F^2)]$)	0.0361	0.0197
wR_2 (F^2)	0.0968	0.0488
GooF	1.056	1.077
parameters	617	139
CCDC #	757609	757610

A similar Lewis acid/Lewis base reaction is assumed for weakly coordinating anions of the type $[Al(OR^F)_4]^-$ in the presence of very electrophilic cations, where the decomposition is initiated either by ligand (R^FO^-) or fluoride ion abstraction, finally leading to $[(R^FO)_3Al-F-Al(OR^F)_3]^-$.[31]

X-ray Crystallography. The structures of $[Li(Et_2O)_4][B(C_6F_5)_4]$, $[Li(toluene)][B(C_6F_5)_4]\cdot$toluene, $[Li(Et_2O)_2][B(C_6F_5)_4]\cdot CH_2Cl_2$, $[Ag(Et_2O)_3][B(C_6F_5)_4]$, $[Ag(toluene)_3][B(C_6F_5)_4]$, and $AgC_6F_5\cdot CH_3CN$ have been determined. Tables 1 and 2 present the X-ray crystallographic data. The molecular structures and coordination spheres of the cations along with selected molecular parameters are depicted in Figures 2−6 and S1−S3 (see Supporting Information).

(29) Bochmann, M.; Sarsfield, M. J. *Organometallics* **1998**, *17*, 5908.
(30) See also: Korolev, A. V.; Ihara, E.; Guzei, I. A.; Young, V. G.; JordanR., F. *J. Am. Chem. Soc.* **2001**, *123*, 8291.
(31) (a) Krossing, I.; Reisinger, A. *Coord. Chem. Rev.* **2006**, *250*, 2721. (b) Gonsior, M.; Krossing, I.; Müller, L.; Raabe, I.; Jansen, M.; Van Wullen, L. *Chem.—Eur. J.* **2002**, *8*, 4475. (c) Krossing, I. *Dalton Trans.* **2002**, *4*, 500. (d) Krossing, I.; Raabe, I. *Chem.—Eur. J.* **2004**, *10*, 5017.

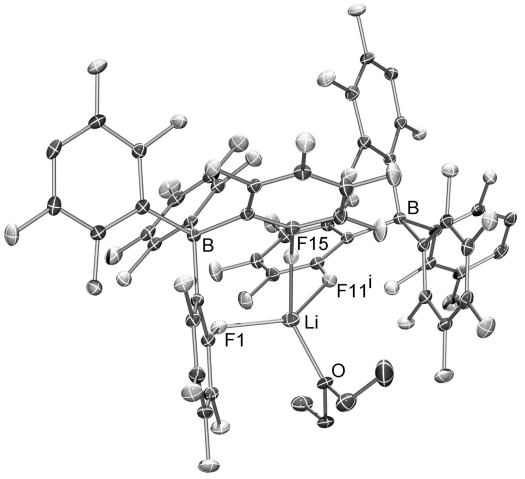

Figure 2. ORTEP drawing of the tetrahedral coordination around the Li^+ in the crystal of $[Li(Et_2O)][B(C_6F_5)_4]\cdot CH_2Cl_2$. Thermal ellipsoids are shown with 50% probability at 173 K. Selected distances in Å, angles in deg: Li−O1 1.946(6), Li−$F11^i$ 1.996(3), Li−F15 2.003(3), Li−F1 2.020(3), Li−$F12^i$ 2.489(4); O1−Li−$F12^i$ 129.1(2), O1−Li−F15 122.2(2), $F11^i$−Li−F1 135.3(2), $F11^i$−Li−F15 86.7(1), F15−Li−F1 88.8(1). Symmetry code: i $-x+1/2$, $y-1/2$, $-z+3/2$.

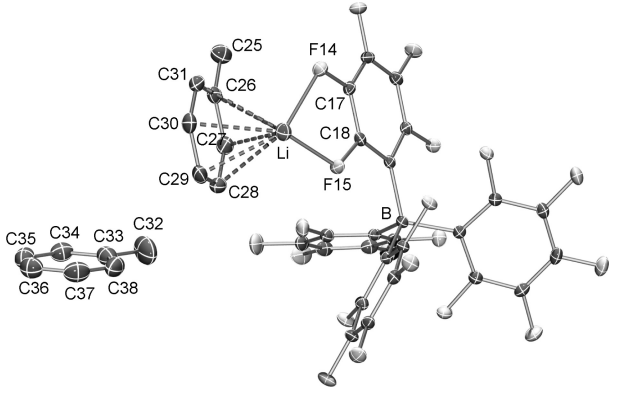

Figure 3. ORTEP drawing of the molecular structure of **3** (only one of the two independent molecules is shown) in the crystal. Thermal ellipsoids are shown with 50% probability at 228 K. Selected distances in Å, angles in deg: C25−C26 1.497(3), C26−C31 1.388(3), C26−C27 1.392(3), C27−C28 1.394(3), C28−C29 1.386(3), C29−C30 1.377(3), C30−C31 1.390(3), C32−C33 1.487(4), C33−C34 1.367(3), C33−C38 1.421(4), C34−C35 1.365(3), C35−C36 1.345(3), C36−C37 1.345(4), C37−C38 1.364(4); C31−C26−C27 118.5(2), C31−C26−C25 120.7(2), C27−C26−C25 120.8(2), C29−C28−C27 119.7(2), C30−C29−C28 119.8(2), C29−C30−C31 120.5(2), C34−C33−C38 115.7(2), C34−C33−C32 122.6(3), C38−C33−C32 121.7(3), C35−C34−C33 122.8(2) .

$[Li(Et_2O)_4][B(C_6F_5)_4]$ crystallizes in the triclinic space group $P\bar{1}$ with two formula units per cell. The structure consists of separated Li^+(diethyl ether)$_4$ and tetrakis(pentafluorophenyl)borate units ($[B(C_6F_5)_4]^-$) with no significant cation···anion contacts. Only weak (ether)C−H···F−C(aryl) interactions are found. The crystallographic asymmetric unit contains one ion pair, $[Li^+(\text{diethyl ether})_4]$-$[B(C_6F_5)_4]^-$ (Figure S1, see Supprting Information). The Li^+ ion is bonded to each oxygen atom of the four diethyl ether molecules, forming a tetrahedral coordination environment around the cation with Li−O distances between 1.952(5) and 1.970(5) Å. Two of the diethyl ether molecules are disordered.

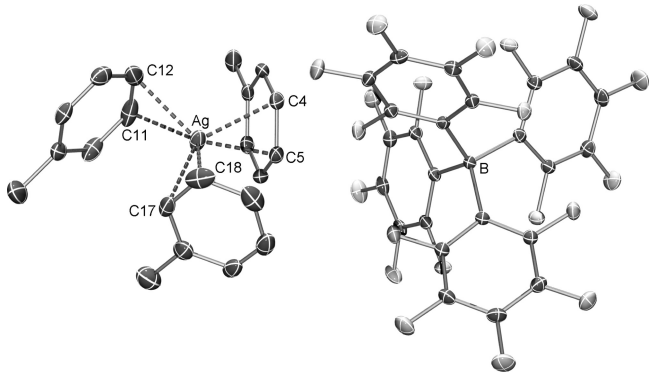

Figure 4. ORTEP drawing of the asymmetric unit of $[Ag(\text{toluene})_3][B(C_6F_5)_4]$ in the crystal. Thermal ellipsoids are shown with 50% probability at 173 K.

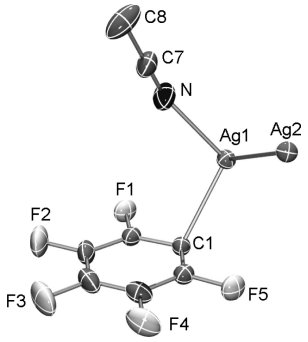

Figure 5. ORTEP drawing of the molecular structure of $Ag(C_6F_5)(CH_3CN)$ (the asymmetric unit is shown) in the crystal. Thermal ellipsoids are shown at 50% probability at 173 K.

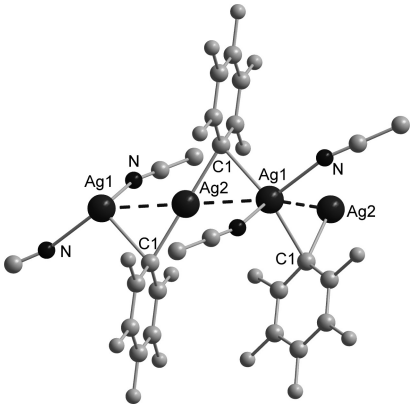

Figure 6. Part of the packing diagram of $Ag(C_6F_5)(CH_3CN)$ in the crystal. Thermal ellipsoids are shown with 50% probability at 228 K. Selected distances in Å, angles in deg: Ag1−$C1^i$ 2.381(2), Ag1−N1 2.392(2), Ag1−Ag2 2.802(1), Ag2−$C1^i$ 2.147(2); C1i−Ag1−C1 138.70(7), $C1^i$−Ag1−N1 105.33(6), C1−Ag1−N1 101.91(6), N1−Ag1−$N1^i$ 96.24(9), $C1^i$−Ag1−Ag2 48.11(4), C1−Ag1−Ag2 105.05(4), N1−Ag1−Ag2 85.39(5), $N1^i$−Ag1−Ag2 148.52(4). Symmetry codes: (i) $-x$, y, $-z+1/2$; (ii) x, $-y$, $z-1/2$; (iii) $-x$, $-y$, $-z$.

The central boron atom of the $[B(C_6F_5)_4]^-$ anion is tetracoordinated. The average length of the B−C(aryl) linkage

amounts to 1.649 Å (between 1.643 and 1.655 Å). The coordination geometry around boron in the BC_4 core is slightly distorted, with the smallest angle of 104.4(2)° and the largest 115.5(2)°.

$[Li(Et_2O)][B(C_6F_5)_4]\cdot CH_2Cl_2$ crystallizes in the monoclinic space group $P2_1/n$ with four formula units per cell. The asymmetric unit consists of one $[Li(Et_2O)]^+$ and $[B(C_6F_5)_4]^-$, as well as one CH_2Cl_2 molecule. Both the CH_2Cl_2 and the ether molecule are disordered. While the CH_2Cl_2 fills only the voids in the unit cell, the Et_2O molecules coordinate via the oxygen atom (d(Li−O) = 1.946(6) Å). Furthermore, three F···Li^+ contacts are observed, resulting in a strongly distorted tetrahedral Li^+ coordination geometry with F−Li−F and F−Li−O bonding angles of 135.3(2)°, 88.8(1)°, 86.7(1)° and 109.8(2)°, 110.2(2)°, 122.2(2)°, respectively, as depicted in Figure 2. Two types of coordination modes are found for the three F···Li^+ contacts: (i) monodentate via $F11^i$ atom (d(Li−$F11^i$) = 1.996(6) Å); (ii and iii) bidentate via two F atoms (d(Li−F1) = 2.020(2), d(Li−F15) = 2.003(3) Å) of another adjacent $[B(C_6F_5)_4]^-$ ion. The sum of van der Waals radii for lithium and fluorine is 3.3 Å.[32] Taking this value into consideration, an additional weak F···Li^+ contact is found (d(Li−$F12^i$) 2.489(4) Å), so that the coordination around the Li^+ ion is best described as a 4+1 coordination. Such weak F···Li^+ contacts (with distances of 2.3−3.3 Å) were already observed by Strauss in lithium salts of the type $Li[Al\{OCH(CF_3)_2\}_4]$ and $Li[Al\{OCH(CF_3)_2\}_4]$.[33]

[Li(toluene)][$B(C_6F_5)_4$]·toluene crystallizes in the triclinic space group $P\bar{1}$ with two formula units per cell. The asymmetric unit consists of one $[Li(toluene)]^+$ and $[B(C_6F_5)_4]^-$, as well as one noncoordinating toluene molecule (Figure 3). The most interesting structural feature is the coordination of the Li^+ ion, which coordinates to nine atoms (Figure S2, see Supporting Information). Besides one strongly interacting toluene molecule, which coordinates via all six ring carbon atoms in a η^6 fashion with Li−C distances of 2.515(4)−2.731(4) Å (cf. 2.533(16)−2.751(11) Å in [Li(benzene)][$B(C_6F_5)_4$]·benzene),[34] four F···Li^+ contacts with three different $[B(C_6F_5)_4]^-$ ions are observed, resulting in a strongly distorted pseudo-square-pyramidal Li^+ coordination geometry (toluene considered as one donor). Among these four F···Li^+ contacts are one bidentate (d(Li−F14) = 2.210(3) and d(Li−F15) = 2.052(3) Å) and two monodentate coordination modes (d(Li−$F9^i$) = 2.038(3) and d(Li−$F18^{ii}$ = 2.151(3) Å; cf. $\sum r_{ion}(Li^+F^-)$ = 1.90 (CN = 4) and 2.09 (CN = 6) Å).[35] The known [Li(benzene)][$B(C_6F_5)_4$]·benzene compound crystallizes isotypically as centrosymmetric dimers, also with two η^6-coordinated and two uncoordinated molecules of benzene per dimer.[34] Similar to [Li(toluene)][$B(C_6F_5)_4$]·toluene, each Li^+ cation is linked by two $[B(C_6F_5)_4]$ anions via short Li···F contacts to form a centrosymmetric dimer. In addition, the Li^+ cation displays a short contact to an F atom of a neighboring $[[B(C_6F_5)_4]^-$ anion.

Comparison of the $(C-C)_{toluene}$ bond lengths in the η^6-coordinated toluene molecule with those in the noncoordinating toluene molecule indicates that the coordinated $(C-C)_{toluene}$ bonds are slightly affected upon coordination in the $[Li(toluene)]^+$ ion, leading to slightly longer bonds on average (Figure 4).

$[Ag(Et_2O)_3][B(C_6F_5)_4]$ crystallizes in the triclinic space group $P\bar{1}$ with two formula units per cell. The silver cation is coordinated by three oxygen atoms of the diethyl ether molecules at significantly different distances. The local coordination environment, however, is almost planar. These fairly different Ag−O structural parameters can be attributed to steric repulsion between the ethyl groups. It should be noted that only a poor data set was obtained, which do not allow a detailed discussion of structural parameters but are good enough to prove unambiguously the existence of the $[Ag(Et_2O)_3]^+$ ion and the structural motif, in accord with structural data, published recently for $[Ag(Et_2O)_3][N(CN)_2\cdot 2B(C_6F_5)_3]$.[25] In agreement with these experimental observations, theoretical results by Feller and Dixon obtained for the gas-phase species $[Ag(Me_2O)_n]^+$ (n = 1−4, Me_2O = dimethyl ether) show the same picture.[36] The synthesis of $[Ag(Et_2O)_3][BF_4]$ has already been reported but without any structural data,[37] and in agreement with our observation this salt loses the ether molecules at room temperature. Weakly coordinating anions such as $[B(C_6F_5)_4]^-$ and $[N(CN)_2\cdot 2B(C_6F_5)_3]^-$ seem to stabilize this unusual tricoordination and lead to a larger thermal stability.

$[Ag(toluene)_3][B(C_6F_5)_4]$ also crystallizes in the triclinic space group $P\bar{1}$ with two formula units per cell. The asymmetric unit consists of one independent $[Ag(toluene)_3]^+$ and one $[B(C_6F_5)_4]^-$ ion (Figure 4). No significant cation···anion contacts are found (besides small $F_{aryl}\cdots H_{toluene}$ contacts, > 2.4 Å, and one Ag···F contact < 4.0 Å at 3.415 Å, cf. $\sum r_{vdW}$(Ag···F) = 3.2 Å).[35] The silver cation is coordinated by two carbon atoms (d(Ag−C) < 2.89 Å) of each of the three toluene molecules in an η^2 fashion (Figure S3, see Supporting Information), resulting in a coordination number of six. Each toluene molecule forms a short (d(Ag1−C17) = 2.413(2), d(Ag−C5) = 2.419(2), d(Ag−C12) = 2.440(2) Å) and a slightly longer bond (d(Ag−C4) = 2.552(2), d(Ag−C11) = 2.559(3), d(Ag1−C18) = 2.630(3) Å). The remaining four $Ag-C_{toluene}$ distances are in the range 2.89−3.80 Å (Figure S3) and can be considered to be weak van der Waals interactions (cf. $\sum r_{cov}$(Ag−C) = 2.215 and $\sum r_{vdW}$(Ag···C) = 3.4 Å).[35] The observed Ag−C distances are in good agreement with other Ag−C bonds in silver complexes; for example, in $[Ag(toluene)_2\{Al(OR^F)_4\}]$ (R^F = $CH(CF_3)_2$) Ag−C bonds in the range 2.363(5)−2.647(6) Å are found.[28] In the latter complex besides the η^2 coordination of the two toluene molecules, two strong Ag−O and two weak Ag···F interactions with the alkoxy anion are observed, while in $[Ag(toluene)_3][B(C_6F_5)_4]$ no strong stabilizing Ag···anion contacts are found.

The local silver coordination environment is slightly distorted pseudo trigonal planar with $C_{short}-Ag-C_{short}$ angles of 111.91°, 118.67°, and 128.81° (angle sum 359.39°). The distortion from perfect planarity can be attributed to packing effects. Recently, it was shown that weakly coordinating

(32) (a) Pauling, L. *The Nature of Chemical Bond*, 3rd ed.; Cornell University Press: Ithaca, NY, 1960. (b) Bondi, A. *J. Phys. Chem.* **1964**, *68*, 441.

(33) Ivanova, S. M.; Nolan, B. G.; Kobayashi, Y.; Miller, S. M.; Anderson, O. P.; Strauss, S. H. *Chem.—Eur. J.* **2001**, *7*, 503.

(34) Bolte, M.; Ruderfer, A.; Müller, T. *Acta Crystallogr.* **2005**, *E61*, m1581.

(35) Holleman, A. F.; Wiberg, E. N. *Lehrbuch der Anorganischen Chemie*, 102 ed.; Walter de Gruyter: Berlin, 2007; p 2002.

(36) Feller, D.; Dixon, D. *J. Phys. Chem. A* **2002**, *106*, 5136.

(37) Meerwein, H.; Hederich, V.; Wunderlich, K. *Ber. Deutsch. Pharm. Ges.* **1958**, *291*, 541.

anions[26] stabilize unusual tricoordination at Ag^+ as shown in $[Ag(Et_2O)_3][N[(CN)\cdot B(C_6F_5)_3]_2$ and $[Ag(\eta^2\text{-}C_2H_4)_3][Al\{OC(CF_3)_3\}_4]$, respectively.[25,38] Especially the $[Ag(\eta^2\text{-}C_2H_4)_3]^+$ ion, prepared by Krossing et al., and $[Ag(benzene)_3][B(C_6F_5)_4]$, prepared by Kitagawa, Komatsu, et al.,[39] strongly resemble the $[Ag(toluene)_3]^+$ ion with respect to structure and bonding. In all cases the key to formation of these complexes is the utilization of weakly coordinating ions, which formally generate pseudo-gas-phase conditions.[26a,40] Like $[Ag(toluene)_3]^+$ in $[Ag(toluene)_3][B(C_6F_5)_4]$, the $[Ag(\eta^2\text{-}C_2H_4)_3]^+$ ion forms an almost trigonal-planar, spokewheel arrangement. Furthermore, also no significant $(C-C)_{coordinated}$ bond elongation was found. The $(C-C)_{toluene}$ bond lengths compare well to those in uncoordinated toluene (cf. d(C4−C5) = 1.389(3), d(C11−C12) = 1.365(4), d(C17−C18) = 1.400(4), vs $d(C-C)_{uncoordinated}$ 1.327−1.391 Å in Figure S3 (see Supporting Information); in d(C−C) = 1.363−1.393 Å in pure toluene),[41] indicating that the coordinated $(C-C)_{toluene}$ bond is unaffected upon coordination in the $[Ag(toluene)_3]^+$ ion.

In comparison with the $[Ag(benzene)_3]^+$ ion it was found that the difference between the smaller and the longer Ag−C bonds (see above) is significantly smaller in $[Ag(toluene)_3]^+$ (average difference 0.284 vs 0.156 Å). Hence, in the case of $[Ag(benzene)_3]^+$ the authors concluded a nearly η^1 coordination, while in $[Ag(toluene)_3]^+$ an η^2 coordination like in $[Ag(\eta^2\text{-}C_2H_4)_3]^+$ can be assumed.

Examples of structurally characterized silver(I) compounds are still rare because of inter- and intramolecular exchange equilibria exhibiting a diverse complexity. Hence, the $[Ag(toluene)_3][B(C_6F_5)_4]$ fills this gap and represents an interesting extension to the $[Ag(\eta^2\text{-}C_2H_4)_3]^+$ and $[Ag(benzene)_3][B(C_6F_5)_4]$ ions. The first structural report on a "tris-benzene" Ag^+ complex, $[Ag(C_6D_6)_3][BF_4]$, was obtained by accident in the reaction of $[(dppe)RhCl]_2$ with EtCl in C_6D_6 and $AgBF_4$ as facilitator.[42] However, here the silver ion coordinates only one benzene-d_6 in a η^2 fashion, while the other two are coordinated in a η^1 fashion. The overall environment of the Ag^+ is trigonal-bipyramidal with one apical position occupied by a fluorine atom (d(Ag−F) = 2.488(8) Å).

$AgC_6F_5\cdot CH_3CN$ crystallizes in the monoclinic space group $C2/c$ with eight formula units per cell, which is isotypic to the related $AgC_6F_5\cdot C_2H_5CN$ compound.[5] The asymmetric unit consists of an $Ag_2(C_6F_5)$ unit attached to one CH_3CN molecule (Figure 5). In the unit cell two crystallographically different Ag ions, Ag1 and Ag2, are present (Figures 5 and 6), with Ag2 in linear coordination (d(Ag2−C) = 2.147(2), cf. 2.128(5) Å in $AgC_6F_5\cdot C_2H_5CN$) with two carbon atoms ($\angle(C1^{i}-Ag2-C1^{ii})$ = 180.00(7)°) of two bridging phenyl groups, while a bent C1−Ag−$C1^{i}$ moiety is found (d(Ag1−$C1^{i}$) = 2.387(5), cf. 2.128(5) Å in $AgC_6F_5\cdot C_2H_5CN$).[5,24,18] The acetonitrile molecule coordinates only to Ag1 at a distance of 2.392(2) Å,[22] which results in a distorted tetrahedral coordination.

Usually arylsilver[20−23] and perfluoroalkenylsilver[43] are tetrameric in the solid state, while diaryl argentates are built up from separated ion pairs.[24] Due to the existence of C_6F_5 bridges in $AgC_6F_5\cdot CH_3CN$, infinite chains are formed in the unit cell as depicted in Figure 6. While most silver compounds with a bridging aryl ligand form polynuclear complexes,[5,16−18,20−22] the first reported example, exhibiting an infinite chain, was the $AgC_6F_5\cdot C_2H_5CN$ compound.[5]

3. Experimental Section

General Information. All manipulations were carried out under oxygen- and moisture-free conditions under argon using standard Schlenk or drybox techniques.

Dichloromethane was purified according to a literature procedure,[44] dried over P_4O_{10}, and freshly distilled prior to use. *n*-Hexane and *n*-pentane were dried over Na/benzophenone/tetraglyme and freshly distilled prior to use. Acetonitrile was dried over P_4O_{10} and freshly distilled prior to use. Toluene was dried over Na/K/benzophenone and freshly distilled prior to use. Bromopentafluorobenzene (99%, Alfa Aesar) was freshly distilled prior to use. Boron trichloride (99.9%, Aldrich) was recondensed prior to use. Silver fluoride (Aldrich, 99%) and *n*-BuLi (2.5 M, in hexanes, Acros) were used as received. Tris(pentafluorophenyl)borane $B(C_6F_5)_3$,[27] lithium tetrakis(pentafluorophenyl)borate diethyl etherate, $Li[B(C_6F_5)_4]\cdot Et_2O$,[27] and silver tetrakis(pentafluorophenyl)borate diethyl etherate, $Ag[B(C_6F_5)_4]\cdot Et_2O$,[45,46] have been reported previously, but were prepared according to modified procedures.

NMR. $^{19}F\{^1H\}$, $^{13}C\{^1H\}$, ^{13}C-DEPT, $^{11}B\{^1H\}$, and ^1H NMR spectra were obtained on a Bruker AVANCE 250 or 300 spectrometer and were referenced internally to the deuterated solvent (^{13}C, CD_2Cl_2: $\delta_{reference}$ = 54 ppm, CD_3CN: $\delta_{reference}$ = 118.1 ppm, C_6D_6: $\delta_{reference}$ = 128 ppm) or to protic impurities in the deuterated solvent (^1H, $CDHCl_2$: $\delta_{reference}$ = 5.31 ppm, C_6D_5H: $\delta_{reference}$ = 7.16 ppm). CD_2Cl_2 and CD_3CN were dried over P_4O_{10}; C_6D_6 was dried over Na/benzophenone. IR: Nicolet 380 FT-IR with Smart Orbit ATR device was used. Raman: Bruker VERTEX 70 FT-IR with RAM II FT-Raman module, equipped with a Nd:YAG laser (1064 nm) was used.[47] CHN analyses: Analysator Flash EA 1112 from Thermo Quest or C/H/N/S-Mikronalysator TruSpec-932 from Leco was used. Melting points are uncorrected (EZ-Melt, Stanford Research Systems). Heating rate 20 °C/min (clearing points are reported). DSC: DSC 823e from Mettler-Toledo, heating rate 5 °C/min, was used.

For details concerning X-ray structure determination see Supporting Information.

Synthesis of Lithium Tetrakis(pentafluorophenyl)borate, Li[B(C_6F_5)$_4$]. To a stirred solution of C_6F_5Br (4.939 g, 20 mmol) in *n*-pentane (80 mL) is added dropwise *n*-BuLi (2.5 M, 8.2 mL, 20.5 mmol) at −80 °C over a period of 5 min. The resulting colorless suspension is stirred for 30 min at this temperature. A suspension of finely ground $B(C_6F_5)_3$ (10.75 g, 21 mmol) in *n*-pentane (40 mL) is then added in one portion. The resulting colorless suspension is stirred for a further 5 min at this temperature and is then slowly warmed to ambient temperatures over a period of one hour. The resulting colorless suspension is filtered (F4) and washed three times by repeated back distillations of solvent. Removal of solvent and drying *in vacuo* at 110 °C for 10 hours

(38) (a) Krossing, I.; Reisinger, A. *Angew. Chem.* **2003**, *115*, 5903; *Angew. Chem., Int. Ed.* **2003**, *42*, 5725. (b) Reisinger, A.; Trapp, N.; Krossing, I.; Altmannshofer, S.; Herz, V.; Presnitz, M.; Scherer, W. *Angew. Chem.* **2007**, *119*, 8445; *Angew. Chem., Int. Ed.* **2007**, *46*, 8295.

(39) Ogawa, K.; Kitagawa, T.; Ishida, S.; Komatsu, K. *Organomet.* **2005**, *24*, 4842.

(40) Cameron, T. S.; Decken, A.; Dionne, I.; Fang, M.; Krossing, I.; Passmore, J. *Chem.—Eur. J.* **2002**, *8*, 3386.

(41) Anderson, M.; Bosio, L.; Bruneaux-Poulle, J.; Fourme, R. *J. Chim. Phys. Phys.-Chim. Biol.* **1977**, 68.

(42) Batsanov, A. S.; Crabtree, S. P.; Howard, J. A. K.; Lehmann, Ch. W.; Kilner, M. *J. Organomet. Chem.* **1998**, *550*, 59.

(43) Jeffries, P. M.; Wilson, S. R.; Girolami, G. S. *J. Organomet. Chem.* **1993**, *449*, 203.

(44) Fischer, C. B.; Xu, S.; Zipse, H. *Chem.—Eur. J.* **2006**, *12*, 5779.

(45) Mukaiyama, T.; Maeshima, H.; Jona, H. *Chem. Lett.* **2001**, 388.

(46) Hayashi, Y.; Rohde, J. J.; Corey, E. J. *J. Am. Chem. Soc.* **1996**, *118*, 5502.

(47) Raman and IR data are given in the Supporting Information.

yields 9.199 g (13.4 mmol, 67%) of $Li[B(C_6F_5)_4]$ as a colorless solid. Mp: 253 °C (dec). Anal. Calcd (found): C, 42.02 (41.58); H, 0.00 (0.11). ^{11}B NMR (25 °C, C_6D_6, 96.3 MHz): δ −16.4. $^{13}C\{^1H\}$ NMR (25 °C, C_6D_6, 75.5 MHz): δ 123 (br, *ipso-C*), 137.3 (dm, *m-C*F, $^1J(^{13}C-^{19}F)$ = 246 Hz), 139.2 (dm, *p-C*F, $^1J(^{13}C-^{19}F)$ = 251 Hz), 148.6 (dm, *o-C*F, $^1J(^{13}C-^{19}F)$ = 238 Hz). $^{19}F\{^1H\}$ NMR (25 °C, C_6D_6, 282.4 MHz): δ −164.1 (m, *m-CF*, $^1J(^{13}C-^{19}F)$ = 246 Hz), −158.7 (dm, *p-CF*, $^1J(^{13}C-^{19}F)$ = 251 Hz), −134.9 (dm, *o-CF*, $^1J(^{13}C-^{19}F)$ = 238 Hz). Recrystallization from toluene gives $Li[B(C_6F_5)_4]\cdot 2$ toluene. Prolonged exposure to vacuum at elevated temperatures leads to a complete loss of the two toluene molecules.

Synthesis of Lithium Tetrakis(pentafluorophenyl)borate Diethyletherate, $Li[B(C_6F_5)_4]\cdot Et_2O$. To a stirred solution of C_6F_5Br (10.13 g, 41 mmol) in diethyl ether (200 mL) is added dropwise *n*-BuLi (2.5M, 16.4 mL, 41 mmol) at −80 °C over a period of 5 min. The resulting colorless suspension is stirred for 30 min at this temperature. A suspension of $B(C_6F_5)_3$ (20.48 g, 40 mmol) in diethyl ether (100 mL) is then added by means of PTFE tubing in one portion. The resulting colorless suspension is stirred for a further 10 min at this temperature and is then slowly warmed to ambient temperatures over a period of one hour. The solvent is removed *in vacuo*, resulting in a colorless, crystalline residue, which is washed two times with 100 mL portions of *n*-pentane and dried *in vacuo* (this crude product contains about 2.5 molecules of diethyl ether and shows a melting point of 120 °C). The crystalline residue is then slowly heated to 120 °C *in vacuo*, which yields 29.92 g (39.4 mmol, 98%) of $Li[B(C_6F_5)_4]\cdot Et_2O$ as a colorless solid. Mp: 184 °C. Anal. Calcd (found): C, 44.24 (44.06); H, 1.33 (1.47). ^1H NMR (25 °C, CD_2Cl_2, 300.13 MHz): δ 1.17 (t, 6H, CH_3, $^3J(^1H-^1H)$ = 7.1 Hz), 3.64 (q, 4H, CH_2, $^3J(^1H-^1H)$ = 7.1 Hz). ^{11}B NMR (25 °C, CD_2Cl_2, 80.3 MHz): δ −16.6. $^{13}C\{^1H\}$ NMR (25 °C, CD_2Cl_2, 62.9 MHz): δ 14.4 (s, CH_3), 67.5 (s, CH_2), 123.1 (br, *ipso-C*), 137.4 (dm, *m-C*F, $^1J(^{13}C-^{19}F)$ = 244 Hz), 139.3 (dm, *p-C*F, $^1J(^{13}C-^{19}F)$ = 249 Hz), 148.8 (dm, *o-C*F, $^1J(^{13}C-^{19}F)$ = 239 Hz). $^{19}F\{^1H\}$ NMR (25 °C, CD_2Cl_2, 282.4 MHz): δ −165.7 (m, *m-CF*, $^1J(^{13}C-^{19}F)$ = 244 Hz), −160.8 (dm, *p-CF*, $^1J(^{13}C-^{19}F)$ = 249 Hz), −135.5 (dm, *o-CF*, $^1J(^{13}C-^{19}F)$ = 239 Hz). The residual equivalent of diethyl ether may be removed by dissolution of $Li[B(C_6F_5)_4]\cdot Et_2O$ in excess toluene, removal of solvent, and drying for five hours at 60 °C *in vacuo*.

Synthesis of Silver Tetrakis(pentafluorophenyl)borate Diethyl Etherate, $Ag[B(C_6F_5)_4]\cdot Et_2O$. To a stirred solution of lithium tetrakis(pentafluorophenyl)borate diethyl etherate, $Li[B(C_6F_5)_4]\cdot Et_2O$ (7.601 g, 10 mmol), in diethyl ether (80 mL) is added ddropwise a solution of $AgNO_3$ (3.397 g, 20 mmol) in H_2O (20 mL, acidified with a few drops of HNO_3(conc)) at ambient temperatures, resulting in a colorless, clear aqueous layer and a colorless, clear diethyl ether layer. The mixture is shaken in a separation funnel and the ethereal layer is separated and washed again with H_2O (10 mL). The solvent is removed *in vacuo*, resulting in a pale brown residue, which is dried at 60 °C for two hours *in vacuo*. The resulting brownish solid is dissolved in dichloromethane (10 mL) and filtered (F4), resulting in a clear, colorless solution. Removal of solvent and drying *in vacuo* for three hours at 50 °C yields 8.206 g (9.53 mmol, 95%) of $Ag[B(C_6F_5)_4]\cdot Et_2O$ as a colorless microcrystalline solid. Mp: 117 °C (dec). Anal. Calcd (found): C, 39.06 (39.77); H, 1.17 (1.80). ^1H NMR (25 °C, CD_2Cl_2, 300.13 MHz): δ 1.30 (t, 6H, CH_3, $^3J(^1H-^1H)$ = 7.0 Hz, $^1J(^{13}C-^1H)$ = 126.4 Hz), 3.69 (q, 4H, CH_2, $^3J(^1H-^1H)$ = 7.0 Hz, $^1J(^{13}C-^1H)$ = 144.0 Hz). ^{11}B NMR (25 °C, CD_2Cl_2, 96.3 MHz): δ −14.7. $^{13}C\{^1H\}$ NMR (25 °C, CD_2Cl_2, 75.5 MHz): δ 16.0 (s, CH_3), 68.2 (s, CH_2), 124.8 (br, *ipso-C*), 136.9 (dm, *m-C*F, $^1J(^{13}C-^{19}F)$ = 245 Hz), 138.8 (dm, *p-C*F, $^1J(^{13}C-^{19}F)$ = 247 Hz), 148.7 (dm, *o-C*F, $^1J(^{13}C-^{19}F)$ = 239 Hz). $^{19}F\{^1H\}$ NMR (25 °C, CD_2Cl_2, 282.4 MHz): δ −165.7 (m, *m-CF*, $^1J(^{13}C-^{19}F)$ = 245 Hz), −161.8 (dm, *p-CF*, $^1J(^{13}C-^{19}F)$ = 247 Hz), −131.2 (dm, *o-CF*, $^1J(^{13}C-^{19}F)$ = 239 Hz).

Synthesis of Silver Tetrakis(pentafluorophenyl)borate Toluene Solvate, $Ag[B(C_6F_5)_4]\cdot 2$ Toluene. Silver tetrakis(pentafluorophenyl)-borate diethyl etherate, $Ag[B(C_6F_5)_4]\cdot Et_2O$ (1.722 g, 2 mmol), is dissolved in toluene (20 mL) at ambient temperatures, resulting in a colorless, oily outer layer and a colorless, clear upper layer. Removal of solvent results in a colorless solid, which is dried *in vacuo* for five hours at 50 °C. The resulting residue is dissolved in a minimum of hot toluene and cooled to ambient temperature over a period of 10 hours, resulting in the deposition of colorless crystals. The supernatant is removed, and the crystalline residue is washed with *n*-pentane (5 mL) and dried *in vacuo* for five hours at 50 °C, which yields 1.616 g (1.66 mmol, 83%) of $Ag[B(C_6F_5)_4]\cdot 2$ toluene as a microcrystalline solid. Mp: 94 °C (dec). Anal. Calcd (found): C, 47.00 (46.46); H, 1.66 (1.73). ^1H NMR (25 °C, CD_2Cl_2, 250.13 MHz): δ 2.39 (s, 3H, CH_3), 6.8−7.7 (m, 5H, *CH*-aryl). $^{11}B\{^1H\}$ NMR (25 °C, CD_2Cl_2, 80.3 MHz): δ −16.6. $^{13}C\{^1H\}$ NMR (25 °C, CD_2Cl_2, 62.9 MHz): δ 21.8 (s, CH_3, toluene), 123.1 (s, *p-C*H, toluene), 124 (br, *ipso-C*), 127.2 (s, *C*H, toluene), 129.8 (s, *C*H, toluene), 136.9 (dm, *m-C*F, $^1J(^{13}C-^{19}F)$ = 244 Hz), 138.9 (dm, *p-C*F, $^1J(^{13}C-^{19}F)$ = 244 Hz), 114.5 (s, *ipso-C*, toluene), 148.8 (dm, *o-C*F, $^1J(^{13}C-^{19}F)$ = 236 Hz). $^{19}F\{^1H\}$ NMR (25 °C, CD_2Cl_2, 282.4 MHz): δ −167.4 (m, *m-CF*, $^1J(^{13}C-^{19}F)$ = 244 Hz), −163.4 (dm, *p-CF*, $^1J(^{13}C-^{19}F)$ = 244 Hz), −133.3 (dm, *o-CF*, $^1J(^{13}C-^{19}F)$ = 236 Hz).

Synthesis of Pentafluorophenyl Silver, AgC_6F_5. Lithium tetrakis(pentafluorophenyl)borate, $Li[B(C_6F_5)_4]$ (6.859 g, 10 mmol), and silver fluoride (1.649 g, 13 mmol) were combined and suspended in dichloromethane (60 mL). The resulting orange-colored suspension was sonicated in an ultrasonic bath at 40−60 °C for eight hours. The resulting grayish suspension is filtered (F5), resulting in a brownish, clear solution. The solvent is removed *in vacuo*, and the resulting pale brownish solid is redissolved in *n*-hexane (30 mL), filtered (F4), and washed four times by repeated back distillations of solvent. Removal of solvent and drying *in vacuo* yields 2.461 g (8.95 mmol, 90%) of pure $Ag[B(C_6F_5)_4]$ as an off-white solid. Mp: 276 °C. Anal. Calcd (found): C, 26.21 (25.89); H, 0.00 (0.00). $^{13}C\{^1H\}$ NMR (25 °C, CD_3CN, 62.9 MHz): δ 121.7 (br, *ipso-C*), 137.0 (dm, *m-C*F, $^1J(^{13}C-^{19}F)$ = 252 Hz), 140.1 (dm, *p-C*F, $^1J(^{13}C-^{19}F)$ = 244 Hz), 150.0 (dm, *o-C*F, $^1J(^{13}C-^{19}F)$ = 221 Hz). $^{19}F\{^1H\}$ NMR (25 °C, CD_3CN, 282.4 MHz): δ −163.1 (m, *m-CF*), −159.1 (dm, *p-CF*), −106.5 (dm, *o-CF*). $^{19}F\{^1H\}$ NMR (25 °C, CD_2Cl_2, 282.4 MHz): δ −158.3 (m, *m-CF*), −143.8 (br, *p-CF*), −100.4 (dm, *o-CF*). Recrystallization from CH_3CN gives $AgC_6F_5\cdot(CH_3CN)$.

Recovering of $B(C_6F_5)_3$. The washing solutions from the synthesis of $Li[B(C_6F_5)_4]$ and AgC_6F_5 contain mainly $B(C_6F_5)_3$, which is recovered by sublimation at 110 °C for six hours (cf. 3.2). This procedure yields about 73% of the possible quantity of $B(C_6F_5)_3$ as a colorless solid, which can directly be used for further syntheses.

Acknowledgment. Financal support by the Deutsche Forschungsgemeinschaft (SCHU 1170/4-1) is gratefully acknowledged.

Supporting Information Available: Crystallographic data in CIF data format. The CIF files are also available online from the Cambridge Crystallographic Data Centre (CCDC Nos. 757606−757610). This material is available free of charge via the Internet at http://pubs.acs.org.

5.3 Blue Imino(pentafluorophenyl)phosphane and Its Iron Carbonyl Complexes

Marcus Kuprat, Mathias Lehmann, Axel Schulz, Alexander Villinger

Manuskript in Vorbereitung.

Blue Imino(pentafluorophenyl)phosphane and Its Ion Carbonyl Complexes

Marcus Kuprat,[a] Mathias Lehmann,[a] Axel Schulz,[a,b*] Alexander Villinger[a]

[a] *Universität Rostock, Institut für Chemie, Abteilung Anorganische Chemie, Albert-Einstein-Straße 3a, 18059 Rostock, Germany;* [b] *Leibniz-Institut für Katalyse e.V. an der Universität Rostock, Albert-Einstein-Str. 29a, 18059 Rostock, Germany.*

Abstract. The reaction of AgC_6F_5 in CH_2Cl_2 at ambient temperature gives imino(pentafluorophenyl)phosphane, Mes*N=P(C_6F_5) (**1**) in almost quantitative yield (96%), which could be isolated as highly viscous blue oil. The same reaction with LiC_6F_5 results in the formation of imino(amino)phosphane $(C_6F_5)_2$P–N(Mes*)–P=NMes* (**2**) (yield 93%). In a second series of experiments the analogous reaction of MC_6F_5 (M = Ag, Li) with dimeric [Cl–P(μ-N–Dipp)]$_2$ was studied leading to the formation of [R–P(μ-N–Dipp)]$_2$ (R = C_6F_5) (**3**) for M = Ag, while only decomposition products such as P(C_6F_5)$_3$ were observed in the reaction with the Li salt.

Highly labile Mes*–N=P–C_6F_5 (**1**) decomposes at ambient temperature forming amongst other products the diphosphane $(C_6F_5)_2$P–P(C_6F_5)$_2$ (**4**). Reaction of **1** with $Fe_2(CO)_9$ yields the iron carbonyl complexes Mes*–N=P(C_6F_5) · $Fe(CO)_4$ (**5**) and [Mes*–N=P(C_6F_5)]$_2$· $Fe(CO)_3$ (**6**). The structure, bonding and potential energy surface is discussed on the basis of B3LYP/6-31G(d,p) computations. According to time-dependent B3LYP calculations, the blue color of **1** arises from an n→π* electronic transition.

Introduction

The low-coordination number chemistry of phosphorus-nitrogen compounds has been extensively developed in the last almost 40 years thanks to the use of bulky groups.[i,ii] It has been possible to characterize these reactive PN species due to their kinetic and thermodynamic stabilization by appropriate substitution.

It was not until 1973 that Flick and Niecke were able to isolate a phosphorus(III)-nitrogen compound with the structural feature of a phosphazene, –P=N–.[iii] This first iminophosphane, a phosphazene with phosphorus in the coordination number two, was yielded from the reaction of bis(trimethylsilyl)aminodifluorophosphane with lithium-bis(trimethylsilyl)amide (eq. 1)

$$(Me_3Si)_2NPF_2 \xrightarrow[-\ LiF\ -\ Me_3SiF]{+\ LiN(SiMe_3)_2} (Me_3Si)_2NPNSiMe_3 \quad (eq.1)$$

Monomeric halogeno(imino)phosphanes, R–N=P–X (X = halogen), have been isolated only for derivatives involving the bulky Mes* (Mes* = 2,4,6-tri-*tert*-butylphenyl) substituent at nitrogen,[iv] which imposes a relative destabilization of the corresponding dimer due to substituent steric strain.[v] Slightly smaller substituents attached at the nitrogen atom such as the Dipp group (Dipp = 2,6 diisopropylphenyl) lead to 1,3-dihalogeno-*cyclo*-1,3-diphospha-2,4-diazanes.[vi] The electronic and kinetic reasons for this R–N=P–X / [ClP(μ-NR)]$_2$ dimerization process has been addressed recently.[vii] Furthermore it is known that electron-rich iminophosphanes of the type R–N=P–R (R = aryl, alkyl) can dimerize in a [2+1] cycloaddition.

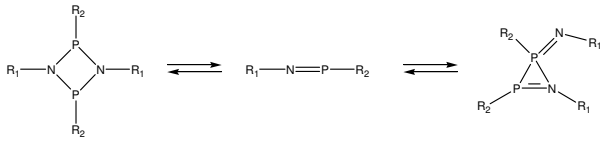

Scheme 1. Different channels for the dimerization of R–N=P–R.

Today, compounds bearing NP bonds are perhaps the most extensively studied inorganic species,[ii,viii] and a vast body of structural and spectroscopic data is available. However, much less is known about iminophosphane compounds containing the pentafluorophenyl group.[viiie] Herein we report on the synthesis of pentafluorophenyl substituted iminophosphanes and their iron carbonyl complexes.

Results and Discussion

Synthesis. Monomeric iminophosphanes of the type R–N=P–X (X = halogen) are only known for R = Mes*. Thus it was of interest to study, if it is possible to introduce the formal pseudohalogen pentafluorophenyl instead of the halogen X. The halogen/C_6F_5 substitution was attempted by means of the silver and the lithium C_6F_5 salts, MC_6F_5 (M = Ag, Li), as illustrated in Scheme 2. Surprisingly, only the reaction of AgC_6F_5 in CH_2Cl_2 at RT gives the desired product Mes*–N=P–C_6F_5 (**1**) in almost quantitative yield (96%), while 1,1-bis(pentafluorophenyl)-2,4-bis(2,4,6-tri-*tert*-butylphenyl)-1,3-diphospha-2,4-diazene, $(C_6F_5)_2$P–N(Mes*)–P=N–Mes* (**2**), was obtained in the reaction of LiC_6F_5 with Mes*–N=P–Cl in diethyl ether (yield 93%).

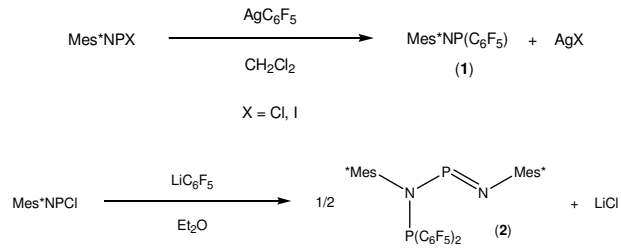

Scheme 2. Reaction of Mes*N=P–X with MC_6F_5 (M = Ag, Li).

While the synthesis of **1** can be cayrried out at ambient temperature, in the case of **2**, the reaction was carried out at –80°C and then slowly warmed to ambient temperatures over a

period of one hour. Obviously, the Lewis-acidic metal center plays an important role. Since the silver iodide and chloride, respectively, are sparingly soluble in contrast to lithium chloride, it can be assumed that the formation of **2** is mediated by solvated Li^+ species.

In a second series of experiments we studied the analogous reaction of MC_6F_5 (M = Ag, Li) with dimeric $[Cl–P(\mu\text{-}N–Dipp)]_2$ in order to investigate if there are also different reaction channels for the Cl/C_6F_5 substitution depending on the used metal. Indeed two different reaction pathways were detected too. While the reaction with the silver salt in CH_2Cl_2 at –80°C yielded the expected 1,3-bis(pentafluorophenyl)-2,4-bis(2,6-di-*iso*propylphenyl)-*cyclo*-1,3-diphospha-2,4-diazene $[DippNP(C_6F_5)]_2$ (**3**) (yield 65%, Scheme 3), only decomposition products such as $P(C_6F_5)_3$, characterized by X-ray structure elucidation, were obtained from the reaction with LiC_6F_5 in diethyl ether at –80°C, which is followed by a slow warming up. To the best of our knowledge $[DippNP(C_6F_5)]_2$ (**3**) has not been described yet.

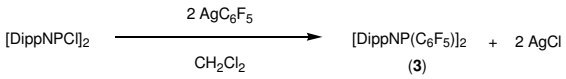

Scheme 3. Reaction of $[Cl–P(\mu\text{-}N–Dipp)]_2$ with AgC_6F_5.

Properties and characterization. Mes*–N=P–C_6F_5 (**1**) can be isolated as highly viscous, deep blue liquid in contrast to **2**, which is an orange crystalline solid. The blue color is rather unusual taking into account that the vast majority of PN species are either yellow or red colored. That together with the liquid state is the reason why **1** is called "blue magic" in our laboratory. The UV-Vis spectrum of the deep blue CH_2Cl_2 solution of **1** exhibits one very weak characteristic n→π* electronic transition at 592 nm (besides strong π→π* electronic transitions in the range < 380nm), which could be assigned on the basis of TD-B3LYP calculation (Tables supporting). The blue colour arises from the weak n→π* HOMO-LUMO electronic transition (Figure 1). The HOMO describes a delocalized mainly nonbonding molecular orbital with large coefficients along the C–N–P–C unit, while the LUMO displays an antibonding PN π* bond.

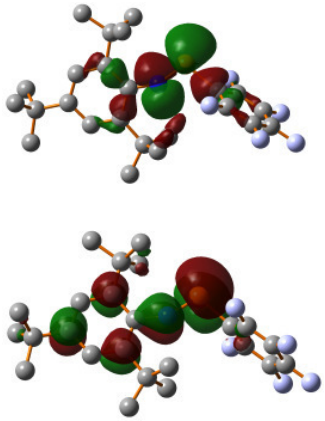

Figure 1. HOMO and LUMO in **1**.

Furthermore, **1** was characterized by elemental analysis, Raman / IR and NMR spectroscopy as well as mass spectrometry (ESI-TOF/MS: 457 [Mes*–N=P–C_6F_5]$^+$). The ^{31}P NMR spectrum of **1** displayed one singlet resonance at δ = 361.6, which is shifted to low field compared to the two resonances found for **2**, which are observed at δ = 11.49 (m, *P*NP) and 290.15 (d, $^2J(^{31}P\text{-}^{31}P)$ = 6.7 Hz, N*P*N), respectively. For comparison, the ^{31}P NMR shift of Mes*–P=N–Cl is found at δ = 139 and for Mes*–N≡P^+ at δ = 79.[iv]

In contrast to **2**, which is thermally stable at ambient temperature (Mp 123°C), compound **1** is thermally labile, moisture sensitive but stable under argon atmosphere over a long period at low temperature (–80 °C) as solid but slowly decomposes in benzene solution. Both compounds (**1** and **2**) can be prepared in bulk. This together with the very good solubility in common organic solvents makes both compounds good precursors for further synthesis.

Slow decomposition of **1** is already observed at ambient temperatures. Thermal treatment of **1** up to 120°C in vacuum (10^{-3}mbar) led to a fast decomposition yielding a yellow oil. Amongst the decomposition products diphosphane $(C_6F_5)_2P–P(C_6F_5)_2$ (**4**) could be isolated and characterized by X-ray single crystallography. Diphosphane $(C_6F_5)_2P–P(C_6F_5)_2$, which is easily prepared from the reaction of $(C_6F_5)_2PBr$ with mercury or magnesium, has already been reported,[ix] but so far, its structural data have not been published yet.

Table 1. ^{31}P NMR data (chemical shift in ppm) and selected structural data (distances in Å, angles in °) of amino(imino)phosphanes of the type $R^1R^2N–P=N–Mes^*$,[a] **1, 2**, Mes*–N=P–Cl, and Mes*$NP^+AlCl_4^-$.

R^1, R^2	P=N	PNC	^{31}P shift
H, Mes*	1.573(8)	126.1(7)	272
Me_3Si, Me_3Si	1.566(2)	117.6(2)	327
*i*Pr, *i*Pr	1.555(2)	129.6(2)	268
Me, Me	1.538(3)	140.7(4)	203
Mes*–N=P–Cp*	1.552(5)	125.9(4)	194
*t*Bu–N=P–Mes*	1.556(5)	122.7(5)	-
Mes*–N=P–*t*Bu	-	-	490
1[b]	1.565	153.2	363
2	1.541(2)	133.6(2)	11.5, 290
Mes*–N=P–I	1.480(3)	172.5(3)	218
Mes*–N=P–Br	1.499(6)	161.0(6)	153
Mes*–N=P–Cl [c]	1.506(2)	146.7(2)	139
Mes*–N=P–F	-	-	87
Mes*$NP^+AlCl_4^-$ [c]	1.475(8)	177.0(7)	79

[a] taken from reference x, [b] calculated values at the B3LYP/6-31G(d,p) level of theory, [c] taken from reference iv or xi.

Since it was impossible to obtain crystals of **1** suitable for single crystal structure elucidation (even at low temperature), **1** was reacted with $Fe_2(CO)_9$ to obtain iron-carbonyl adducts. The iron carbonyl adduct formation reaction is straightforward and can easily be followed by ^{31}P NMR experiments. Upon addition of a solution of **1** in *n*-hexane to a stirred suspension of $Fe_2(CO)_9$ in *n*-hexane at –50°, an immediate reaction occurred leading to a brown suspension (Scheme 4). The suspension was slowly warmed to ambient temperature. Filtration gave a dark red solution from which after concentration black crystals of $Fe_3(CO)_{12}$ were obtained. Decantation of the supernatant, further

concentration and storage at ambient temperature gave red crystals of *N*-(2,4,6-tri-*tert.*butylphenyl)imino(pentafluorophenyl)phosphane iron tetracarbonyl adduct Mes*NP(C_6F_5) · Fe(CO)$_4$ (**5**) which could be isolated in good yields (82%). It should be mentioned that [Mes*NP(C_6F_5)]$_2$· Fe(CO)$_3$ (**6**) was observed when no excess of $Fe_2(CO)_9$ was used.

Power *et al.* have frequently used iron carbonyl complexes to stabilize element-element double bonds, *e.g.* diphosphenes, RP=PR.[xii] For example, the reaction of $Na_2Fe(CO)_4$, with different bulky monosubstituted phosphorus(III) halides $RPCl_2$, where R = 2,4,6-$Me_3C_6H_2$, CH_2SiMe_3, $CH(SiMe_3)_2$, $N(SiMe_3)_2$, -OC_6H_2-2,6-tBu_2-4-Me, or -OC_6H_2-2,4,6-tBu_3) yielded products in which the phosphorus center behaves as either a diphosphene or a bridging phosphinidene group. Complexes **5** and **6** are rare examples of iron carbonyl complexes featuring an iminophosphane as ligand.

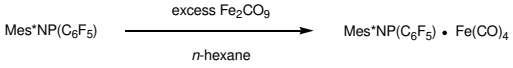

Scheme 4. Synthesis of **4**

Computations. Inspection of the conformational space at the B3LYP/6-31G(d,p) level of theory displayed two different monomeric structures for **1** (Figure 2): (i) a *cis* isomer (*cis*-**1**) and (ii) a *trans* arrangement (*trans*-**1**) with respect to the C_{Mes*}–N=P–C_{C6F5} moiety. Our calculation revealed that the *trans*-*cis* energy gap is rather small, with *trans* form being the most stable isomer (ΔE^{tot}(*cis*-*trans*) = +0.1 kcal/mol, ΔG^{298}(*cis*-*trans*) = 0.8 kcal/mol). Different dimerization processes must be considered. As shown in Figure 2, three different dimers were found: (i) a cyclic imino(amino)phosphane (**2**) with a NPNP connectivity and a diphosphene with a NPPN connectivity, and (ii) two isomers for *cyclo*-diphosphadiazane. In agreement with experiment, all computed dimerization processes are endergonic (*e.g.* ΔG^{298}(**2** – 2**trans*-**1**) = +16.1 kcal/mol). It should be noted that at least dimerization to **2** represents an exothermic process (G^{298}(**2** – 2**trans*-**1**) = –3.3 kcal/mol (see supporting information).

Since it was impossible to obtain experimental structural data for **1**, its structure was calculated for the gas phase at the B3LYP level of theory. Selected structural data of *trans*-**1** and *cis*-**1** along with data of different dimers are summarized in Table 2. The most interesting structural features of aryl substituted iminophosphanes are the short PN double bond and rather large CNP angles. While for *trans*-**1** and *cis*-**1** the PN distances of 1.555 and 1.552 Å, respectively, are fairly similar and in the expected range (*cf.* Σr_{cov}(P=N) = 1.52 Å),[xiii] the C_{Mes*}–N distance in *trans*-**1** (1.370 Å) is significantly shorter compared to that in *cis*-**1** (1.397 Å). Since for both species the CNPC unit is planar and allow delocalization of the 6π aryl electrons, the computed difference in the CN bond can be attributed to a larger steric strain in *cis*-**1**. In both species the C_6F_5 ring adopts a perpendicular position to the Mes* ring.

MO and NBO[xiv] calculations for **1** displayed highly polarized P–N and P–C bonds. While for the P–C bond only 31% of the NBO electron density is localized at the P atom, for the P–N σ bond this value is further decreased to 24 % but increased for the π bond to 39 %. The hybrid orbital at the P atom used for the P–C bond possesses 12% s atomic orbital character, which increases to 17% in the P–N bond. The calculated natural atomic orbital population (NAO) net charges are $q(C_{Mes*})$ = +0.14, –0.85 (N), +0.96 (P), and –0.49 *e* (C_{C6F5}) and alternate along the C_{Mes*}–N–P–C_{C6F5} unit. Charge comparison of the PN unit in **1** with neutral PN (q(P) = +0.77, q(N) = –0.77*e*) shows a charge transfer of only 0.10*e*, although the entire Mes* group donates 0.41 electrons of which, however, 0.30 electrons are accepted by the C_6F_5 group, describing a classic push pull situation.[ii]

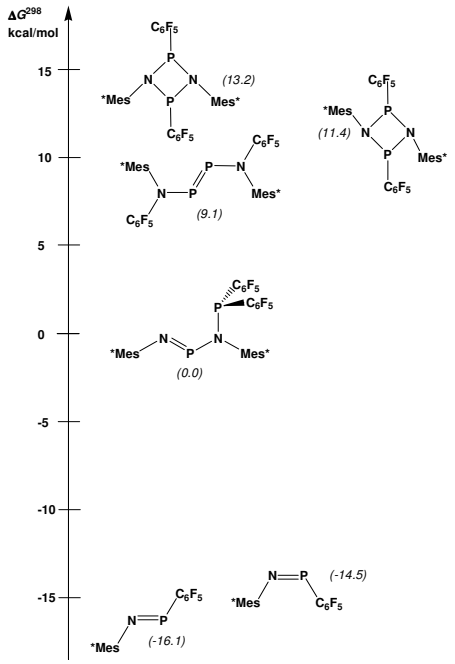

Figure 2. Relative Gibbs energies for the isomers of [Mes*NP(C_6F_5)]$_y$ (y = 1, 2) The exact values are given in parenthesis.

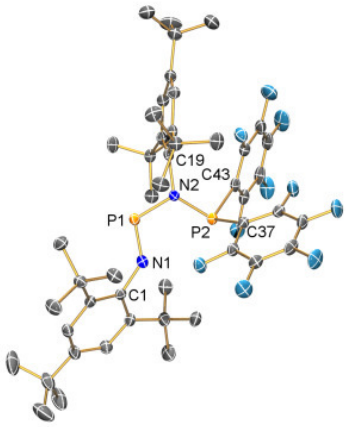

Figure 3. ORTEP drawing of the molecular structure of **2** in the crystal. Thermal ellipsoids with 50% probability at 173 K (hydrogen atoms omitted for clarity). Selected bond lengths (Å) and angles (°): P1–N1 1.541(2), P1–N2 1.726(2), P2–N2 1.740(2), P2–C43 1.846(2), P2–C37 1.872(2), N1–C1 1.419(3), N2–C19 1.473(3); N1–P1–N2 108.47(9), N2–P2–C43 104.09(9), N2–P2–C37 109.61(9), C43–P2–C37 101.1(1), C1–N1–P1 133.6(2), C19–N2–P1 111.5(1), C19–N2–P2 125.8(1), P1–N2–P2 120.7(1), N1–C1–C6 117.0(2), N1–C1–C2 124.2(2), C38–C37–P2 128.6(2), C42–C37–P2 115.6(2), C48–C43–P2 128.5(2), C44–C43–P2 115.9(2), N2–P1–N1–C1 –174.1(2), N1–P1–N2–C19 178.5(1), N1–P1–N2–P2 13.6(2).

Table 2. Calculated selected structural data of *trans*-**1**, *cis*-**1**, **2**, and dimers of **1**.

	CN	NP	PC	CNP	NPC	CNPC
trans-**1**	1.370	1.565	1.903	153.2	103.8	180.0
cis-**1**	1.397	1.552	1.905	148.2	113.9	0.3
2	1.410	1.568	1.862	111.5	104.4	-22.3
	1.472	1.756	1.893	124.9	110.2	85.9
		1.780		131.9		
trans-dimer	1.437	1.772	1.899	119.6	102.3	-46.1
	1.437	1.763	1.900	119.6	102.8	-113.4
		1.764		134.9	106.4	48.6
		1.774		135.3	107.2	112.4
cis-dimer	1.444	1.757	1.918	122.3	104.8	-74.8
	1.451	1.763	1.920	122.9	106.8	-77.0
	-	1.764	-	138.2	108.2	61.3
	-	1.768	-	138.8	110.1	88.4

MO and NBO[xv] calculations for **1** displayed highly polarized P–N and P–C bonds. While for the P–C bond only 31% of the NBO electron density is localized at the P atom, for the P–N σ bond this value is further decreased to 24 % but increased for the π bond to 39 %. The hybrid orbital at the P atom used for the P–C bond possesses 12% s atomic orbital character, which increases to 17% in the P–N bond. The calculated natural atomic orbital population (NAO) net charges are $q(C_{Mes*})$ = +0.14, –0.85 (N), +0.96 (P), and –0.49 *e* (C_{C6F5}) and alternate along the C_{Mes*}–N–P–C_{C6F5} unit. Charge comparison of the PN unit in **1** with neutral PN (q(P) = +0.77, q(N) = –0.77*e*) shows a charge transfer of only 0.10*e*, although the entire Mes* group donates 0.41 electrons of which, however, 0.30 electrons are accepted by the C_6F_5 group, describing a formal classic push pull situation.[ii]

X-ray crystallography. The structures of compounds **2** - **6** have been determined. Tables 2 and 3 present the X-ray crystallographic data. Selected molecular parameters are listed in Figures 3 - 6. X-ray quality crystals of all considered species were selected in Kel-F-oil (Riedel deHaen) or Fomblin YR-1800 (Alfa Aesar) at ambient temperature. All samples were cooled to –100(2)°C during the measurement.

*Mes*N=P–N(Mes*)–P(C_6F_5)$_2$* (**2**) crystallizes in the triclinic space group *P*-1 with two formula units per cell. The structure consist of separated Mes*N=P–N(Mes*)–P(C_6F_5)$_2$ and triply disordered CH_2Cl_2 molecules with no significant intermolecular contacts. In contrast to the trigonal pyramidal P2 atom, both nitrogen atoms and the di-coordinated P1 atom sit in a trigonal planar environment with a PN double bond of 1.541(2) (P1–N1), and two PN single bonds of 1.726(2) (P1–N2), and 1.740(2) Å (P2–N2), respectively, which lies in the expected range for amino(imino)phosphanes, for example P=N 1.545(6) and P–N 1.632(6) in MeN(H)–P=N–Mes* (Σr_{cov}(P–N) = 1.76 and Σr_{cov}(P=N) = 1.52 Å).[ii,x,xiii]

Since the phenyl ring of the Mes* group attached to N1 lies orthogonal to the plane composed of N1, P1, N2 and P2 there is no interaction between the PN π-bond and the π system of the phenyl ring (Figure 3). A look along the N1, P1, N2 and P2 unit displays a *cis* conformation and an almost planar arrangement of all four atoms (<N1–P1–N2–P2 13.6(2)°). While a rather small angle is found around the di-coordinated P1 atom (<N1–P1–N2 108.47(9)°), due to steric repulsion the angle around the di-coordinated N1 atom is fairly large with 133.6(2)° (<C1–N1–P1).

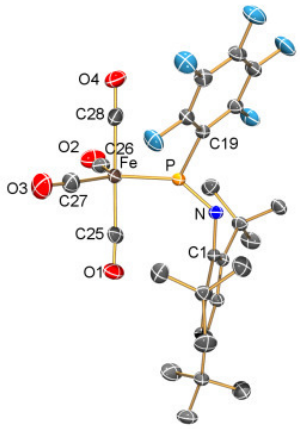

Figure 4. ORTEP drawing of the molecular structure of **5** in the crystal. Thermal ellipsoids with 50% probability at 173 K (hydrogen atoms omitted for clarity). Selected bond lengths (Å) and angles (°): P–N 1.558(1), P–C19 1.825(1), P–Fe 2.1225(3), N–C1 1.417(1), Fe–C28 1.803(1), Fe–C27 1.804(1), Fe–C26 1.812(1), Fe–C25 1.819(1), O1–C25 1.130(2), O2–C26 1.135(2), O3–C27 1.141(2), O4–C28 1.134(2); N–P–C19 101.66(5), N–P–Fe 138.80(4), C19–P–Fe 119.52(4), C1–N–P 125.47(8), C28–Fe–C27 90.09(6), C28–Fe–C26 90.32(6), C27–Fe–C26 115.08(7), C28–Fe–C25 178.19(5), C27–Fe–C25 89.78(6), C26–Fe–C25 91.38(5), C28-Fe–P 88.84(4), C27–Fe–P 122.33(5), C26–Fe–P 122.58(5), C25–Fe–P 89.71(4), C19–P–N–C1 177.23(9).

Table 3. Crystallographic details of **2**, **5** **6** and **4**.

	2	**5**	**6**	**4**
Chem. Formula	$C_{48.98}H_{59.96}Cl_{1.96}F_{10}N_2P_2$	$C_{28}H_{29}F_5FeNO_4P$	$C_{51}H_{58}F_{10}FeN_2O_3P_2$	$C_{24}F_{20}P_2$
Form. Wght. [g mol^{-1}]	998.13	625.34	1054.78	730.18
Colour	Orange	Red	Red	Colourless
Cryst. system	Monoclinic	Triclinic	Monoclinic	Tetragonal
Space group	$P2_1/n$	P-1	$P2_1/n$	P-42_1c
a [Å]	18.2786(7)	8.6162(3)	20.3424(6)	12.9649(16)
b [Å]	10.6517(4)	10.4409(3)	22.6247(7)	12.9649(16)
c [Å]	26.1221(10)	17.9784(6)	24.7584(8)	42.228(12)
α [°]	90.00	93.508(2)	90.00	90.00
β [°]	99.774(2)	98.424(2)	112.2600(10)	90.00
γ[°]	90.00	113.3970(10)	90.00	90.00
V [Å^3]	5012.1(3)	1455.60(8)	10545.6(6)	7098(2)
Z	4	2	8	12
$\rho_{calc.}$ [g cm^{-3}]	1.323	1.427	1.329	2.050
μ [mm^{-1}]	0.264	0.639	0.424	0.359
$\lambda_{MoK\alpha}$ [Å]	0.71073	0.71073	0.71073	0.71073
T [K]	173(2)	173(2)	173(2)	173(2)
Measured reflections	44100	48927	77741	19726
Independent reflections	11440	10458	18565	5223
Reflections with $I > 2\sigma(I)$	8501	8133	9788	3834
$R_{int.}$	0.0463	0.0331	0.1054	0.0542
F(000)	2085	644	4384	4248
R_1 (R [$F^2 > 2\sigma(F^2)$])	0.0562	0.0339	0.0520	0.0486
wR_2 (F^2)	0.1445	0.0958	0.1101	0.1045
GooF	1.057	1.049	0.919	1.073
Parameters	655	401	1320	622
CCDC #	-	-	-	

*Mes*NP(C_6F_5) · Fe(CO)$_4$* (**5**) crystallizes in the space group $P2_1/n$ with eight molecules per unit cell and one independent molecules per asymmetric unit. The perspective view of the complex is illustrated in Figure 4. The primary coordination sphere consists of an iron centered trigonal bipyramidal arrangement of the four CO ligands and the *trans*-Mes*–N=P–C_6F_5 ligands (C_{axis}–Fe–C/P_{plane} angles between 89.8 and 91.4°, axis: C28–Fe–C25 178.19(5), trigonal plane: C27–Fe–C26 115.08(7), C27–Fe–P 122.33(5), C26–Fe–P 122.58(5) °). Seven CO···F–C intermolecular interactions with three different Mes*NP(C_6F_5) ligands are observed besides numerous C–F···H–C contacts. The O···F distances between 2.802(1) (O1···F2') and 3.000(2) Å (O1···F3'), respectively, lie within the range of weak F···O van der Waals interactions (*cf.* Σr_{vdW}(F–O) = 3.0 Å).[xiii] Due to these van der Waals interactions, in the crystal the iron complexes are arranged in such a manner that stacked chains of alternating polar "Fe(CO)$_4$-units" and non-polar "Mes*-units" are formed.

The Mes*–N=P–C_6F_5 ligand is part of the trigonal plane and attached to the iron atom via the phosphorus with a Fe–P bond lengths of 2.1225(3) Å (*c.f.* 2.232 (l) Å in the diphosphene iron carbonyl complex (CO)$_4$Fe–P(R)=P(R)–Fe(CO)$_4$, R = N(SiMe$_3$)$_2$).[xvi]

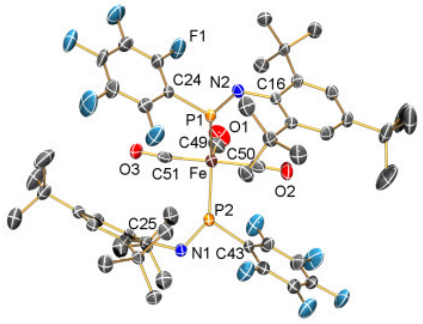

Figure 5. ORTEP drawing of the molecular structure of **6** in the crystal. Thermal ellipsoids with 50% probability at 173 K (hydrogen atoms omitted for clarity). Selected bond lengths (Å) and angles (°):Fe1–C49 1.803(4), Fe1–C51 1.816(4), Fe1–C50 1.819(4), Fe1–P1 2.133 (1), Fe1–P2 2.134(1), P1–N2 1.562(3), P1–C19 1.833(3), P2–N1 1.566(3), P2–C43 1.830(3), N1–C25 1.419(4), N2–C1 1.425(4); C49–Fe1–C51 92.9(2), C49–Fe1–C50 93.8(2), C51–Fe1–C50 173.3(2), C49–Fe1–P1 111.9(1), C51–Fe1–P1 87.1(1), C50–Fe1–P1 89.6(1), C49–Fe1–P2 110.1(1), C51–Fe1–P2 91.9(1), C50–Fe1–P2 86.6(1), P1–Fe1–P2 137.98(4), N2–P1–C19 101.5(2), N2–P1–Fe1 137.5(1), C19–P1–Fe1 120.9(1), N1–P2–43 101.9(2), N1–P2–Fe1 138.1(1), C43–P2–Fe1 119.8(1), C25–N1–P2 121.3(2).

The P–N distance in **2** (1.558(1) Å) is found in the range expected for the free ligand (calculated value for the gas phase species 1.565 Å, in Mes*N=P–N(Mes*)–P(C_6F_5)$_2$ (**2**) 1.541(2) Å). This is probably due to the fact, that the HOMO (Figure 1) represents a nonbonding molecular orbital with a large coefficient at the P atom. Thus, this MO describes mainly the lone pair localized at the P atom in the Lewis picture. The steric effects of binding Fe(CO)$_4$ to the Mes*–N=P–C_6F_5 species in **4** is reflected in the position (trigonal plane) and orientation of the Mes* and C_6F_5 aryl rings. Both rings and the almost planar C1–N–P–C19 unit (C19–P–N–C1 177.23(9)°) are oriented parallel to the Fe(CO)$_4$ fragment.

[Mes*NP(C_6F_5)]$_2$· Fe(CO)$_3$ (**6**) crystallizes in the monoclinic space group $P2_1/n$ with eight formula units (two independent molecules) per cell. In contrast to **2**, only one CO···F–C intermolecular interaction is observed (2.713(3) Å). With respect to bond lengths and angles similar structural features are found for the tricarbonyl iron complex **6** in comparison to the tetracarbonyl iron complex **5**: (i) The molecular structure also displays a slightly distorted trigonal bipyramidal iron center with the two Mes*–N=P–C_6F_5 ligands occupying a position in the trigonal plane. (ii) Both Mes–*N=P–C_6F_5 ligands are attached via the P atom (Fe1–P1 2.133(1), Fe1–P2 2.134(1) Å). (iii) The Mes*–N=P–C_6F_5 ligands adopt a *trans* configuration with an almost planar C–P–N–C unit (<C19–P1–N2–C1 178.8(3) and <C25–N1–P2–C43 177.0(2)°). (iv) Both PN bond lengths (P2–N1 1.566(3), P1–N2 1.562(3) Å) are found in the expected range for a typical double bond (*cf.* Σr_{cov}(P=N) = 1.52 Å.).

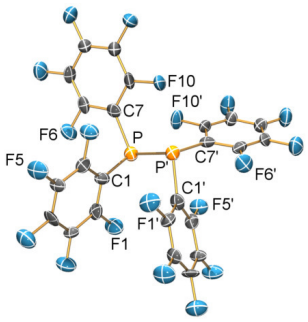

Figure 7. ORTEP drawing of the molecular structure of **4** in the crystal. Thermal ellipsoids with 50% probability at 173 K (hydrogen atoms omitted for clarity). Selected bond lengths (Å) and angles (°):P1–C7 1.848(6), P1–C1 1.868(6), P1–P1^i 2.248(3); C7–P1–C1 99.9(3), C7–P1–P1^i 102.8(2), C1–P1–P1^i 95.0(2). Symmetry codes: (i) $-x$, $-y$+1, z.

Diphosphane (C_6F_5)$_2$P–P(C_6F_5)$_2$ (***4***) crystallizes in the tetragonal space group P-42$_1$c with 12 formula units per cell (three independent molecules). The structure consists of separated (C_6F_5)$_2$P–P(C_6F_5)$_2$ molecules with no significant intermolecular contacts. The main feature of interest is the P–P distance of 2.248(3) Å**,** which is slight1y longer than the sum of the covalent radii 2.2 Å. This slight increase is expected in view of the electronegative C_6F_5 moiety reducing the electron density in the bonding orbitals of the P–P unit. Both PR_2 fragments adopt a C_2 symmetric staggered configuration to each other.

Acknowledgements

We are indepted to Dr. D. Michalik and J. Thomas (Univ. Rostock). Generous support by the University of Rostock is gratefully acknowledged. We would like to thank the Deutsche Forschungsgemeinschaft (SCHU 1170/4-1) for financial support.

Experimental Details

All manipulations were carried out under oxygen- and moisture-free conditions under argon using standard Schlenk or drybox techniques.
Dichloromethane was purified according to a literature procedure,[xvii] dried over P_4O_{10} and freshly distilled prior to use. Diethylether was dried over Na/benzophenone and freshly distilled prior to use, *n*-hexane was dried over Na/benzophenone/tetraglyme and freshly distilled prior to use. *N*-BuLi (2.5M, Acros) was used as received. Pentafluorophenylsilver AgC_6F_5,[xviii] *N*-(2,4,6-tri-*tert.*butyl-phenyl)imino(chloro)phosphine Mes*NPCl, *N*-(2,4,6-tri-*tert.*butylphenyl)imono(iodo)phosphine Mes*NPI[xix] and 1,2-dichloro-2,4-bis(2,6-diisopropylphenyl)-*cyclo*-diphosphadiazane [DippNPCl]$_2$,[xx] were prepared as previously reported. Fe_2CO_9 was a kind gift of Prof.(em.) J. Beck (LMU München).

NMR: $^{31}P\{^1H\}$, $^{13}C\{^1H\}$, $^{11}B\{^1H\}$, $^{19}F\{^1H\}$ and ^1H NMR spectra were recorded on a Bruker spectrometer AVANCE 250, 300 or 400. The chemical shifts were referenced to solvent signals (CD_2Cl_2: δ ^1H = 5.31, δ ^{13}C = 54.0). CD_2Cl_2 was dried over P_4O_{10}, **IR**: Nicolet 380 FT-IR with a Smart Orbit ATR device was used. **Raman**: Bruker VERTEX 70 FT-IR with RAM II FT-Raman module, equipped with a Nd:YAG laser (1064nm) was used. **CHN analyses**: Analysator Flash EA 1112 from Thermo Quest, or C/H/N/S-Mikronalysator TruSpec-932 from Leco were used. **Melting points** are uncorrected (EZ-Melt, Stanford Research Systems). Heating-rate 20 °C/min (clearing-points are reported). **DSC**: DSC 823e from Mettler-Toledo (Heating-rate 5 °C/min) was used. **MS**: Finnigan MAT 95-XP from Thermo Electron was used.

***N*-(2,4,6-tri-*tert.*butylphenyl)imino(pentafluorophenyl)phosphane Mes*NP(C_6F_5) (1).** To a stirred solution of Mes*NPX (X = Cl: 0.160 g, 0.68 mmol, X = I: 0.326 g, 1.0 mmol) in CH_2Cl_2 (5 ml) a suspension of AgC_6F_5 (0.190 g, 0.582 mmol) in CH_2Cl_2 (7 ml) is added dropwise at -80°C over a period of 20 minutes. The resulting dark blue suspension is stirred for 10 minutes and then slowly warmed to ambient temperatures over a period of one hour. The solvent is removed *in vacuo* and the residue is extracted with *n*-hexane (10 mL) and filtered. Removal of solvent and drying *in vacuo* yields 0.256 g (0.559 mmol, 96%) of *N*-(2,4,6-tri-*tert.*butylphenyl)imino(pentafluorophenyl)phosphane Mes*NP(C_6F_5) (**1**) as a blue oil. Anal. calc. % (found) for $C_{24}H_{29}F_5NP$ (457.46): C, 63.01 (61.23); H, 6.39 (5.98); N, 3.06 (2.98). ^{1}H-NMR (25 °C, CD_2Cl_2, 300.13 MHz): δ = 1.35 (s, 9 H, *p*-C(CH_3)$_3$), 1.37 (s, 18 H, *o*-C(CH_3)$_3$), 7.41 (d, 2 H, $^5J(^{31}P-^1H)$ = 7.41 Hz, *m*-C*H*). $^{13}C\{^1H\}$-NMR (25°C, CD_2Cl_2, 75.48 MHz): δ = 32.53 (d, $^5J(^{31}P-^{13}C)$ = 2.8 Hz, *o*-C(CH_3)$_3$), 33.63 (d, $^7J(^{31}P-^{13}C)$ = 4.7 Hz *p*-C(CH_3)$_3$), 35.21 (s, *p*-*C*(CH_3)$_3$), 36.60 (s, *o*-*C*(CH_3)$_3$), 122.52 (s, *m*-*C*H), 133.83 (aryl-*C*), 138.2 (dm, $^1J(^{13}C-^{19}F)$ = 257 Hz, aryl-*C*F), 144.6 (dm, $^1J(^{13}C-^{19}F)$ = 260 Hz, aryl-*C*F), 145.65 (aryl-*C*), 147.4 (dm, $^1J(^{13}C-^{19}F)$ = 250 Hz, aryl-*C*F), 149.16 (aryl-*C*), $^{31}P\{^1H\}$-NMR (25 °C, CD_2Cl_2, 121.51 MHz): δ = 361.6.

$^{19}F\{^{1}H\}$-NMR (25°C, CD_2Cl_2, 282.38 MHz): δ = -160.44 (m, *m*-C*F*), -147.27 (m, *p*-C*F*), -136.54 (m, *o*-C*F*). IR (ATR, 16 scans): 2958 (m), 2907 (m), 2870 (m), 1638 (m), 1597 (w), 1557 (w), 1514 (s), 1470 (s), 1426 (m), 1417 (m), 1392 (m), 1381 (m), 1362 (m), 1347 (w), 1287 (m), 1264 (m), 1240 (m), 1216 (m), 1200 (m), 1141 (w), 1113 (w), 1085 (s), 1023 (w), 974 (s), 955 (m), 923 (m), 877 (m), 852 (w), 823 (w), 793 (w), 765 (m), 739 (w), 726 (m), 716 (w), 686 (w), 665 (w), 645 (m), 631 (m), 608 (w), 584 (w), 546 (w), 532 (w). Raman (100 mW, 25°C, 500 scans, cm^{-1}): = 2963 (9), 2911 (10), 2781 (2), 2712 (2), 1640 (4), 1600 (7), 1552 (1), 1533 (1), 1516 (1), 1451 (4), 1419 (7), 1395 (4), 1381 (2), 1365 (3), 1328 (3), 1288 (6), 1267 (5), 1204 (4), 1184 (2), 1149 (3), 1094 (1), 1069 (1), 1055 (1), 1026 (1), 927 (2), 910 (1), 892 (1), 863 (1), 854 (1), 825 (5), 784 (1), 771 (1), 754 (1), 739 (1), 718 (1), 682 (5), 644 (1), 622 (1), 606 (1), 587 (3), 570 (3), 546 (1), 507 (1), 487 (2), 446 (2), 429 (1), 394 (2), 367 (1), 346 (1), 330 (1), 314 (1), 285 (3), 261 (2), 229 (1), 219 (1), 201 (1), 165 (1), 141 (1), 121 (1). MS (EI, m/z, (>10%)): 41 (11), 57 (33), 69 (18), 77 (10), 110 (12), 198 (27) $[(C_6F_5)P]^+$, 246 (80) $[Mes*H]^+$, 261 (36) $[Mes*NH]^+$, 290 (100) $[Mes*NP]^+$, 366 (18) $[(C_6F_5)_2PH]+$, 493 (14), 550 (10). MS (ESI-TOF/MS): 262 $[Mes*NH_2]^+$, 457 $[Mes*NP(C_6F_5)]^+$. UV/Vis: 591.91 nm.

1,1-bis(pentafluorophenyl)-2,4-bis(2,4,6-tri-*tert.*butylphenyl)-1,3-diphospha-2,4-diazene $(C_6F_5)_2PN(Mes*)PNMes*$ (2). To a stirred solution of C_6F_5Br (0.247 g, 1.0 mmol) in Et_2O (10 ml) *n*-BuLi (2.5 M, 0.4 ml, 1.0 mmol) is added dropwise at -80°C over a period of 15 minutes. The solution of LiC_6F_5 is added quickly to a solution of Mes*NPCl (0.326 g, 1.0 mmol) in Et_2O (5 ml) at -80°C by means of a PTFE tubing, resulting in a yellow suspension. The solvent is removed *in vacuo* and the residue is extracted with *n*-hexane (10 mL) and filtered. Removal of solvent and drying *in vacuo* yields 0.427 g (0.467 mmol, 93.4%) of 1,1-bis(pentafluorophenyl)-2,4-bis(2,4,6-tri-*tert.*butylphenyl)-1,3-diphospha-2,4-diazene $(C_6F_5)_2PN(Mes*)PNMes*$ (**2**) as an orange solid. M.p. 123 °C. Anal. calc. % (found) for $C_{48}H_{58}F_{10}N_2P_2$ (914.92): C, 63.01 (62.99); H, 6.39 (6.81); N, 3.06 (2.82). ^{1}H-NMR (25 °C, CD_2Cl_2, 300.13 MHz): δ = 1.25 (s, 18 H, $C(CH_3)_3$), 1.33 (s, 18 H, $C(CH_3)_3$), 1.37 (s, 18 H, $C(CH_3)_3$), 7.33 (s, 2 H, *m*-C*H*), 7.42 (s, 2 H, *m*-C*H*). $^{13}C\{^{1}H\}$-NMR (25°C, CD_2Cl_2, 125.77 MHz): δ = 31.35 (s, *p*-$C(CH_3)_3$), 31.88 (s, *p*-$C(CH_3)_3$), 32.72 (s, *o*-$C(CH_3)_3$), 35.03 (s, *p*-$C(CH_3)_3$), 35.21 (s, *p*-$C(CH_3)_3$), 36.14 (s, *o*-$C(CH_3)_3$), 36.99 (s, *o*-$C(CH_3)_3$), 39.30 (s, *o*-$C(CH_3)_3$), 111.26 (dm, $^{1}J(^{31}P\text{-}^{13}C)$ = 71 Hz, aryl-C_6F_5), 123.05 (s, *m*-*C*H), 127.27 (s, *m*-*C*H), 136.86 (aryl-*C*), 138.22 (dm, $^{1}J(^{13}C\text{-}^{19}F)$ = 255 Hz, aryl-*C*F), 141.90 (m, $^{2}J(^{31}P\text{-}^{13}C)$ = 12 Hz, aryl-*C*N(P)P), 143.58 (aryl-*C*), 143.94 (dm, $^{1}J(^{13}C\text{-}^{19}F)$ = 257 Hz, aryl-*C*F), 148.99 (dm, $^{1}J(^{13}C\text{-}^{19}F)$ = 249 Hz, aryl-*C*F), 150.05 (aryl-*C*), 150.48 (aryl-*C*).$^{31}P\{^{1}H\}$-NMR (25 °C, CD_2Cl_2, 121.51 MHz): δ = 11.49 (m, *P*NP), 290.15 (d, $^{2}J(^{31}P\text{-}^{31}P)$ = 6.7 Hz, N*P*N).$^{19}F\{^{1}H\}$-NMR (25°C, CD_2Cl_2, 282.38 MHz): δ = -161.43 (m, *m*-C*F*), -148.57 (m, *p*-C*F*), -120.83 (m, *o*-C*F*). IR (ATR, 16 scans): 2953 (m), 2909 (m), 2871 (m), 1639 (m), 1602 (w), 1516 (s), 1473 (s), 1459 (s), 1408 (m), 1393 (m), 1385 (m), 1373 (w), 1361 (m), 1287 (m), 1269 (w), 1243 (m), 1217 (w), 1200 (w), 1190 (w), 1171 (w), 1142 (w), 1130 (w), 1090 (s), 1080 (s), 1041 (w), 1025 (w), 978 (s), 926 (w), 911 (w), 888 (m), 877 (m), 849 (s), 831 (m), 809 (w), 767 (m), 749 (w), 735 (s), 725 (m), 667 (w), 646 (m), 633 (m), 629 (m), 612 (w), 588 (w), 567 (w), 552 (w). Raman (250 mW, 25°C, 549 scans, cm^{-1}): = 2964 (1), 2926 (3), 2911 (3), 2884 (3), 2786 (1), 2712 (1), 1641 (2), 1603 (3), 1535 (1), 1518 (1), 1470 (1), 1453 (2), 1410 (3), 1373 (1), 1363 (1), 1296 (10), 1251 (1), 1211 (1), 1192 (1), 1159 (1), 1144 (1), 1098 (1), 1043 (1), 929 (1), 858 (1), 847 (1), 827 (1), 810 (1), 788 (1), 770 (1), 644 (1), 614 (1), 589 (1), 572 (1), 504 (1), 486 (1), 449 (1), 410 (1), 399 (1), 390 (1), 357 (1), 295 (1), 284 (1), 259 (1), 229 (1), 218 (1), 188 (1), 174 (1), 143 (1), 123 (1).MS (EI, m/z, (>10%)): 57 (69), 246 (60), 247 (11), 259 (12), 261 (18), 290 (31) $[Mes*NP]^+$, 402 (97), 403 (30), 418 (100), 442 (17), 457 (56) $[Mes*NP(C_6F_5)]^+$, 475 (12), 652 (14), 912 (10) $[M - 2 H]^+$. UV/Vis: 432.02 nm. Crystals suitable for X-ray crystallographic analysis were obtained, by cooling a saturated dichloromethane solution of **2** to -25°C over a period of ten hours.

1,3-bis(pentafluorophenyl)-2,4-bis(2,6-di-*iso*propylphenyl)-*cyclo*-1,3-diphospha-2,4-diazene $[DippNP(C_6F_5)]_2$ (3). To a stirred solution of $[DippNPCl]_2$ (0.242 g, 0.5 mmol) in CH_2Cl_2 (5 ml) a solution of AgC_6F_5 (0.275 g, 1.0 mmol) in CH_2Cl_2 (20 ml) is added dropwise at -80°C over a period of 15 minutes. The resulting brownish solution is slowly warmed to ambient temperatures and stirred for three resulting in an yellow suspension. The solvent is removed *in vacuo* and the residue is extracted with *n*-hexane (10 mL) and filtered. Removal of solvent and drying *in vacuo* yields 0.244 g (0.327 mmol, 65%) of 1,3-bis(pentafluorophenyl)-2,4-bis(2,6-di-*iso*propylphenyl)-*cyclo*-1,3-diphospha-2,4-diazene $[DippNP(C_6F_5)]_2$ (**3**) as an yellow solid. M.p. 133 °C. Anal. calc. % (found) for $C_{36}H_{34}F_{10}N_2P_2$ (746.60): C, 57.91 (57.81); H, 4.59 (4.72); N, 3.75 (3.50). IR (ATR, 16 scans): 3059 (w), 2962 (m), 2929 (m), 2868 (m), 1639 (m), 1582 (w), 1512 (s), 1461 (s), 1436 (m), 1384 (m), 1376 (w), 1363 (m), 1323 (m), 1303 (w), 1282 (m), 1253 (w), 1244 (m), 1195 (m), 1161 (w), 1137 (w), 1103 (w), 1074 (s), 1053 (w), 1040 (w), 1014 (w), 997 (w), 972 (s), 937 (m), 915 (m), 887(s), 798(s), 759 (w), 746 (w), 723(m), 681 (w), 638 (w), 619 (w), 589 (w), 551 (w), 539 (w). Raman (450 mW, 25°C, 2920 scans, cm^{-1}): = 3061 (2), 3023 (1), 2965 (7), 2935 (8), 2911 (7), 2867 (6), 2759 (1), 2715 (1), 1639 (4), 1589 (7), 1514 (1), 1465 (3), 1441 (4), 1366 (1), 1335 (3), 1305 (1), 1274 (10), 1218 (1), 1178 (1), 1162 (1), 1148 (1), 1104 (2), 1043 (2), 972 (1), 955 (1), 924 (1), 881 (2), 812 (1), 727 (1), 639 (2), 613 (2), 585 (2), 552 (2), 540 (1), 519 (1), 497 (4), 445 (3), 391 (2), 363 (1), 281 (2), 187 (2), 170 (1), 132 (4), 69 (9). MS (CI^+, isobutane): 747 $[[DippNP(C_6F_5)]_2 + H]^+$, 430 $[DippNP(C_6F_5) + i\text{-}Pr - H]^+$, 416 $[DippNP(C_6F_5) + i\text{-}Pr]^+$, 373 $[DippNP(C_6F_5)]^+$. Crystals suitable for X-ray crystallographic analysis were obtained, by cooling a saturated *n*-hexane solution of **3** to -25°C over a period of ten hours.

***N*-(2,4,6-tri-*tert.*butylphenyl)imino(pentafluorophenyl)-phosphane iron tetracarbonyl adduct $Mes*NP(C_6F_5) \cdot Fe(CO)_4$ (5).** To a stirred suspension of $Fe_2(CO)_9$ (0.363g, 1.0 mmol) in *n*-hexane (8 ml), a solution of $Mes*NPC_6F_5$ (0.457 g, 1.0 mmol) in *n*-hexane (10 ml) is added quickly at -50° without stirring. The suspension is then slowly warmed to ambient temperature over a period of two hours. The resulting brown suspension is stirred for three hours at this temperature and filtered (F4). The resulting browish red solution is concentrated to an approximate volume of 5 ml and cooled to 5°C for ten hours, resulting in the deposition of $Fe_3(CO)_{12}$. The supernatant is removed by filtration and further concentrated which results in the deposition of red crystals. Removal of supernatant by decantation and drying *in vacuo* yields 0.824 g (0.824 mmol, 82%) of *N*-(2,4,6-tri-*tert.*butylphenyl)imino(pentafluorophenyl)phosphane iron tetracarbonyl adduct $Mes*NP(C_6F_5) \cdot Fe(CO)_4$ (**5**) as red crystals. M.p. 103 °C (dec.). Anal. calc. % (found) for $C_{28}H_{29}F_5FeNO_4P$

(625.34): C, 53.78 (53.74); H, 4.67 (4.55); N, 2.24 (2.14). ^{1}H-NMR (25 °C, CD_2Cl_2, 300.13 MHz): δ = 1.28 (s, 9 H, *p*-C(CH_3)$_3$), 1.43 (s, 18 H, *o*-C(CH_3)$_3$), 7.32 (d, 2 H, ^{5}J(^{31}P-^{1}H) = 2.5 Hz, *m*-C*H*). ^{13}C{^{1}H}-NMR (25°C, CD_2Cl_2, 75.48 MHz): δ = 31.74 (s, *p*-C(CH_3)$_3$), 32.05 (s, *o*-C(CH_3)$_3$), 35.12 (d, ^{6}J(^{31}P-^{13}C) = 1.1 Hz, *p*-*C*(CH_3)$_3$), 36.64 (d, ^{4}J(^{31}P-^{13}C) = 1.9 Hz, *o*-*C*(CH_3)$_3$), 122.99 (d, ^{4}J(^{31}P-^{13}C) = 4.7 Hz, *m*-*C*H), 138.00 (aryl-*C*), 146.23 (aryl-*C*), 208.93 (d, ^{2}J(^{31}P-^{13}C) = 9.9 Hz, *C*O). ^{31}P{^{1}H}-NMR (25 °C, CD_2Cl_2, 121.51 MHz): δ = 300.60. ^{19}F{^{1}H}-NMR (25°C, CD_2Cl_2, 282.38 MHz): δ = -159.13 (m, *m*-C*F*), -148.63 (m, *p*-C*F*), -132.82 (m, *o*-C*F*). Raman (600 mW, 25°C, 1000 scans, cm^{-1}): = 3111 (1), 3090 (1), 2999 (2), 2959 (3), 2907 (3), 2777 (1), 2709 (1), 2082 (6), 2034 (5), 2003 (7), 1964 (1), 1643 (2), 1598 (4), 1460 (2), 1445 (2), 1418 (4), 1395 (2), 1362 (1), 1274 (10), 1201 (2), 1151 (2), 1129 (1), 1092 (1), 1041 (2), 926 (2), 890 (1), 850 (2), 822 (2), 789 (1), 753 (1), 621 (2), 598 (1), 586 (1), 567 (2), 535 (1), 506 (1), 492 (1), 445 (2), 423 (3), 413 (3), 386 (2), 350 (1), 335 (2), 312 (1), 278 (1), 258 (1), 233 (1), 150 (2), 112 (5), 86 (6).MS (EI, m/z, (>10%)): 41 (13), 57 (37), 246 (18) [Mes*]$^{+}$, 260 (11), 290 (25) [Mes*NP]$^{+}$, 297 (11), 313 (18), 315 (43), 440 (13), 513 (100) [Mes*NP(Fe)C_6F_5]$^{+}$, 541 (17) [Mes*NP(FeCO)C_6F_5]$^{+}$, 625 (10) [M]$^{+}$. Crystals suitable for X-ray crystallographic analysis were obtained, by storage of a saturated *n*-hexane solution of **5** at ambient temperature for ten hours.

(i) (a) *Multiple Bonds and Low Coordination in Phosphorus Chemistry*, ed. Regitz, M.; Scherer, O. J. Weinheim, 1990. (b) Weber, L. *Chem. Rev.* **1992**, *92*, 1839. (c) Weber, L. *Chem. Ber.* **1996**, *129*, 367.

(ii) Niecke, E.; Gudat, D. *Angew. Chem.* **1991**, *103*, 251 – 270; *Angew. Chem., Int. Ed. Engl.* **1991**, *30(3)*, 217 – 37 and references therein.

(iii) Niecke, E.; Flick, W. *Angew. Chem.* **1973**, *85(13)*, 586 – 587; *Angew. Chem., Int. Ed. Engl.* **1973**, *12*, 585 – 586.

(iv) E. Niecke, M. Nieger, F. Reichert *Angew. Chem.* **1988**, *12*, 1781–1782; *Angew. Chem. Int. Ed.* **1988**, *27*, 1715–1716.

(v) (a) Burford, N.; Clyburne, J. A. C.; Chan, M. S. W. *Inorg. Chem.* **1997**, *36*, 3204-3206. B) Burford, N.; Cameron, T. S.; Conroy, K. D.; Ellis, B.; Lumsden, M. D.; Macdonald, C. L. B.; McDonald, R.; Phillips, A. D.; Ragogna, P. J.; Schurko, R. W.; Walsh, D.; Wasylishen, R. E. *J. Am. Chem. Soc.* **2002**, *124*, 14012-14013.

(vi) M. S. Balakrishna, D. J. Eisler, T. Chivers *Chem. Soc. Rev.* **2007**, *36*, 650–664, and references therein.

(vii) M. Lehmann, A. Schulz, A. Villinger *Struc. Chem.* **2010** in press.

(viii) (a) A. Villinger, A. Westenkirchner, R. Wustrack, A. Schulz *Inorg. Chem.* **2008**, *47*, 9140 – 9142; (b) A. Schulz, A. Villinger *Eur. J. Inorg. Chem.* **2008**, 4199 – 4203; (c) Ch. Hubrich, D. Michalik, A. Schulz, A. Villinger *Z. Anorg. Allg. Chem.* **2008**, 1403 – 1408; (d) M. Schaffrath, A. Villinger, D. Michalik, U. Rosenthal, A. Schulz *Organomet.*, **2008**, *27*, 1393 – 1398; (e) M. Kowalewski, B. Krumm, P. Mayer, A. Schulz, A. Villinger *Eur. J. Inorg. Chem.* **2007***,* 5319 – 5322; (f) G. Fischer, S. Herler, P. Mayer, A. Schulz, A. Villinger, J. J. Weigand *Inorg. Chem.* **2005**, *44*, 1740 – 1751; (g) N. Götz, S. Herler, P. Mayer, A. Schulz, A. Villinger *Eur. J. Inorg. Chem.* **2006***,* 2051 – 2057.

(ix) a) M. Fild, I. Hollenberg, O. Glemser, *Naturwissenschaften* **1967**, *54*(4), 89-99; b), H. G. Ang, J. M. Miller, *Chem. & Ind.* (London) **1966**, 945.

(x) R. Detsch, E. Niecke, M. Nieger, F. Reichert *Chem. Ber.* **1992**, *125*, 321 – 330.

(xi) M. Kuprat, R. Kuzora, M. Lehmann, A. Schulz, A. Villinger, R. Wustrack *J. Organomet. Chem.* **2010**, *695*, 1006–1011.

(xii) (a) Ruth A. Bartlett, H. V. Rasika Dias, Kathy M. Flynn, Marilyn M. Olmstead, Philip P. Power *J. Am. Chem. Soc.* **1987**, *109*, 5699-5703; (b) Flynn, K. M.; Olmstead, M. M.; Power, P. P.; *J. Am. Chem. Soc.* **1983**, *105*, 2085; (c) Flynn, K. M .; Murray, B. D.; Olmstead, M. M.; Power, P. P. *J. Am. Chem. Soc.* **1983**, *105*, 7460. (d) Flynn, K. M.; Hope, H.; Murray, B. D.; Olmstead, M M.; Power, P. P. *J. Am. Chem. Soc.* **1983**, *105*, 7750; (e) Flynn, K. M.; Bartlett, R. A,; Olmstead, M. M.; Power, P. P. *Organometallics* **1986**, *5*, 813.

(xiii) Values have been corrected according to the Schomaker-Steveson equation for highly polar bonds: *d*AB = *r*A + *r*B – c|χA–χB|,, Holleman Wiberg, *Lehrbuch der Anorganischen Chemie*, 101. Aufl., Walter de Gruyter, 1995, Anhang V.Holleman Wiberg, Lehrbuch der Anorganischen Chemie, 102. Aufl., Walter de Gruyter, Berlin, 2007, Anhang IV.

(xiv) (a) E. D. Glendening, A. E. Reed, J. E. Carpenter, F. Weinhold NBO Version 3.1; (b) A. E. Reed, L. A. Curtiss, F. Weinhold *Chem. Rev.* **1988**, *88*, 899-926.

(xv) (a) E. D. Glendening, A. E. Reed, J. E. Carpenter, F. Weinhold NBO Version 3.1; (b) A. E. Reed, L. A. Curtiss, F. Weinhold *Chem. Rev.* **1988**, *88*, 899-926.

(xvi) Kathy M. Flynn, Brendan D. Murray, Marilyn M. Olmstead, Philip P. Power *J. Am. Chem. SOC.* **1983,** *105,* 7460–7461.

(xvii) C. B. Fischer, S. Xu, H. Zipse, *Chem. Eur. J.* **2006**, *12*, 5779.

(xviii) M. Kuprat, M. Lehmann, A. Schulz, A. Villinger, *Organometallics* **2010**, *29*, 1421.

(xix) (a) E. Niecke, M. Nieger, F. Reichert, *Angew. Chem.* **1988**, *100*, 1781. (b) N. Burford, J. A. C. Clyburne, P. Losier, T. M. Parks, In *Handbuch der Präparativen Anorganischen Chemie*, 4th ed., Engl.; Karsch, H. H. Ed.; Thieme-Verlag: Stuttgart.

(xx) N. Burford, T. S. Cameron, K. D. Conroy, B. Ellis, C.L.B. Macdonald, R. Ovans, A. D. Phillips, P. J. Ragogna, D. Walsh, *Can. J. Chem.* **2002**, 80, 1404–1409.

6. Zusammenfassung

Bei dem Versuch aus Mes*NPCl (Mes* = 2,4,6-tri-*tert*-butylphenyl) und $[HypNPCl]_2$ (Hyp = $(Me_3Si)_3Si$) die reaktiven PN-Kationen $[Mes^*NP]^+$ und $[Hyp_2N_2P_2Cl]^+$aufgrund von Chlorid-eliminierung durch Umsetzung mit Silbertetrakis(1,1,1,3,3,3-hexafluor-2-propoxy)-aluminat, $Ag[Al(OCH(CF_3)_2)_4]$, zu erhalten und durch das schwach koordinierende Anion $[Al(OCH(CF_3)_2)_4]^-$ zu stabilisieren, zeigte sich, dass die Reaktivität beider Kationen zur Zersetzung des Anions führt. Es bildete sich die freie Lewis-Säure $[Al(OCH(CF_3)_2)_3]_2$; zugleich erfolgte ein Chlor/Hexafluoroisopropylaustausch. Diese neue Austauschreaktion verläuft selektiv und unter milden Bedingungen und besitzt daher großes präparatives Potential.

Die Untersuchung der Stabilität von Silbersalzen des Tetrakis(pentafluorphenyl)boratanions, $[B(C_6F_5)_3]^-$ in verschiedenen Lösemitteln führte zu einem neuen Syntheseweg für die Bildung des bekannten Pentafluorphenylsilbers, AgC_6F_5, ausgehend vom Tri*s*pentafluorphenylboran, $B(C_6F_5)_3$. Da das Boran am Ende des Reaktionszyklus wieder zurückgewonnen werden kann, handelt es sich hierbei um eine formale Lewis-Säure katalysierte Reaktion. Entsprechende Silber- und Lithium-Lösemittelkomplexe des Pentafluorphenylborats wurden strukturell charakterisiert.

Zudem wurden über einen Chlor/Pentafluorphenylaustausch durch Reaktion von AgC_6F_5 mit Mes*NPCl oder $[DippNPCl]_2$ (Dipp = 2,6-Di*iso*propylphenyl) das Pentafluorophenyl-substituierte Iminophosphan sowie das entsprechende *cyclo*-Diphosphadiazan dargestellt. Das ungewöhnliche, blaue $Mes^*NPC_6F_5$ konnte gebunden an Fe(CO)-Fragmenten in Form verschiedener Eisencarbonylkomplexe kristallisiert und strukturell charakterisiert werden.

7. Literatur

[1] A. Michaelis, G. Schroeter, *Ber. Dtsch. Chem. Ges*. **1894**, *27*, 490.

[2] a) N. Burford, T. S. Cameron, K. D. Conroy, B. Ellis; M. Lumsden, C. L. B. Macdonald, R. McDonald, A. D. Phillips, P. J. Ragogna, R. W. Schurko; D. Walsh, R. E. Wasylishen, *J. Am. Chem. Soc.* **2002**, *124*, 14012; b) N. Burford; T. S. Cameron, D. J. LeBlanc, A. D. Phillips, T. E. Concolino, K.-C. Lam, A. L. Rheingold, *J. Am. Chem. Soc.* **2000**, *122*, 5413; c) N. Burford, P. J. Ragogna, R. McDonald, M. J. Ferguson, *Chem. Commun.* **2003***,* 2066, d) N. Merceron, K. Miqueu, A. Baceiredo, G. Bertrand, *J. Am. Chem. Soc*. **2002**, *124*, 6806.

[3] a) N. Burford, K. D. Conroy, J. C. Landry, P. J. Ragogna, M. J. Ferguson, R. McDonald, *Inorg. Chem*. **2004**, *43*, 8245; b) N. Burford, J. C. Landry, M. J. Ferguson, R. McDonald, *Inorg. Chem.* **2005**, *44*, 5897.

[4] E. Niecke, M. Nieger, F. Reichert, *Angew. Chem.* **1988**, *100*, 1781; *Angew. Chem. Int. Ed. Engl.* **1988**, *27*, 1715.

[5] A. Cowley, M. Lattman, J. Wilburn, *Inorg. Chem*. **1981**, *20*, 2916–2919.

[6] A. Schulz, A. Villinger. *Inorg. Chem.* **2009**, *48*, 7359–7367.

[7] G. David, E. Niecke, M. Nieger, V. v. d. Goenna, W. Schoeller, *Chem. Ber.* **1993**, *126* (7), 1513.

[8] A. Villinger, P. Mayer, A. Schulz, *Chem. Comm.* **2006**, *11*, 1236.

[9] I. Krossing, I. Raabe, Angew. Chem. **2004**, 116, 2116.

[10] C. A. Reed, K.-C. Kim, R. D. Bolskar, L. J. Mueller, *Science* **2000**, *289*, 101.

[11] I. Krossing*, Chem. Eur. J*. **2001**, *7*, 490.

[12] a) T. J. Barbarich, S. T. Handy, S. M. Miller, O. P. Anderson, P. A. Grieco, S. H. Strauss, *Organometallics* **1996**, *15*, 3776; b) T. J. Barbarich, S. M. Miller, O. P. Anderson, S. H. Strauss, J. *Mol. Catal. A* **1998**, *128*, 289; c) S. M. Ivanova, B.G. Nolan, Y. Kobayashi, S. M. Miller, O. P. Anderson, S. H. Strauss, *Chem. Eur. J*. **2001**, *7*, 503.

[13] C. Reed, *Acc. Chem. Res*. **1998**, *31*, 133.

[14] Übersichten: a) J. B. Lambert, L. Kania, S. Zhang, *Chem. Rev*. **1995**, *95*, 1191; b) C. A. Reed *Acc. Chem. Res*. **1998**, *31*, 325.

[15] K.-C. Kim, C. A. Reed, G. Long, A. Sen, *J. Am. Chem. Soc.* **2002**, *124*, 7662.

[16] S. H. Strauss, S. V. Ivanov, WO 2002036557, **2002**.

[17] M. Lehmann, A. Schulz, A. Villinger, *Angew. Chem.* **2009**, *121*, 7580.

[18] A. Vij, W. Wilson, V. Vij, F. S. Tham, J. Sheehy, K. Christe, *J. Am. Chem. Soc*. **2001**, *123*, 6308.

[19] a) I. Krossing, A. Reisinger *Angew. Chem.* **2003**, *115*, 5903; *Angew. Chem., Int. Ed.* **2003**, *42*, 5725. (b) A. Reisinger, N. Trapp, I. Krossing, S. Altmannshofer, V. Herz, M. Presnitz, W. Scherer *Angew. Chem*. **2007**, *119*, 8445; *Angew. Chem., Int. Ed*. **2007**, 46, 8295.

[20] Ogawa, K.; Kitagawa, T.; Ishida, S.; Komatsu, K. *Organometallics* **2005**, *24*, 4842.

Lebenslauf

Persönliche Daten:

Geburtstag:	19.11.1984
Geburtsort:	Ludwigslust
Nationalität:	Deutsch
Familienstatus:	ledig

Schule:

1991 - 1995 Diesterweg-Grundschule Kühlungsborn
1995 - 2004 Fritz-Reuter-Gymnasium Kühlungsborn
2004 - 2005 Zivildienst (Median Klinik Heiligendamm)

Universität:

10/2005 Immatrikulation (Reformierter Diplomstudiengang Chemie, Universität Rostock)
04/2008 Vordiplom
09/2008 Abschluss Basisstudium

Berufstätigkeit:

10/2002	Wissenschaftliche Hilfskraft (Schülervertrag) am Leibniz-Institut für Atmosphärenphysik an der Universität Rostock e.V., Kühlungsborn, Abteilungen Lidar/ Sonar, Leitung: Prof. Dr. F.-J. Lübken
06/2005 – 07/2005	Stationshelfer Median Kinik Heiligendamm (Medizin. und Pflegedienst, Chefarzt Dr. Schütt)
10/2008 – 09/2009	Wissenschaftliche Hilfskraft am Institut für Chemie, Universität Rostock, Abteilung Physikalische Chemie, Leitung: Prof. Dr. E. Vogel
10/2009 – 03/2010	Wissenschaftliche Hilfskraft am Institut für Chemie, Universität

	Rostock, Abteilung Physikalische Chemie, Leitung: PD Dr. J. Wagner
04/2010 – 09/2010	Wissenschaftliche Hilfskraft am Institut für Chemie, Universität Rostock, Abteilung Anorganische Chemie, Leitung: Prof. Dr. A. Schulz